



Omid Saberi

# **Embankment dam failure outflow hydrograph development**

**DOCTORAL THESIS**

to achieve the university degree of

Doktor der technischen Wissenschaften

submitted to

**Graz University of Technology**

Tutor

Univ.-Prof. Dipl.-Ing. Dr.techn. Gerald Zenz

Institute of Hydraulic Engineering and Water Resources Management

Reviewer

Prof. Leif lia

NTNU University- Department of Hydraulic and Environmental Engineering

Graz, October 2016

# ABSTRACT

In this thesis four different instances of embankment dams affected by overtopping flow are investigated. In the first investigation new relationships for predicting fill-dam failures based on the available history of dam failures around the world are introduced. These new relationships facilitate the estimation of the maximum discharge and breach formation time in the embankment dams which failed due to overtopping flow. The relationship for maximum discharge estimation is derived by introducing a new method for handling the outflow hydrograph. In this method, the flow duration curve is split into three shapes and superimposed to calculate the peak outflow discharge. The relationship for predicting the breach formation time was obtained by using regression analysis. The accuracy of the breach formation time is improved considerably by introducing a parameter related to the dam construction type.

In the second investigation a one-dimensional program is developed in order to calculate the breach outflow hydrograph during embankment dam failure. This program calculates the flow parameters by solving the one-dimensional Saint-Venant equation. Furthermore, it calculates bed evolution by solving the Exner equation with finite difference method. Herein, the model accuracy is increased by dividing the bed slopes into three categories: small slope (0.0–1%), mild slope (1–20%), and steep slope (> 20%). At each time step, based on the real bed slope, bed load transport is modelled by using the relevant equations. In addition, the two-dimensional open-source TELEMAC software has been applied and a subroutine modified in order to model the embankment dam failure. This modification is done by calibrating the slope correction formulas in the sediment part of this software.

In the third investigation of this study, the influence of different geometrical parameters on the breach outflow hydrograph are numerically modelled and compared with each other. The modelling results infer that the downstream slope has more influence on the breach outflow hydrograph in comparison to the other geometrical parameters.

Finally, two new relationships are introduced in order to estimate the hydraulic parameters of the flood resulting from a dam breach which travels through channels and floodplains. The first relationship is concerned about calculating the peak outflow discharge curve. This curve is obtained by connecting the maximum values of cross section hydrographs downstream of a dam. The second relationship calculates the flood wave arrival time using a new method. In this method, it is assumed that arrival time increases linearly along the channel. This means that by calculating the slope of this line, arrival time can be calculated at each point of the channel.

In conclusion, to evaluate the accuracy of the empirical and numerical approaches, reliable dam failure data are collected from a variety of sources around the world. The final results show that estimation of the breach outflow hydrograph and flood wave parameters have been improved by using the new approaches. These improvements are demonstrated by comparing the new approaches results against the existing formulas and observed results.

# STATUTORY DECLARATION

I declare that I have authored this thesis independently, that I have not used other than the declared sources / resources, and that I have explicitly marked all material which has been quoted either literally or by content from the used sources.

*October 5, 2016*

*Omid Saberi*

---

*Date*

*Signature*

# ACKNOWLEDGEMENTS

First of all I would like to say gratitude to Univ.-Prof. Dipl.-Ing. Dr.techn. Gerald Zenz for his review, guidance, critical thoughts and advises. Without our fruitful discussion this thesis wouldn't have possible the way it is.

I also want to express my sincere gratitude to Prof. Lief Lia for his reviewing and helpful comments to improve this thesis.



## **“Brief Resume”**

### **Omid Saberi**

**E-Mail : [omidsaberi@gmail.com](mailto:omidsaberi@gmail.com)**

Born: 1979  
Nationality: Iranian

#### **Scientific background**

- **2012-2016:**  
PhD in Civil Engineering and water resource management, Austria, Graz, Technical University of Graz
- **2004-2008:**  
MSc. Civil Engineering-water branch, Tehran Azad University, Tehran, Iran.
- **1997 -2002:**  
BSc. Civil Engineering, Mashhad Azad University, Mashhad, Iran.
- **1993- 1997:**  
Diploma, Math & Physics, Mashhad, Iran.

#### **Work experience**

- **2012- 2016:** PhD student, Institute of Hydraulic Engineering and Water Resources Management, Graz, Austria
- **2010- 2011:** Civil Manager, KOOMEH Company, Tehran, Iran
- **2007- 2010:** Civil Unit Manager, Rafsanjan Industry Company (R.I.C) Company, Tehran, Iran.
- **2005- 2007:** Civil Supervisor, PERSIA KOLBEH Company (structure, constructor and Utilities Company), Tehran, Iran.
- **2004- 2005:** Civil Engineer, PERSIA KOLBEH Company (structure, constructor and Utilities Company), Tehran, Iran.

#### **Publication**

- Omid Saberi, Clemens Dorfmann and Zenz Gerald (2013). 2-D hydraulic modelling of a dam break scenario. 12th INTERNATIONAL BENCHMARK WORKSHOP ON NUMERICAL ANALYSIS OF DAMS, pp. 267-276.
- Omid Saberi, Zenz Gerald (2015). Empirical Relationship for Calculate Outflow Hydrograph of Embankment Dam Failure due to Overtopping Flow. International Journal of Hydraulic Engineering, 2015 4(3), 10.5923/j.ijhe.20150403.01, pp. 45-53.
- Omid Saberi, Zenz Gerald (2016). Numerical investigation on 1D and 2D embankment dams failure due to overtopping flow, International Journal of Hydraulic Engineering, 2016 5(1), 10.5923/j.ijhe.20160501.02, pp. 9-18.

# CONTENTS

<b>LIST OF FIGURES .....</b>	<b>iv</b>
<b>LIST OF SYMBOLS.....</b>	<b>ix</b>
<b>I INTRODUCTION.....</b>	<b>xiv</b>
<b>1 Design measure.....</b>	<b>17</b>
1.1 Introduction.....	17
1.2 Upstream slope.....	18
1.3 Downstream slope.....	21
1.3.1 Minimum energy loss (MEL) for inlet .....	21
1.3.2 Gabion stepped weir .....	24
1.3.3 Site-cast concrete .....	26
1.3.4 Pre-cast concrete.....	28
<b>2 Empirical method to predict breach outflow hydrograph .....</b>	<b>30</b>
2.1 Introduction.....	30
2.1.1 Dataset collection and preparation.....	30
2.2 Calculation of dam failure time .....	33
2.2.1 Literature review.....	33
2.2.2 New relationships for dam failure time .....	34
2.2.3 New approach to increase the accuracy of dam failure time equations.....	35
2.3 Calculation of peak outflow discharge.....	37
2.3.1 Literature review.....	37
2.3.2 New method for calculating the peak outflow discharge .....	38
2.4 Validation of peak outflow discharge and failure time equations.....	41
2.4.1 IMPACT project .....	41
2.4.2 Chaq-Chaq Dam failure.....	44
2.4.3 ICOLD Benchmark workshop.....	46
2.4.4 Comparison all validation.....	48
<b>3 Numerical modelling of dam overflow .....</b>	<b>49</b>
3.1 Introduction.....	49
3.1.1 Partial differential equation (PDE).....	50
3.1.2 Finite difference method (FDM) .....	52
3.2 Embankment dam failure modelling.....	54

3.2.1	Introduction .....	54
3.2.2	Literature review.....	54
3.3	One-dimensional modelling.....	56
3.3.1	Introduction .....	56
3.3.2	Hydrodynamic part .....	57
3.3.3	Model verification (Modelling flow over bump).....	65
3.3.4	Erosion part.....	68
3.3.5	Sliding.....	75
3.4	TELEMAC-MASCARET Software .....	76
3.4.1	TELEMAC-2D software .....	77
3.4.2	SISYPHE software .....	78
3.5	Validation of 1-D program and TELEMAC-2D software .....	80
3.5.1	One-dimensional (d = 0.31 mm).....	81
3.5.2	One-dimensional (d = 2.0 mm).....	82
3.5.3	TELEMAC-2D (d = 2.0 mm) .....	83
3.5.4	TELEMAC-2D (d = 0.31 mm) .....	84
3.5.5	Comparison of 1-D program and TELEMAC-2D software .....	85
<b>4</b>	<b>Influence of geometrical parameters on outflow hydrograph.....</b>	<b>86</b>
4.1	Introduction.....	86
4.2	Influence of geometrical parameters on the outflow hydrograph .....	87
4.2.1	Influence of downstream slope .....	87
4.2.2	Influence of upstream slope .....	88
4.2.3	Influence of upstream and downstream slopes .....	90
4.2.4	Influence of crest width .....	91
4.3	Influence of initial breach on outflow hydrograph .....	93
4.3.1	IMPACT project (Test No.2).....	93
4.3.2	Modelling IMPACT project by using TELEMAC-2D software .....	94
4.3.3	Modelling IMPACT project by using 1-D program .....	96
4.3.4	Compare results of the 1-D program, TELEMAC-2D software and empirical formula .....	97
4.3.5	Influence of the sediment response angles on the outflow hydrograph.....	98
4.3.6	Influence of the crest width on the outflow hydrograph.....	100
<b>5</b>	<b>Flood Wave Propagation downstream of the dam.....</b>	<b>102</b>
5.1	Introduction.....	102

5.2	Calculation of the peak outflow discharge and flood wave arrival time.....	104
5.2.1	Dataset collection and preparation.....	104
5.2.2	New approach to find the peak outflow discharge .....	106
5.2.3	New approach to find flood wave arrival time .....	109
5.3	Validation of both relationships at same dam failure.....	111
5.3.1	ICOLD Benchmark Workshop .....	111
5.4	Excel sheet program.....	114
<b>6</b>	<b>Conclusion.....</b>	<b>116</b>
6.1	Empirical formula .....	116
6.2	Numerical modelling .....	117
6.3	Change of geometrical parameters.....	117
6.4	Flood Wave propagation.....	118
6.5	Recommendations for Future Work.....	118
<b>7</b>	<b>Reference.....</b>	<b>119</b>
<b>8</b>	<b>Appendix.....</b>	<b>127</b>
8.1	Appendix-A.....	127
8.2	Appendix-B.....	129
8.3	Appendix-C.....	130
8.4	Appendix-D.....	133
8.5	Appendix-E.....	136
8.6	Appendix-F .....	144
8.7	Appendix-G.....	152

# LIST OF FIGURES

<b>Figure 1-1.</b> $W_{50}$ and $d_{50}$ chart (Sentürk 1994).....	19
<b>Figure 1-2.</b> Determine wave height (Yarde 1996).....	19
<b>Figure 1-3.</b> Upstream slope protection design.....	20
<b>Figure 1-4.</b> Riprap protection, Mugie Dam, Kenya, 2009.....	20
<b>Figure 1-5.</b> Side view of Minimum energy loss (MEL).....	22
<b>Figure 1-6.</b> Plan view of Minimum energy loss (MEL).....	22
<b>Figure 1-7.</b> Minimum energy loss, Chinchilla weir, Australia, 1971.....	23
<b>Figure 1-8.</b> Gabion stepped weir.....	24
<b>Figure 1-9.</b> Gabion stepped weir, Pacific Pines, Australia, 2010.....	25
<b>Figure 1-10.</b> Gabion stepped weir, Pacific Pines, Australia, 2010.....	25
<b>Figure 1-11.</b> Site-cast concrete.....	26
<b>Figure 1-12.</b> Site-cast concrete, Georgia Dam, USA.....	27
<b>Figure 1-13.</b> Site-cast concrete, Log Creek Dam, USA, 2012.....	27
<b>Figure 1-14.</b> Pre-cast concrete: (a) without overlapping (b) with overlapping.....	28
<b>Figure 1-15.</b> Pre-cast concrete without overlapping, Klinkner Dam, USA, 2005.....	29
<b>Figure 1-16.</b> Pre-cast concrete with overlapping, Barriga Dam, Spain, 2008.....	29
<b>Figure 2-1.</b> R square value : (a) $(V_w/H_w) \leq 1.0$ (b) $(V_w/H_w) > 1.0$ .....	35
<b>Figure 2-2.</b> Convert hydrograph to simplified shapes.....	38
<b>Figure 2-3.</b> Simplified hydrograph.....	38
<b>Figure 2-4.</b> Simplified hydrograph based on the calibrated parameters.....	40
<b>Figure 2-5.</b> A picture from the IMPACT project area.....	41
<b>Figure 2-6.</b> New formula result for the IMPACT test.....	42
<b>Figure 2-7.</b> Comparison of gained results for the IMPACT project.....	43
<b>Figure 2-8.</b> Chaq-Chaq dam (K.Abdulrahman. (2014)).....	44
<b>Figure 2-9.</b> Comparison of gained results for the Chaq-Chaq dam.....	45
<b>Figure 2-10.</b> A hypothetic image of the dam given in the ICOLD Benchmark Workshop.....	46
<b>Figure 2-11.</b> Comparison of gained results for ICOLD Benchmark Workshop.....	47
<b>Figure 2-12.</b> Comparison results of all equations.....	48
<b>Figure 3-1.</b> Finite difference mesh.....	53
<b>Figure 3-2.</b> Different approaches for dam failure modelling.....	54
<b>Figure 3-3.</b> Embankment dam failure procedure.....	56
<b>Figure 3-4.</b> Control volume in the open channel.....	57
<b>Figure 3-5.</b> Cross section of channel.....	57
<b>Figure 3-6.</b> Forces in the rectangular channel.....	57
<b>Figure 3-7.</b> MacCormack method.....	62
<b>Figure 3-8.</b> MacCormack procedure in 1-D program.....	62
<b>Figure 3-9.</b> Geometry of the channel.....	65
<b>Figure 3-10.</b> Subcritical Flow over bump.....	66
<b>Figure 3-11.</b> Supercritical with hydraulic jump.....	66
<b>Figure 3-12.</b> Supercritical without hydraulic jump.....	67
<b>Figure 3-13.</b> Velocity and Stress profile in the fluid.....	69
<b>Figure 3-14.</b> Forces in the fluid.....	69
<b>Figure 3-15.</b> Grain distribution chart to characterize the sediments grain sizes.....	70

LIST OF FIGURES

---

<b>Figure 3-16.</b> Shield diagram.....	71
<b>Figure 3-17.</b> Choose proper sediment transport equation, Van Emelen (2013).....	74
<b>Figure 3-18.</b> Sliding in 1-D numerical modelling.....	75
<b>Figure 3-19.</b> TELEMAC-MASCARET system.....	76
<b>Figure 3-20.</b> Schmocker et al. (2013) dam failure tests.....	80
<b>Figure 3-21.</b> Schmocker outflow hydrograph:(a) Measurement results, (b) 1-D results for d=0.31 mm.....	81
<b>Figure 3-22.</b> Schmocker outflow hydrograph:(a) Measurement results, (b) 1-D results for d=2.0 mm.....	82
<b>Figure 3-23.</b> Schmocker outflow hydrograph:(a) Measurement results, (b) TELEMAC- 2D results for d=2.0 mm.....	83
<b>Figure 3-24.</b> Schmocker outflow hydrograph:(a) Measurement results, (b) TELEMAC- 2D results for d=0.31 mm.....	84
<b>Figure 3-25.</b> 1-D program, TELEMAC-2D software and measurement results: (a) For d=2.0 mm, (b) For d=0.31 mm.....	85
<b>Figure 4-1.</b> Downstream slopes variation.....	87
<b>Figure 4-2.</b> Influence of different downstream slope on the outflow hydrograph.....	87
<b>Figure 4-3.</b> Influence of different downstream slope on the crest elevation (erosion rate).....	88
<b>Figure 4-4.</b> Upstream slopes variation.....	88
<b>Figure 4-5.</b> Influence of different upstream slope on outflow hydrograph.....	89
<b>Figure 4-6.</b> Influence of different upstream slope on crest elevation (erosion rate).....	89
<b>Figure 4-7.</b> Change in both upstream and downstream slopes.....	90
<b>Figure 4-8.</b> Influence of different upstream and downstream slope on outflow hydrograph.....	90
<b>Figure 4-9.</b> Influence of different upstream and downstream slope on crest elevation.....	91
<b>Figure 4-10.</b> Change crest width.....	91
<b>Figure 4-11.</b> Influence of different width of the crest on outflow hydrograph.....	92
<b>Figure 4-12.</b> Influence of different width of the crest on crest elevation(erosion rate).....	92
<b>Figure 4-13.</b> Influence of initial breach on the outflow hydrograph.....	93
<b>Figure 4-14.</b> The IMPACT project site picture.....	94
<b>Figure 4-15.</b> Modelling the IMPACT project using TELEMAC-2D software.....	94
<b>Figure 4-16.</b> IMPACT outflow hydrograph: (a) Measurement results, (b) TELEMAC- 2D results....	95
<b>Figure 4-17.</b> Influence of initial breach (Second scenario).....	96
<b>Figure 4-18.</b> 1-D dam failure modelling assumptions.....	96
<b>Figure 4-19.</b> 1-D result for the IMPACT project.....	97
<b>Figure 4-20.</b> Compare results between 1-D program, TELEMAC-2D, empirical method and measurement result.....	97
<b>Figure 4-21.</b> Influence of sediment response angle on outflow hydrograph( $\psi=30$ ).....	98
<b>Figure 4-22.</b> Influence of sediment response angle on outflow hydrograph( $\psi=35$ ).....	99
<b>Figure 4-23.</b> Influence of sediment response angle on outflow hydrograph( $\psi=40$ ).....	99
<b>Figure 4-24.</b> Influence of sediment response angle on outflow hydrograph( $\psi=45$ ).....	99
<b>Figure 4-25.</b> Compare all results.....	100
<b>Figure 4-26.</b> Influence of different width of the crest on outflow hydrograph ( $H_d = 5.0$ m).....	101
<b>Figure 4-27.</b> Influence of different width of the crest on outflow hydrograph ( $H_d = 50.0$ m).....	101
<b>Figure 5-1.</b> The plan view of a hypothetical dam along with the downstream area.....	102
<b>Figure 5-2.</b> Dam-break flood wave parameters: (a) Peak outflow discharge curve (b) Arrival time line.....	103

---

LIST OF FIGURES

---

<b>Figure 5-3.</b> Procedure to find the peak outflow discharge and arrival time .....	104
<b>Figure 5-4.</b> Peak outflow discharge curve (Test No.30).....	106
<b>Figure 5-5.</b> The ‘reduction value’ ( $\delta_R$ ) parameter on the peak outflow discharge curve .....	106
<b>Figure 5-6.</b> Time discretization (time steps) concept on the peak outflow discharge curve .....	107
<b>Figure 5-7.</b> Flood arrival time assumption (Test No.30).....	109
<b>Figure 5-8.</b> General form of wave arrival time line.....	109
<b>Figure 5-9.</b> A schematic picture showing the ICOLD Benchmark Workshop dam and its downstream region.....	111
<b>Figure 5-10.</b> Plan view of ICOLD Benchmark Workshop downstream of the dam .....	112
<b>Figure 5-11.</b> Excel sheet program: (a) Calculating dam failure parameters (b) Calculating flood wave parameters .....	115
<b>Figure 8-1.</b> Boundary condition in 1-D program.....	127
<b>Figure 8-2.</b> P. Garcia-Navarro & J. M. Saviron (1992) method.....	127
<b>Figure 8-3.</b> Outflow hydro graph for dam number 1 and 2 .....	134
<b>Figure 8-4.</b> Outflow hydro graph for dam number 3 and 4 .....	134
<b>Figure 8-5.</b> Outflow hydro graph for dam number 5 and 6 .....	134
<b>Figure 8-6.</b> Outflow hydro graph for dam number 7 and 8 .....	135
<b>Figure 8-7.</b> Outflow hydro graph for dam number 9 and 10.....	135
<b>Figure 8-8.</b> Outflow hydro graph for dam number 11 and 12.....	135
<b>Figure 8-9.</b> Outflow hydro graph for dam number 13 and 14.....	136
<b>Figure 8-10.</b> Peak outflow discharge curve for test number 1 and 6.....	138
<b>Figure 8-11.</b> Peak outflow discharge curve for test number 7 and 12.....	138
<b>Figure 8-12.</b> Peak outflow discharge curve for test number 13 and 18.....	138
<b>Figure 8-13.</b> Peak outflow discharge curve for test number 19 and 24.....	139
<b>Figure 8-14.</b> Peak outflow discharge curve for test number 25 and 30.....	139
<b>Figure 8-15.</b> Peak outflow discharge curve for test number 31 and 36.....	139
<b>Figure 8-16.</b> Peak outflow discharge curve for test number 37 and 42.....	140
<b>Figure 8-17.</b> Peak outflow discharge curve for test number 34 and 40.....	142
<b>Figure 8-18.</b> Peak outflow discharge curve for test number 22 and 16.....	142
<b>Figure 8-19.</b> Peak outflow discharge curve for test number 4.....	142
<b>Figure 8-20.</b> Compare all peak outflow discharge curve.....	143
<b>Figure 8-21.</b> Arrival time for test number 1 and 6.....	146
<b>Figure 8-22.</b> Arrival time for test number 7 and 12.....	146
<b>Figure 8-23.</b> Arrival time for test number 13 and 18.....	146
<b>Figure 8-24.</b> Arrival time for test number 19 and 24.....	147
<b>Figure 8-25.</b> Arrival time for test number 25 and 30.....	147
<b>Figure 8-26.</b> Arrival time for test number 31 and 36.....	147
<b>Figure 8-27.</b> Arrival time for test number 37 and 42.....	148
<b>Figure 8-28.</b> Arrival time for test number 22 and 16.....	150
<b>Figure 8-29.</b> Arrival time for test number 34 and 40.....	150
<b>Figure 8-30.</b> Arrival time for test number 4 .....	150
<b>Figure 8-31.</b> Compare all flood wave arrival time .....	151
<b>Figure 8-32.</b> King Mongkut’s University dam failure tests.....	152
<b>Figure 8-33.</b> Erosion rate for 20% and 25% slope .....	154
<b>Figure 8-34.</b> Erosion rate for 33% and 50% slope .....	154

## LIST OF TABLES

<b>Table 2-1</b>	List of the dam failure data for regression analysis.....	31
<b>Table 2-2.</b>	List of the dam failure data to calibrate $\delta$ in the failure time equations.....	31
<b>Table 2-3.</b>	List of dam failure data to validate the failure time and peak outflow equation.....	32
<b>Table 2-4.</b>	List of dam failure to calibrate $\alpha$ and $\beta$ parameters in the peak outflow equation .....	32
<b>Table 2-5.</b>	List of failure time equations ( $t_f$ ).....	33
<b>Table 2-6.</b>	Calculation of dam coefficient ( $\delta$ ) for different type of dams .....	36
<b>Table 2-7.</b>	A list of the existing peak outflow discharge equations.....	37
<b>Table 2-8.</b>	Calibrate $\alpha$ and $\beta$ for the peak outflow discharge.....	39
<b>Table 2-9.</b>	Dam failure data for Test # 2-2002 dam .....	41
<b>Table 2-10.</b>	Measurement of failure parameter for Test # 2-2002.....	41
<b>Table 2-11.</b>	Calculated results for the IMPACT project using the new formulas .....	42
<b>Table 2-12.</b>	Compare results of new relationships with other studies for the IMPACT project .....	43
<b>Table 2-13.</b>	Dam failure parameters for the Chaq-Chaq Dam.....	44
<b>Table 2-14.</b>	Measurement failure parameter for the Chaq-Chaq Dam .....	44
<b>Table 2-15.</b>	Calculated result of new formula for Chaq-Chaq dam.....	44
<b>Table 2-16.</b>	Compare results of the new relationships with other studies for the Chaq-Chaq dam.....	45
<b>Table 2-17.</b>	Dam failure data from ICOLD Benchmark Workshop .....	46
<b>Table 2-18.</b>	Failure parameter given by formulator for ICOLD Benchmark Workshop.....	46
<b>Table 2-19.</b>	Calculated result of new formula .....	47
<b>Table 2-20.</b>	Compare results of new relationships with other studies .....	47
<b>Table 3-1.</b>	Different equations and algorithms for modelling fluid behavior.....	50
<b>Table 3-2.</b>	Literature review for dam failure program.....	55
<b>Table 3-3.</b>	Roughness equations.....	63
<b>Table 3-4.</b>	Roughness coefficient for different surface .....	64
<b>Table 3-5.</b>	Literature review of Erosion modelling software.....	68
<b>Table 3-6.</b>	Different Bed-load transport formula.....	73
<b>Table 3-7.</b>	Calibrated value for $\omega$ parameter .....	75
<b>Table 3-8.</b>	Different bed load equations in SISYPHE .....	78
<b>Table 3-9.</b>	Calibrated value for $\beta_{Tel}$ parameter .....	79
<b>Table 3-10.</b>	Details of the Schmocker et al. (2013) dam failure tests.....	80
<b>Table 4-1.</b>	List of modified geometrical parameters (Chinnarasri et al. (2003)).....	86
<b>Table 4-2.</b>	IMPACT project detail.....	93
<b>Table 4-3.</b>	List of modified sediment response angles (Morris et al. (2008)).....	98
<b>Table 4-4.</b>	List of modified crest width (Morris et al. (2008)) .....	100
<b>Table 5-1.</b>	List of embankment dam failure .....	105
<b>Table 5-2.</b>	Calibrated $\Delta t$ value for calculating maximum discharge .....	108
<b>Table 5-3.</b>	Dam data for ICOLD Benchmark Workshop.....	111
<b>Table 5-4.</b>	Cross sections at downstream of the dam .....	112
<b>Table 5-5.</b>	Calculated results by new formula for cross section 1, 2 and 3 .....	112
<b>Table 5-6.</b>	Calculated results by new formula for cross section 3 and 4 .....	113
<b>Table 5-7.</b>	Compare results of new relationships with formulator results.....	113
<b>Table 8-1.</b>	List of embankment dam failure .....	133
<b>Table 8-2.</b>	List of the peak outflow discharge curve .....	137

---

LIST OF TABLES

---

**Table 8-3.** List of the peak outflow discharge curve ..... 141  
**Table 8-4.** List of the arrival time line ..... 145  
**Table 8-5.** List of the arrival time line ..... 149  
**Table 8-6:** Details of the King Mongkut’s University dam failure tests ..... 152  
**Table 8-7.** Different slope in the King Mongkut’s University dam failure tests ..... 152  
**Table 8-8.** Calibrated  $\omega$  value ..... 153  
**Table 8-9.** Calibrated  $\beta_{Tel}$  parameter ..... 153

**LIST OF SYMBOLS**

$A$	Wetted cross section [m <sup>2</sup> ]
$A_p$	Coefficient in partial differential equation [-]
$A_s$	Surface area of the reservoir in acres corresponding to $H_w$ [m <sup>2</sup> ]
$B$	Width of the channel at $Z_1$ elevation [m]
$B_{avg}$	Average of width of final breach [m]
$B_b$	Bottom width of breach [m]
$B_p$	Coefficient in partial differential equation [-]
$B_t$	Top width of breach [m]
$B_{max}$	The crest width [m]
$C_i^j$	Wave celerity = $\sqrt{(gy)}$ [m/s]
$C_{ni}^j$	Courant number [-]
$C_D$	Drag coefficient [-]
$C_p$	Coefficient in partial differential equation [-]
$C_L$	Lift coefficient [-]
$d$	Mean diameter of sediment [m]
$d_{30}$	Sieve size 30% of the grains by weight pass through [%]
$d_{50}$	Sieve size 50% of the grains by weight pass through [%]
$d_{90}$	Sieve size 90% of the grains by weight pass through [%]
$D$	Deposition formula [-]
$D_I$	The flow depth at inception point [m]
$E$	Erosion formula [-]
$E_s$	Specific energy [m]

---

LIST OF SYMBOLS

---

$F_f$	Friction force term [kg·m/s <sup>2</sup> ]
$F_g$	Gravity force term [kg·m/s <sup>2</sup> ]
$F_p$	Pressure force term [kg·m/s <sup>2</sup> ]
$F_D$	Drag force [kg·m/s <sup>2</sup> ]
$F_L$	Uplift force [kg·m/s <sup>2</sup> ]
$F_r$	Froude number = $u/\sqrt{(gy)}$ [-]
$F$	Fetch length [m]
$g$	Acceleration of gravity [m/s <sup>2</sup> ]
$H_{Wave}$	The design wave height [m]
$H$	Height of water in channel [m]
$H_b$	Maximum height of the final breach [m]
$H_w$	Height of the water above the final breach bottom at failure time [m]
$H_d$	Height of the dam [m]
$H_{des}$	The design upstream head [m]
$h$	The step heights [m]
$(H1 - z)$	The upstream head above spillway crest [m]
$I_1$	Hydrostatic pressure [N/m <sup>2</sup> ] or [kg·m <sup>-1</sup> ·s <sup>-2</sup> ]
$I_2$	Force because of change in width [kg·m/s <sup>2</sup> ]
$K_s$	Roughness of channel [T/L <sup>1/3</sup> ]
$K_{rr}$	Stability coefficient =2.5 [-]
$L_I$	The inception distance from crest [m]
$L_C$	Length of the crest [m]
$L$	The step width [m]

---

LIST OF SYMBOLS

---

$m$	Mass [kg]
$n$	Manning number [s/ (m <sup>1/3</sup> )]
$n'$	Global manning number [s/ (m <sup>1/3</sup> )]
$Q$	Discharge [m <sup>3</sup> /s]
$q_b$	Unit discharge [m <sup>3</sup> /s][1/m]
$Q_p$	Peak outflow discharge at dam [m <sup>3</sup> /s]
$Q_{ob}$	Discharge [m <sup>3</sup> /s]
$Q_b$	Modified discharge [m <sup>3</sup> /s]
$q$	Lateral inflow [m <sup>3</sup> /s]
$p$	Sediment porosity [%]
$R$	Hydraulic radius [m]
$R_{fb}$	is the freeboard height [m]
$S$	Bed slope [%]
$s_{rel}$	Relative density = $\frac{\rho_s}{\rho_w}$ [-]
$S_0$	Bed slope [%]
$S_f$	Energy line slope [%]
$S_r$	Specific gravity of the riprap [ $\gamma_r/\gamma_w$ ]
$S_{res}$	Reservoir volume at the time of failure [m <sup>3</sup> ]
$t_f$	Dam failure time [h]
$t_p$	Time to reach peak outflow discharge [T]
$t$	The thickness of riprap [m]
$T$	Wave period [s]
$U$	Design wind velocity over water [m/s]

---

LIST OF SYMBOLS

---

$U_i$	Velocity in x direction [m/s]
$u_*$	Shear velocity $=\sqrt{gRS}$ [m/s]
$V_{er}$	Volume of material eroded [m <sup>3</sup> ]
$V_w$	Reservoir volume at the time of failure [m <sup>3</sup> ]
$W$	Submerged weight [kg·m/s <sup>2</sup> ]
$W_{cst}$	Width of the crest [m]
$W_c$	Width of the channel [m]
$W_s$	Speed of the object relative to the fluid [m/s]
$W_{50}$	The weight in the Kilo Newton of 50% size in the riprap
$y$	Height of water in channel [m]
$Z_b$	Side slope of the breach [%]
$Z$	Bed elevation [m]
$Z_1$	any elevation above the toe [m]
$\gamma_r$	Unit weight of the riprap rocks [ $\frac{kN}{m^3}$ ]
$\delta$	Parameters for defining type of dam in failure time equation [-]
$\alpha_{stab}$	Stability parameter [-]
$\alpha$	Parameter for defining shape of the hydrograph [-]
$\alpha_{Up}$	Upstream slope [%]
$\beta$	Parameter for defining shape of the hydrograph [-]
$\gamma_Q$	Instantaneous flow reduction factor $= 23.4 \times \left(\frac{A_s}{B_{avg}}\right)$
$\Delta t$	Time step [s]
$\Delta x$	Cell space [m]
$\mu$	Sediment Courant number [-]

---

LIST OF SYMBOLS

---

$d$	Mean diameter of sediment [m]
$\theta_o$	The angle between the pseudo-bottom formed by the step and horizontal [°]
$\theta$	Shield parameter = $\frac{u_*^2}{(s-1)gd}$ [-]
$\theta_c$	Critical shield parameter [-]
$\theta_{c0}$	Slope adjusted critical shield parameter [-]
$\tau_b$	Bottom shear stress [N/m <sup>2</sup> ]
$\tau_z$	Shear stress in vertical distance above the channel bottom [N/m <sup>2</sup> ]
$\rho_s$	Density of sediment particles [kg/m <sup>3</sup> ]
$\rho_w$	Water density [kg/m <sup>3</sup> ]
$\emptyset$	Bed slope [%]
$\emptyset_s$	Sediment respond angle [°]
$\omega$	Calibrated parameter in the Smart equation [-]
$\beta_{Tel}$	Calibrated parameter in the Koch and Flokstra formula [-]
$\eta$	Vertical distance above the channel bottom [m]
$\Theta_T$	Arrival time line slope [-]
$\delta_R$	Reduction parameter [-]
$\forall$	Volume of water in the control volume [m <sup>3</sup> ]
$\Phi$	Dimensionless sediment transport rate [-]
$\dot{m}$	Mass flow [kg/s]

## INTRODUCTION

Dams are engineered to serve in a robust manner to store water for power production, irrigation purposes or flood protection. Spilling facilities are foreseen to prevent uncontrolled increase of the storage water level and therefore overtopping of the dam. In addition reservoir and dam monitoring systems provide together with a forecasting system the basis to intervene and start with safety measures.

However, in very uncertain cases the uncontrolled overtopping of a fill dam could cause regressive erosion, uncontrolled loss of water and finally the failure of the retention structure. For rescue forces and protection measures to endangered areas downstream it is of highest interest to know the failure path, the time to failure and the flow duration curve to account for the flood risk.

The International Commission on Large Dams (ICOLD 1995 and 2011) have reported 176 failures among the 17,406 registered dams in the world (Figure I-1). In this report, the failure rate for embankment dams is higher than concrete dams. It also reveals that overtopping failure is the most common cause of failure in embankment dams compared with other types of failures like piping and slope failure (Figure I-1). Therefore, in hydraulic engineering, water resource management and risk management fields, overtopping failure is categorized as a more dangerous failure compared to other types of failure. In this study, dam failure due to overtopping is reassessed.

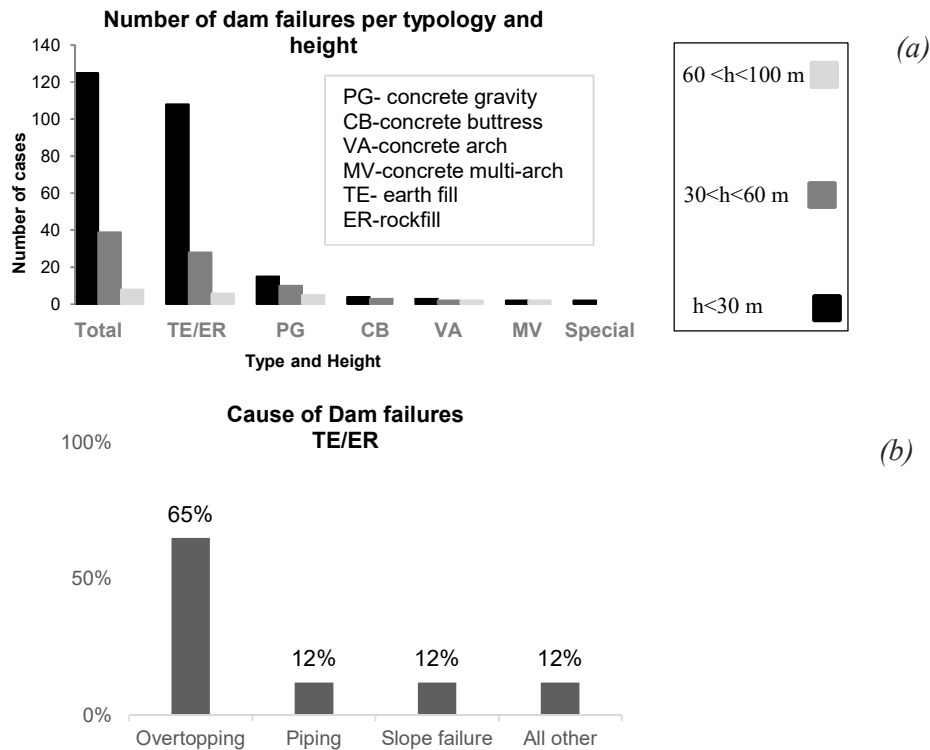


Figure I- 1. Dam failure statistics: (a) Number of dam failure (b) Cause of dam failure

To achieve a better understanding of such failure mechanisms, it is essential to identify dam failure parameters. Dam failure parameters are split into two categories; geometrical and hydrographical parameters (Figure I-2).

Geometrical parameters normally refer to the geometric characteristics of a dam's breach shape:

- Height of breach ( $H_b$ )
- Top width of breach ( $B_t$ )
- Average width of breach ( $B_{ave}$ )
- Bottom width of breach ( $B_b$ )
- Side slope of breach ( $Z_b$ )

The hydrographic parameters describe factors which affect the breach outflow hydrograph (Figure I-2):

- Peak outflow discharge ( $Q_p$ )
- Time of failure ( $t_f$ )

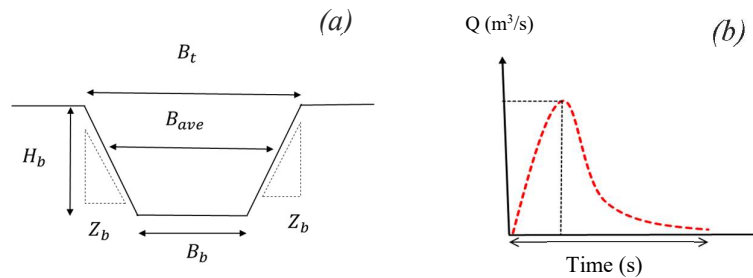


**Figure I- 2.** Failure parameters: (a) Geometrical parameters (b) Hydrographic parameters

Generally, in overtopping failure the hydrographic parameters can be calculated in two different ways:

- Based on empirical method
- Numerical simulation

In the empirical method, dam failure parameters are predicted by finding relationships between previous dam failures parameters by using regression analysis. The main disadvantage of this method is ignoring many site-specific parameters like grain size, roughness, density, velocity, stress, etc. Therefore, using these simplifications can lead to errors and the necessity to include more additional appropriate parameters.

In the numerical method to calculate dam failure parameters the governing equations of fluid like Navier-Stokes, shallow water or Saint-Venant are solved. The main advantage of this method is considering more reasonable parameters based on mechanical relationships like cohesion, friction, etc. This means if appropriate parameters are available, the numerical method is more accurate in comparison to the empirical method.

In this thesis, we will find relationships to aid the prediction of hydrographic breach parameters by using empirical and numerical methods.

To communicate the findings, this thesis is laid out in the following chapters:

**- Chapter one**

In this chapter, different design measures to protect embankment dams against erosion and failure are discussed and presented. This chapter includes the following methods: The minimum energy loss (MEL) weirs, site-cast concrete, pre-cast concrete and gabion stepped weir.

**- Chapter two**

Two new relationships for predicting dam failure parameters are introduced. In the first relationship dam failure time is calculated by using regression analysis on the previous dam failure data. In the second relationship, the peak outflow discharge is calculated by using a new method. In this method the area under the outflow hydrograph is split into the three primitive shapes. The peak outflow discharge is calculated from the sum of the areas of these three shapes.

**- Chapter three**

In the third chapter, a one-dimensional program is developed. In this program the breach outflow hydrograph of non-cohesive embankment dams which are failed by overtopping flow is calculated. Furthermore, the two-dimensional open-source TELEMAC software is modified to model sediment transport over the steep slopes during the failure process.

**- Chapter four**

The influences of geometrical parameters like upstream slope, downstream slope, crest width and initial breach on the breach outflow hydrograph are numerically modelled. Furthermore, the final results are compared against each other to define which geometrical parameters have a significant influence on the breach outflow hydrograph.

**- Chapter five**

In the last chapter, two new relationships are introduced to calculate the flood wave parameters downstream of the dam. The first relationship concerns about calculating peak outflow discharge curve. This curve is obtained by connecting the maximum values of the cross section hydrographs downstream of the dam. The second relationship calculates the flood wave arrival time by using a new method. In this method, it is assumed that the arrival time increases linearly along the channel. Therefore, by determining its slope, the arrival time can be calculated at any point in the downstream valley.

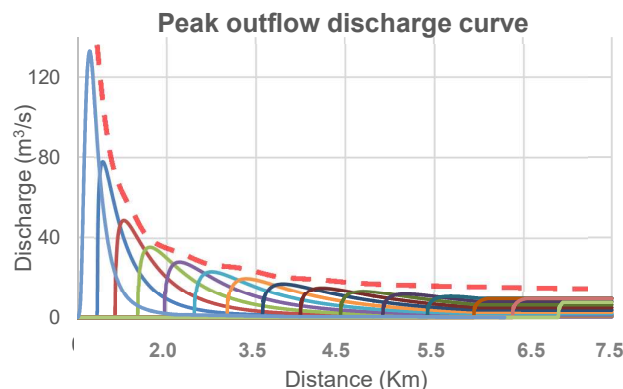


**Figure I- 3.** Peak outflow discharge curve

# Chapter 1

## Design measure

---

### 1.1 Introduction

Dam overtopping could cause disaster if flood control facilities like spillways and freeboard are not adequately designed or worked properly. Overtopping can cause a huge amount of uncontrolled water release above the dam body which may lead to instability and dam collapse. Recent studies on failure of the embankment dams like ICOLD (1995 and 2011), show that overtopping failure is one of the most common causes of failure in comparison to other failure types like piping and slope failure as shown in Figure I-1. The results of these studies clearly indicate the importance of modelling and designing elements in such dams to protect against erosion and failure of the structure.

There are several conventional methods known to overcome possible overtopping failure like using larger spillway or increase height of the dam. However, using these methods have limitations such as additional construction costs and implementation problems. In order to address these issues, new methods have been introduced and developed as substitute approaches for dealing with the overtopping protection in embankment dams like reducing downstream slope (minimum energy loss), gabion stepped weir and concrete stepped spillway. In these methods, water flow is permitted to overtop the dam body by considering special element against any erosion. Design and construction of these methods are considered as the best alternative compared to other methods like enlargement of spillway capacity or increase the height of the dam. According to the USBR (1992, 2012a) regulations, such protection elements are normally used for dam under the following conditions:

- Maximum water elevation in the reservoir is close to the crest elevation. Wind can generate wave, therefore, erosion on the dam body could happen.
- Maximum water elevation in the reservoir is higher than crest elevation.

In general, overtopping and erosion protection measures are designed in any of the two different portions of a dam body:

- Upstream slope
- Downstream slope

## 1.2 Upstream slope

Upstream slope protection is usually needed in rock-fill dams against erosions caused by wave impact on the reservoir slope. This type of protection is normally done with the help of riprap. The used materials in such construction should have the following specifications to secure the effectiveness of this method:

- The riprap material should be large enough to dissipate wave's energy without displacement and settlement by filter erosion.
- The riprap material should be durable and strong enough without any destruction.

However, the main parameters which affect the successfulness of the riprap structure are:

- Material size
- Layer thickness
- Freeboard height

In the following the equations which are restated to calculate these parameters are explained in more detail (Barker et al. (2000)).

$$W_{50} = (\gamma_r H_{Wave}^3) / (K_{rr} (S_r - 1)^3 \cos \alpha_{Up}) \quad 1-1$$

$$t = 2 \sim 3 d_{50} \quad 1-2$$

$$T = 0.07118 F^{0.3} U^{0.4} \quad 1-3$$

$$L = 5.12 T^2 \quad 1-4$$

$$R_{fb} = \frac{H_{Wave}}{(0.4 + (\frac{H_{Wave}}{L})^{0.5} \cos \alpha_{Up})} \quad 1-5$$

Here:

$W_{50}$  [KN] the weight of 50% size in the riprap

$\gamma_r$  [ $\frac{KN}{m^3}$ ] the unit weight of the riprap rocks

$H_{Wave}$  [m] the wave height

$S_r$  [ $\frac{\gamma_r}{\gamma_w}$ ] the specific gravity of the riprap

$\alpha_{Up}$  [-] the upstream slope

$K_{rr}$  [-] the stability coefficient =2.5

$F$  [m] the fetch length

$U$  [m/s] the wind velocity

$T$  [s] the wave period

$t$  [m] the thickness of riprap

$L$  [m] the water wave length

$R_{fb}$  [m] the freeboard height

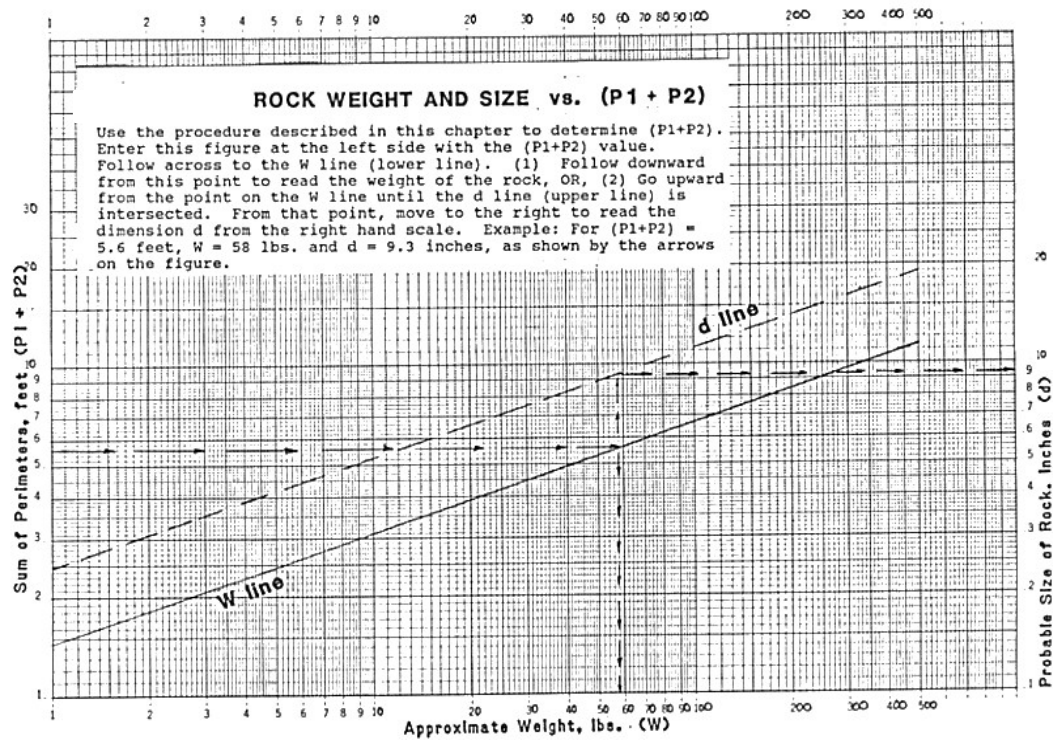


Figure 1-1. W<sub>50</sub> and d<sub>50</sub> chart (Sentürk 1994)

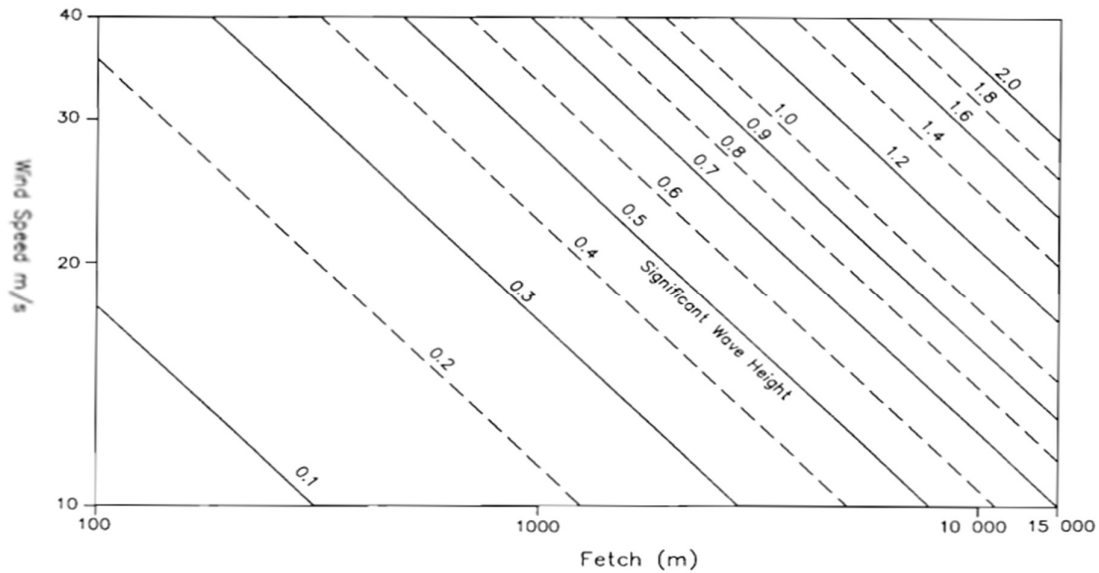


Figure 1-2. Determine wave height (Yarde 1996)

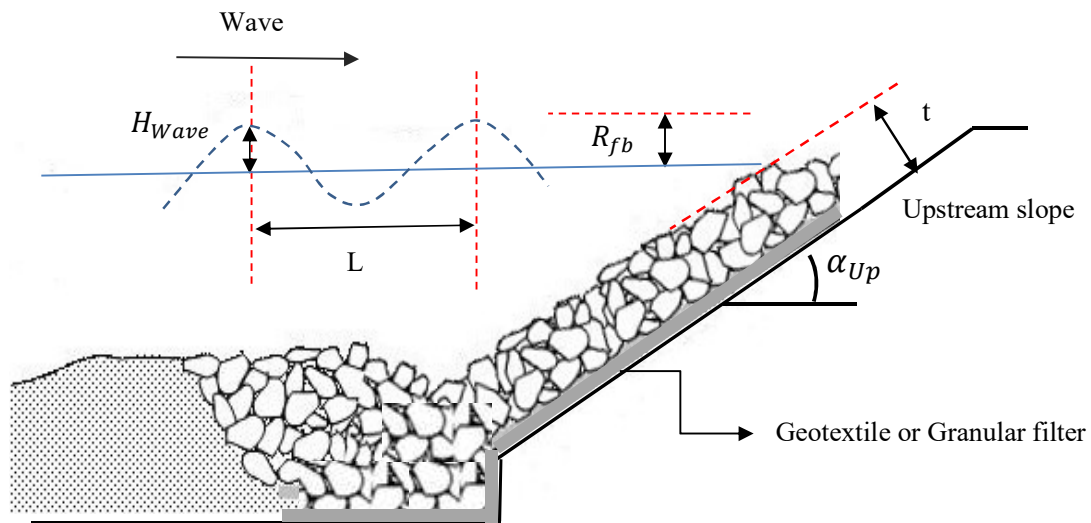


Figure 1-3. Upstream slope protection design



Figure 1-4. Riprap protection, Mugie Dam, Kenya, 2009

Link: [http://design-of-small-dams.appspot.com/quick\\_links/photos/ch12/dam-construction](http://design-of-small-dams.appspot.com/quick_links/photos/ch12/dam-construction)

### 1.3 Downstream slope

Downstream slope protection is required to protect slope against erosion by overtopping flow and can be implemented in several ways:

- Minimum energy loss (MEL) for inlet
- Gabion stepped weir
- Concrete stepped spillway
- Precast concrete block spillway

In the following, these methods are explained in more detail.

#### 1.3.1 Minimum energy loss (MEL) for inlet

This method was designed and introduced by Mackay (1971) and is one of the unusual overtopping protection designs. First built was on the Redcliffe weir in Australia and it is still in use without any damage. The MEL inlet system was developed for embankment dams where the river catchment is characterized by large rainfalls and a very small bed slope. This system is working based on the minimize energy dissipation of large flood during passing on the embankment dams to prevent any erosion and damage at weir foot.

By assuming a wide crest and negligible energy loss along the inlet the discharge capacity of the MEL inlet is determined by using the following equation:

$$Q = \frac{2}{3} C_d B_{\max} \sqrt{2g} (H_1 - Z)^{1.5} \quad 1-6$$

For broad submerge weirs  $C_d \cong 0.58$

$$Q = B_{\max} \sqrt{g} \left(\frac{2}{3}\right) (H_1 - Z)^{1.5} \quad 1-7$$

In order to prevent hydraulic jump at downstream of the dam, a MEL channel should be designed to achieve critical flow conditions at any position along the channel. Therefore width of the MEL channel at any elevation under the crest and above the dam toe should be calculated by using Equation 1-8:

$$B = B_{\max} \left(\frac{H_1 - Z}{H_1 - Z_1}\right)^{1.5} \quad 1-8$$

Furthermore, water depth on a MEL channel is determined by using the following equation.

$$A = \sqrt[3]{\frac{Q^2 B}{g}} \quad 1-9$$

For rectangular channel water depth is calculated as the following equation.

$$y = \sqrt[3]{\frac{q^2}{g}} \quad 1-10$$

The culvert design is defined in the following figures (Chanson (2013)).

Here:

- $A$  [m<sup>2</sup>] Cross section areas  
 $B_{max}$  [m] Crest width  
 $B$  [m] Width of the channel at  $Z_1$  elevation  
 $C_d$  [-] Submerge weir coefficient  
 $H_1$  [m] Upstream head  
 $R$  [m] Hydraulic radius  
 $S_0$  [-] Bed slope  
 $Z_1$  [m] the any elevation above the toe  
 $q$  [m<sup>3</sup>/s][1/m] Unit discharge

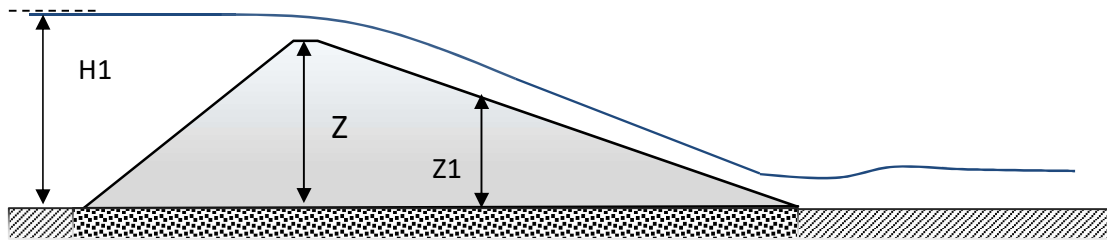


**Figure 1-5.** Side view of Minimum energy loss (MEL)

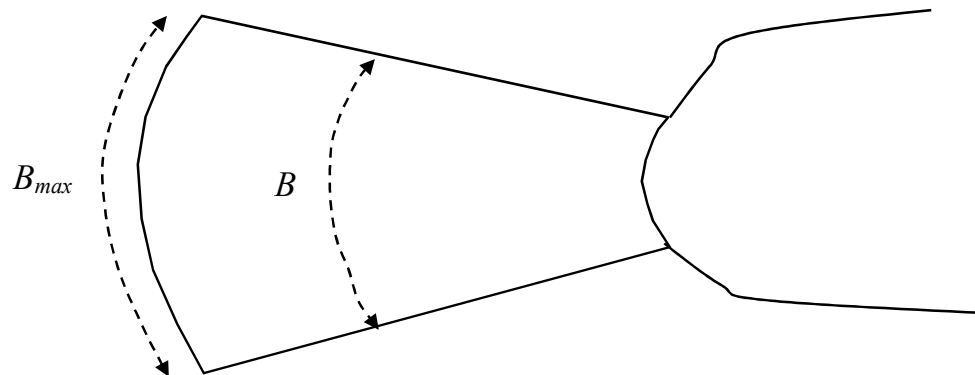


**Figure 1-6.** Plan view of Minimum energy loss (MEL)

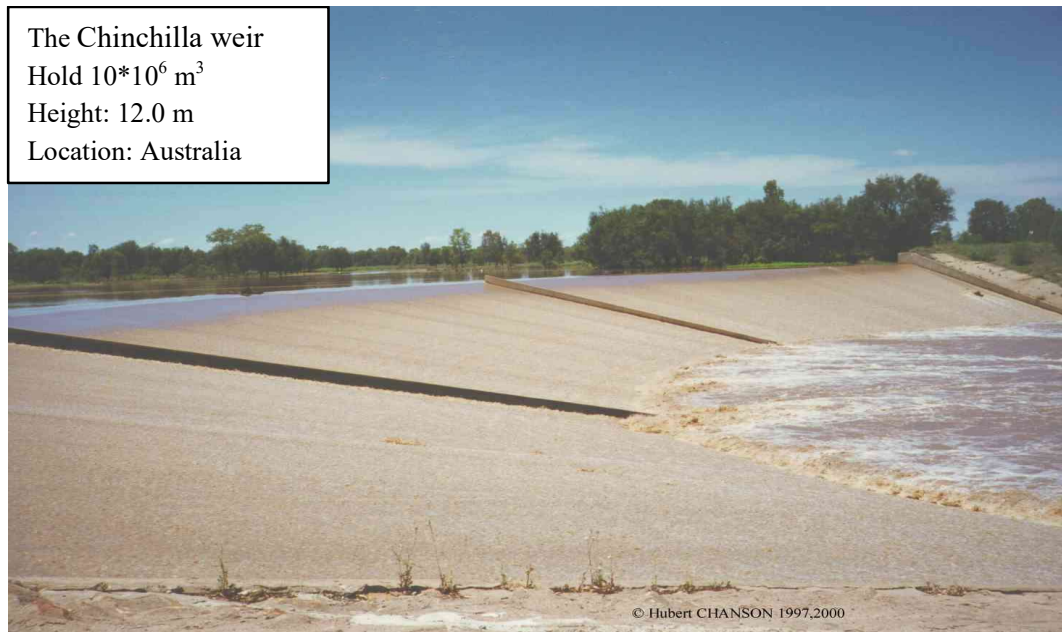


**Figure 1-7.** Minimum energy loss, Chinchilla weir, Australia, 1971

Link: [http://staff.civil.uq.edu.au/h.chanson/mel\\_weir.html](http://staff.civil.uq.edu.au/h.chanson/mel_weir.html)

### 1.3.2 Gabion stepped weir

A gabion stepped weir method consists of a rectangular basket or mesh which is filled with stone or rock. Gabion stepped weir extensively are used for retaining earth structures like embankment dams. The main reasons for extensive usage of gabions in comparison to the other construction materials are:

- Low cost
- High Flexibility and porosity(permeability)

One of the main advantages of the Gabion stepped weir in comparison to other methods is their higher porosity. The high porosity prevents any uplift pressure in steps and makes the embankment dams more stable.

Typical gabion basket has 0.5 to 1.0 m height, 0.5 to 1.0 m width and 2.0 to 4.0 m length. The basket or mesh of gabions is made of steel with zinc coating. Therefore quality and durability of gabions directly depending on mesh wire quality. The size of materials inside the gabions should be 1.0-1.5 times bigger than mesh size. The main disadvantages of gabions stepped weir are:

- Low resistance to the damage
- Stability on steep slopes

Also the sediment which is carried out with stream can affect the mesh gabion. Figures 1-8, 1-9 and 1-10 show the details of this method.

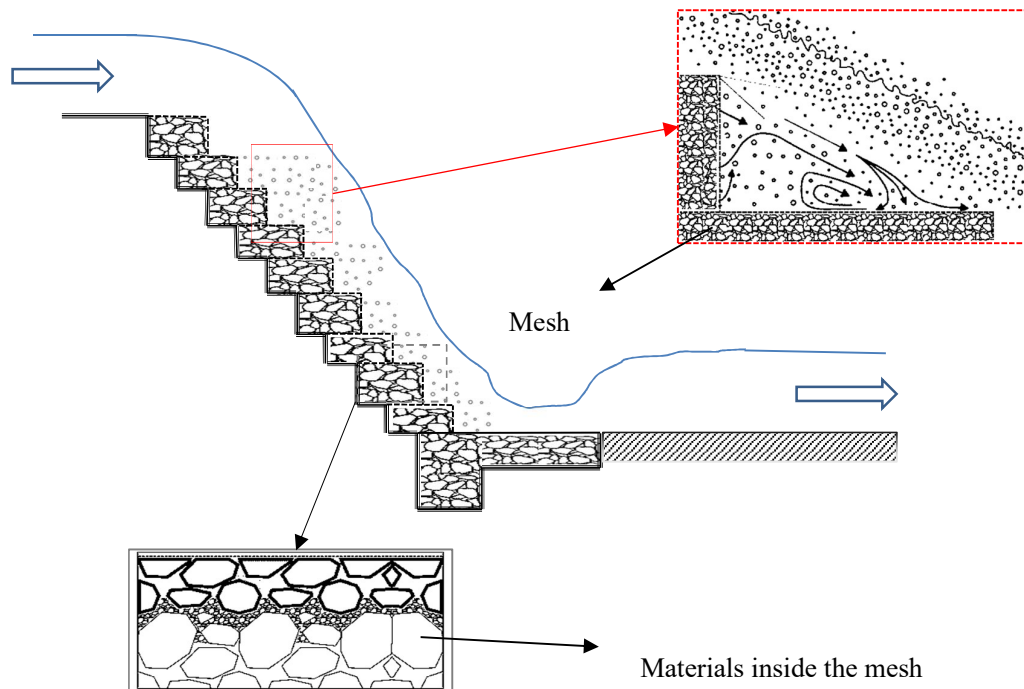


**Figure 1-8.** Gabion stepped weir



**Figure 1-9.** Gabion stepped weir, Pacific Pines, Australia, 2010

Link: [http://www.concrib.com.au/project\\_gallery/project\\_pacificpines.php](http://www.concrib.com.au/project_gallery/project_pacificpines.php)



**Figure 1-10.** Gabion stepped weir, Pacific Pines, Australia, 2010

Link: [http://www.concrib.com.au/project\\_gallery/project\\_pacificpines.php](http://www.concrib.com.au/project_gallery/project_pacificpines.php)

### 1.3.3 Site-cast concrete

The site-cast or cast-in-place concrete system is a roller compact concrete (RCC) method. This method was first time applied for overtopping protection in the beginning of 1980 and is in use during the last decades. This approach is used as the common method to protect slopes from overtopping flows in both concrete and embankment dams. The RCC can be constructed on formed or unformed steps. The typical thickness of the overlay is 0.2 to 0.4 m with the width of 2.5 m for proper evacuation. The advantages of this method are:

- Affordable
- Short construction time

Also in a construction of RCC the drainage should be considered between embankment dam and concrete to prevent any uplift pressure. One of the most important issues remaining in designing concrete stepped spillway is determining inception point of free-surface aeration. In order to determine the location of the inception point the following equations are suggested by Chanson (2013). Figure 1-11 shows the detail of this method.

$$(L_I / (h \times \cos \theta_0)) = 9.72 \times (\sin \theta_0)^{0.08} \times (q / \sqrt{g \times \sin \theta_0} \times (h \times \cos \theta_0)^3)^{0.71} \quad 1-11$$

$$(D_I / (h \times \cos \theta_0)) = (0.403 / (\sin \theta_0)^{0.04}) \times (q / \sqrt{g \times \sin \theta_0} \times (h \times \cos \theta_0)^3)^{0.59} \quad 1-12$$

$L_I$  [m] the inception distance from crest

$h$  [m] the step height  $\cong 0.2 - 0.9$  m

$L$  [m] the step width  $\cong 2.5$  m

$D_I$  [m] the flow depth at the inception point

$\theta_0$  [°] the angle between the pseudo-bottom formed by the step edges and the horizontal

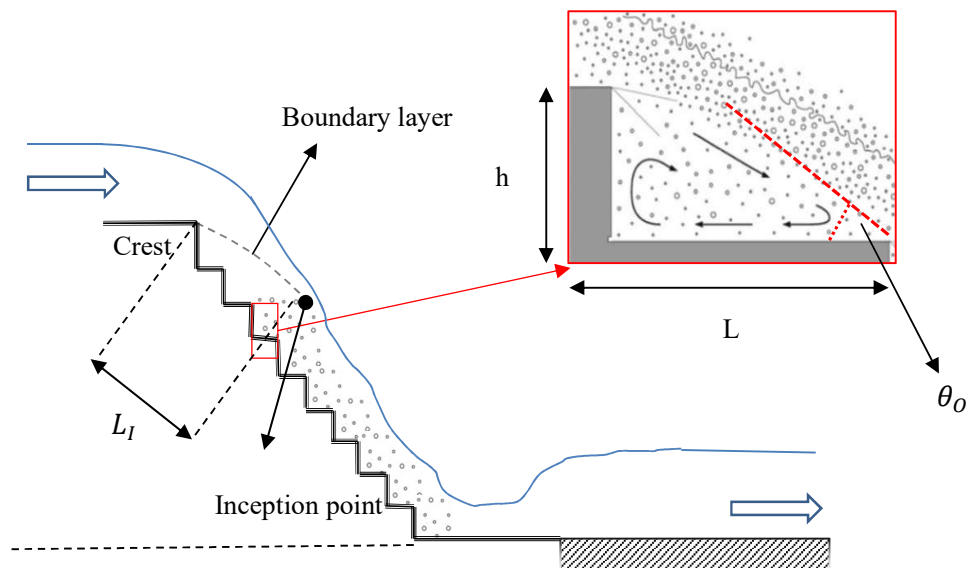


**Figure 1-11.** Site-cast concrete



**Figure 1-12.** Site-cast concrete, Georgia Dam, USA

Link: <http://www.agpeltz.com/rcc-projects/>



**Figure 1-13.** Site-cast concrete, Log Creek Dam, USA, 2012

Link: <http://cenews.com/article/8690/alternative-concrete-for-dams>

### 1.3.4 Pre-cast concrete

The method of pre-cast concrete or Articulating Concrete Blocks (ACBs) first time was implemented in the beginning of 1978. This system consists of individual pre-cast concrete blocks and are placed on the slopes to provide hard surface and protect any surface erosion. The advantages of this method in comparison to other methods are:

- Flexibility
- Short construction time

Furthermore, this method can be implemented in the two ways (Figure 1-14):

- Pre-cast concrete without overlapping
- Pre-cast concrete with overlapping

For a large discharge of overtopping flow, the blocks should be reinforced and tied to the adjacent blocks. To secure the maximum stability, drains must be placed in areas of sub-atmospheric pressure to relieve uplift pressures.

Figures 1-14a and 1-14b show more details about this method.

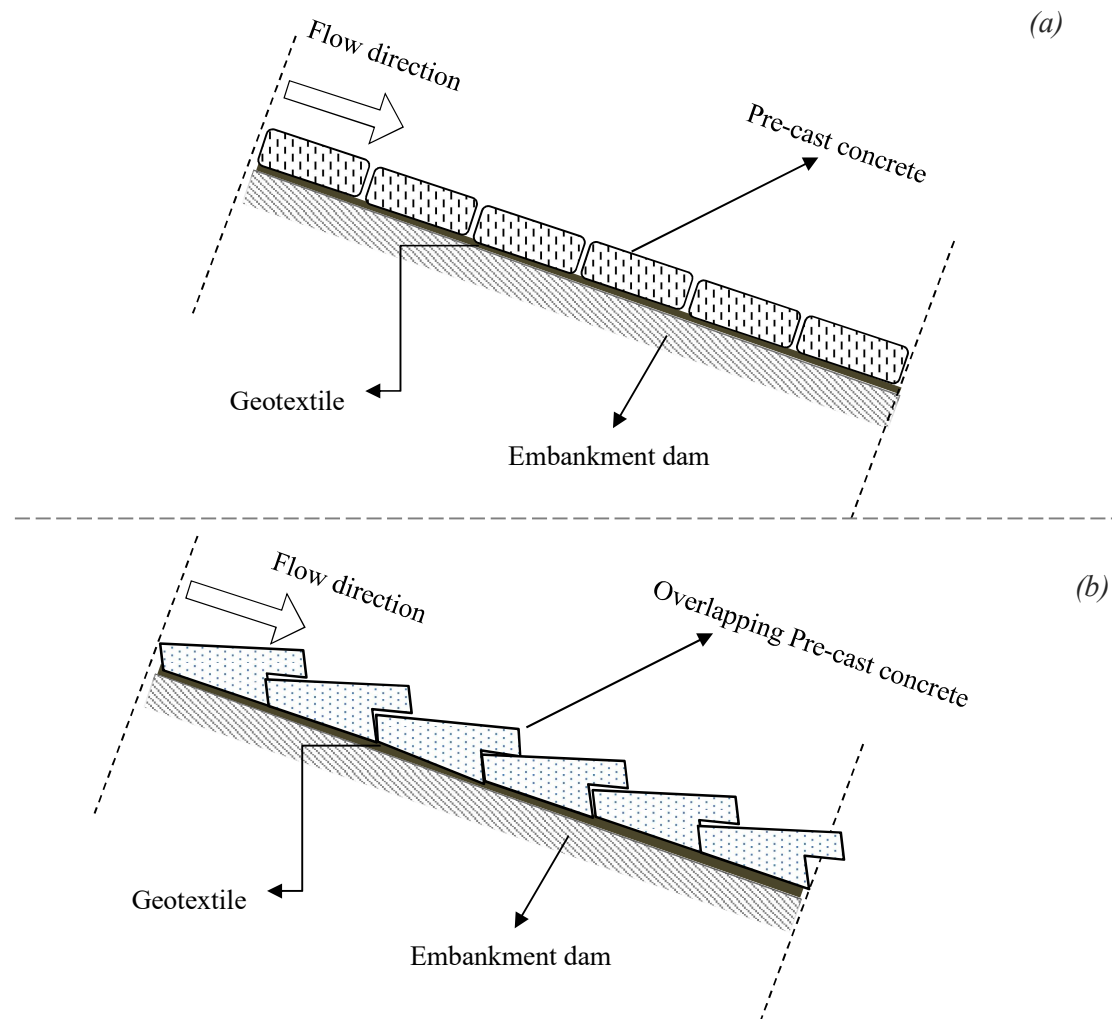


**Figure 1-14.** Pre-cast concrete: (a) without overlapping (b) with overlapping



**Figure 1-15.** Pre-cast concrete without overlapping, Klinkner Dam, USA, 2005

Link: <http://www.vernoncounty.org/lwcd/klinknerRepair.htm>



**Figure 1-16.** Pre-cast concrete with overlapping, Barriga Dam, Spain, 2008

Link: <http://www.damsafety.org>

---

# Chapter 2

## Empirical method to predict breach outflow hydrograph

---

### 2.1 Introduction

Two relationships to predict the peak outflow discharge and failure time for embankment dams which are failed by overtopping flow are introduced.

- In the first relationship dam failure time is calculated by using regression analysis on previous dam failure data. The accuracy of this relationship is improved by considering the influence of different type of fill material through a parameter named  $\delta$ .
- In the second relationship, the peak outflow discharge is calculated by using a new method. In this approach, the area under the hydrograph is split into three shapes and is superimposed to calculate the peak outflow discharge.

#### 2.1.1 Dataset collection and preparation

In the first step, a reliable dataset about dam failures from literature are collected. In this investigation, dam failures data are selected and gathered from different sources to have a certain variety in parameterization and modelling procedure. Then, a close scanning on all datasets is performed to pick up the best quality data that fit to our purpose for this study.

To set up worldwide dataset three main sources are used:

- The Singh V.P. et al (1998) dataset
- The Xu et al. (2009) dam failure data
- The Froehlich (2008) dataset

These data were scanned thoroughly to remove incomplete or duplicated data. Furthermore, only dams which were failed by overtopping failure are selected. These refined dataset construct the basis of this research and are used in the calibration, validation and regression analysis.

Tables 2-1 to 2-4 give a general overview of the selected dataset after data preparation.

**Table 2-1** List of the dam failure data for regression analysis

Dam name	Height of the dam[m]	Crest length [m]	Side slope	Storage [m <sup>3</sup> ]	Peak flow [m <sup>3</sup> /s]	Failure time [hr]	Type of failure
Grand Rapids <sup>1</sup>	7.5	3.7	01:01.5	2.20E+05	-	0.5	O
little creek usa <sup>1</sup>	26	-	-	1.73E+06	1330	0.34	O
Coadty <sup>2</sup>	11	262	-	3.10E+05	-	0.5	O
Cougar Creek <sup>4</sup>	11.1	21.7	-	3.00E+04	-	0.05	O
French Mich. <sup>1</sup>	14.2	34.3	0.97	3.90E+06	-	0.58	O or P
Big Bay Dam <sup>1</sup>	15.5	-	-	1.70E+07	-	0.9	O
Dells wisconsin <sup>1</sup>	18.3	292.6	-	1.30E+07	5440	0.7	O
Schaeffer, Colorado <sup>1</sup>	30.5	-	-	4.25E+06	-	0.5	O
Baldwin Hills <sup>1</sup>	21.3	59.6	0.31	9.10E+05	-	0.34	O or P
South Fork <sup>1</sup>	24.6	64	1.38	1.90E+07	-	0.75	O
Little Deer <sup>1</sup>	27.1	63.1	0.75	1.40E+06	-	0.34	O or P
Bradfield <sup>2</sup>	29	382	-	3.20E+06	1150	0.5	O or P
Hell Hole <sup>1</sup>	56.4	103.2	0.96	3.10E+07	-	0.75	O or P
Erindale canada <sup>4</sup>	10.5	-	-	1.30E+06	-	0.5	O
Lower Otay <sup>1</sup>	40	53.3	1.0	4.90E+07	-	1	O
Quail Creek <sup>1</sup>	21.3	56.6	0.1	3.10E+07	-	1	O or P
Wheat land no <sup>1</sup>	13.6	6.0	-	3.60E+08	-	2.5	O
Oakford Park Dam <sup>1</sup>	6.1	-	-	8.00E+06	-	1	O

O: Overtopping, P: Piping, 1: U.S.A, 2:U.K, 3: Brazil, 4: Canada

**Table 2-2.** List of the dam failure data to calibrate  $\delta$  in the failure time equations

Dam name	Type of the dam	Type of the fill material	Height of the dam [m]	Storage [m <sup>3</sup> ]	peak flow [m <sup>3</sup> /s]	Failure time [hr]	type of failure
Zhonghuaju <sup>5</sup>	HD	HE	16.0	1.4E+05	-	0.4	O
Frias <sup>8</sup>	FD	ME	15.0	2.5E+05	400	0.25	O
Qielinggou <sup>5</sup>	HD	HE	180	7.0E+05	2000	0.17	O
Yuanmen <sup>5</sup>	HD	HE	19.2	6.4E+06	-	0.5	O
Zuocun <sup>5</sup>	DC	HE	35.0	4.0E+07	23600	1.0	O
Wadi Qattarah <sup>7</sup>	HD	LE	28.0	4.8E+06	-	1.5	O
Chenyng <sup>5</sup>	HD	ME	12.0	4.3E+06	1200	1.83	O
Hatfield <sup>1</sup>	-	LE	12.3	6.8E+06	-	2.0	O
Hemet Dam <sup>1</sup>	DC	LE	6.1	8.6E+06	1600	3.0	O
Danghe <sup>5</sup>	DC	LE	46.0	1.6E+07	2500	30	O
Mammoth <sup>1</sup>	DC	ME	21.3	1.4E+07	2520	3.0	O
Machhu <sup>6</sup>	DC	HE	60.0	1.1E+08	7690	2.0	O

O: Overtopping, P: Piping, DC: dam with core, HD: Homogeneous dam, FD: concrete-faced dams, 1: U.S.A, 5: China, 6: India, 7: Libya, 8: Argentina

**Table 2-3.** List of dam failure data to validate the failure time and peak outflow equation

Dam name	Height of the Dam[m]	Crest length [m]	Side slope	Storage [m <sup>3</sup> ]	P.flow [m <sup>3</sup> /s]	Failure time [hr]	Type of failure
Hatfield <sup>1</sup>	6.8	-	-	1.2E+07	3400	2.0	O
Kelly barnes <sup>1</sup>	11.5	6.0	1:1	5.1E+05	680	0.5	O
Ireland No. 5 <sup>1</sup>	5.2	18	0.38	1.6E+05	-	0.5	O or P
Puddingstone <sup>1</sup>	15.2	-	-	6.2E+05	283.0	0.25	O
Hatchtown <sup>1</sup>	18.3	44.8	2.42	1.5E+07	-	1.0	O or P
Kaddam Dam <sup>6</sup>	31.0	3.3	-	1.4E+08	11000	1.0	O
Pierce Reservoir <sup>1</sup>	8.7	-	0.77	4.1E+06	-	1.0	O
Castlewood <sup>1</sup>	21.3	47.4	0.5	6.2E+06	-	0.5	O

O: Overtopping, P: Piping, 1: U.S.A, 6: India

**Table 2-4.** List of dam failure to calibrate  $\alpha$  and  $\beta$  parameters in the peak outflow equation

Dam name	Height of the Dam[m]	Storage [m <sup>3</sup> ]	Peak flow [m <sup>3</sup> /s]	Failure time[hr]	type of failure
Whitewater Brook <sup>1</sup>	19.0	5.18E+05	70.8	3.0	O
Bear Creek Dam <sup>1</sup>	132.3	1.8E+07	10821	0.855	O
Lake Latonka Dam <sup>1</sup>	13.0	1.6E+06	295	3.0	O
Horse Creek Dam <sup>1</sup>	16.8	2.1E+07	3890	3.0	O
Banqiao <sup>5</sup>	24.5	4.92E+08	78100	5.5	O
Kaila Dam <sup>6</sup>	23.1	1.39E+07	1690	4.0	O
Khadkawasla Dam <sup>6</sup>	31.3	8.76E+06	2780	4.0	O
Knife Lake Dam <sup>1</sup>	6.1	9.87E+06	1100	5.0	O
Lake Avalon Dam <sup>1</sup>	14.5	7.77E+06	2320	2.0	O
Shimantan <sup>5</sup>	25.0	9.44E+07	30000	5.5	O
buffalo creek north <sup>5</sup>	32.0	6.10E+05	1420	0.5	O
Frenchman Dam <sup>1</sup>	12.5	8.65E+06	1600	3.0	O

O: Overtopping, P: Piping, 1: U.S.A, 5: China, 6: India

## 2.2 Calculation of dam failure time

### 2.2.1 Literature review

Dam failure time is one of the most important parameters for predicting the breach outflow hydrograph in embankment dams. Any change in this parameter has a significant influence on the magnitude and shape of the outflow hydrograph.

Many researchers already worked on this issue and have found various relationships for predicting dam failure time based on regression analysis. MacDonald and Langridge-Monopolis (1984) relate dam failure time to the volume of soil eroded ( $V_{er}$ ). Froehlich (1995) related dam failure time either to the volume of water behind the dam or to the multiplication between height of the breach and volume of water behind the dam. And recently Froehlich (2008) considered the height of water ( $H_w$ ) along with the height of breach ( $H_b$ ) to find a regression relationship for calculating dam failure time.

These various works with a variety of relationships for defining the dam's failure time emphasize the importance of different dam breach parameters for predicting dam failure time.

**Table 2-5.** List of failure time equations ( $t_f$ )

Investigator	Equations
MacDonald and Langridge-Monopolis (1984)	$t_f = 0.0179(V_{er})^{0.364}$
Froehlich (1995)	$t_f = 0.00254V_w^{0.53}H_b^{-0.9}$
Reclamation (1988)	$t_f = 0.011B_{ave}$
Von Thun and Gillette (hard erosion)(1990)	$t_f = 0.02H_w + 0.25$
Von Thun and Gillette (easy erosion)(1990)	$t_f = 0.015H_w$
Froehlich (2008)	$t_f = 63.2(V_w/9.81H_b^2)^{0.5}$

### 2.2.2 New relationships for dam failure time

Dam failure time in embankment dams is depending on the type of the dams, kind of the failure, soil parameters, soil compaction, reservoir volume, height of the dam, height of the water behind the dam and many other conditions and parameters. Any change in either of these parameters can make sensible change in the breach formation time, maximum discharge of breach and shape of the dam breach. In order to find an accurate relationships for the breach formation time based on the regression method, we need some additional specific parameters in our dam failures data. Most important ones are:

- Height of the dam or height of the water behind dam ( $H_w$ )
- Volume of the reservoir ( $V_w$ )
- Dam failure time ( $t_f$ )

According to prepared dataset on dam failures data, only 50 dams satisfy these requirements and as a result only these dams are considered for further calculation. Furthermore, these selected dams are divided into three different groups for a more accurate analysis:

- The first group is used to find the relationship for the regression formula.
- The dams in the second group are used to define the soil type coefficient.
- The last group is kept to be used later for validating the relationships.

In the group one, regression analysis has been done between all dam failure parameters, as these are:

- Height of the dam ( $H_d$ )
- Length of the crest ( $L_C$ )
- Width of the crest ( $W_{CST}$ )
- Height of the water behind the dam ( $H_w$ )
- Volume of the water behind dam ( $V_w$ )

Based on this analysis, we find out that ( $\frac{V_w}{H_w}$ ) has a good relation with dam failure time ( $t_f$ ). Furthermore, we find out that we can increase the accuracy of the new relationship by using additional two different regression equations based on the parameter ( $\frac{V_w}{H_w}$ ).

These two relationships are given in Equations 2-1 and 2-2

**( $V_w/H_w$ )  $\leq$  1.0:**

$$t_f = 0.1214 \ln\left(\frac{V_w}{H_w}\right) + 0.79 \quad 2-1$$

**( $V_w/H_w$ )  $>$  1.0:**

$$t_f = 0.5063 \ln\left(\frac{V_w}{H_w}\right) + 0.85 \quad 2-2$$

Here,  $t_f$  [Hour] is the failure time of embankment dam,  $V_w$  [ $10^6 \times m^3$ ] is the reservoir volume and  $H_w$  [m] is the height of the water behind the dam.

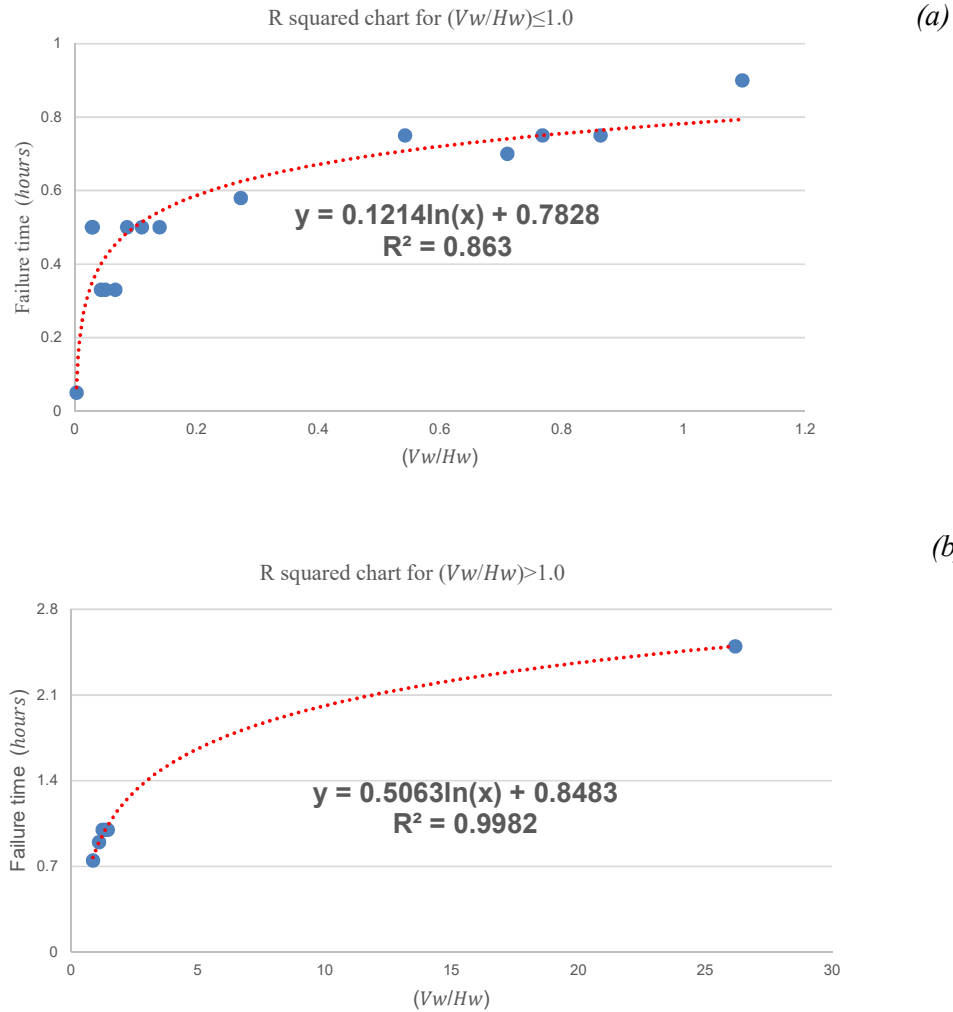


**Figure 2-1.** R square value : (a)  $(Vw/Hw) \leq 1.0$  (b)  $(Vw/Hw) > 1.0$

### 2.2.3 New approach to increase the accuracy of dam failure time equations

In the previous section, the main relationships for the dam failure time (Equations 2-1 and 2-2) were found. These relationships are quite similar to other previous dam failure relationships which were suggested by many other researches. But the most important factor which has significant influence on these equations is the erosion rate of the dam. This factor directly depends on:

- Type of the fill material
- Type of the dam

Therefore, we consider this factor to improve the accuracy of the aforementioned equations (Equations 2-1 and 2-2).

In the following, this technique is explained in more detail.

### Different type of the fill material

In this study, different types of the fill material and dams are defined based on the previous works on the embankment dam erosion fields. One of the essential one is the work of Y. Xu et al. (2009). They proposed two categories for soil erosion in all embankment dams.

- The first category concerns about the dam material composition.
- The second category concerns about the compaction effects.

The compositions of the dam's material have great influence on the erosion rate. For instance rock-fill dams and clay dams have medium to low erosion rate while dams with sands and clay show high to medium erosion. Y. Xu et al. (2009) proposed the second category for considering compaction effects on the soil erodibility.

Furthermore, this issue was discussed by Wan et al. (2004). They indicated that compaction degree has a great influence on the erosion rate parameter especially in the soils with fine materials.

Here in, to improve the accuracy of the new relationships, we consider different type of the soil and different type of the dam in those equations through a new parameter named  $\delta$ . Equations 2-3 and 2-4, are the new relationships where  $\delta$  is included and play the role of erodibility of the dam at failure time. It means that by increasing or decreasing  $\delta$ , failure time ( $t_f$ ) will be increased or decrease respectively.

Different categories of soil erodibility are introduced (high erosion, medium erosion, low erosion) according to Xu et al. (2009). Here, we present two different soil types as high erodibility and low erodibility. The low erosion category, furthermore, contains medium erosion and low erosion.

**(Vw/Hw) ≤ 1.0**

$$t_f = \delta(0.1214 \ln \left( \frac{Vw}{Hw} \right) + 0.79) \quad 2-3$$

**(Vw/Hw) > 1.0**

$$t_f = \delta(0.5063 \ln \left( \frac{Vw}{Hw} \right) + 0.85) \quad 2-4$$

Here,  $\delta$  is the coefficient for defining dam type (Table 2-6).

The optimum value for  $\delta$  parameter is estimated by calibration analysis for each type of the dam. Table 2-6 presents the results of this step.

**Table 2-6.** Calculation of dam coefficient ( $\delta$ ) for different type of dams

Type of the Dam	Coefficient range	Suggested
Dam without core and high erosion	0.5-2.0	1.0
Dam without core with low erosion	2.0-3.0	2.0
Dam with core with low erosion	2.0-3.0	3.0
Dam with core with high erosion	2.0-3.0	2.0

## 2.3 Calculation of peak outflow discharge

### 2.3.1 Literature review

In the second part, the peak outflow discharge by using the aforementioned dataset is calculated. The peak outflow discharge calculation is very important for embankment dam failure in our study. Many methods use regression analysis to predict breach peak outflow discharge. These relationships vary from each other by considering different dam breach parameters as the main reason for their failure relationships.

Table 2-7 summarizes some of the most important relationships in this regard. Here, it can be seen that relationships like Kirkpatrick (1977), SCS (1981), USBR (1982) or Singh (1982) attempt to relate height of the water behind a dam at failure time ( $H_w$ ) to the peak outflow discharge ( $Q_p$ ). On the other hand, some other relationships like the ones given by Evans (1986) mainly relate volume of the water behind a dam at failure time ( $V_w$ ) to the peak outflow discharge ( $Q_p$ ), while Hagen (1982) models focuses on the multiplication between height of the water behind a dam and volume of the water at failure time ( $V_w H_w$ ) as the main reason for the peak outflow discharge ( $Q_p$ ).

Our results indicate that most of these relationships are not accounting for the overall behavior. Moreover, a regression approach was applied to obtain a more appropriate relationship for calculating the peak outflow discharge. The final results reveal that regression analysis is not a proper solution. Therefore, a new method is employed.

**Table 2-7.** A list of the existing peak outflow discharge equations

Investigator	Equations
Kirkpatrick (1977)	$Q_p = 1.268(H_w + 0.3)^{2.5}$
SCS (1981) for dams >31.4m	$Q_p = 16.6(H_w)^{1.85}$
USBR (1982)	$Q_p = 19.1(H_w)^{1.85}$
Singh (1982)	$Q_p = 13.4(H_d)^{1.85}$
Evans (1986)	$Q_p = 0.72(V_w)^{0.53}$
Hagen (1986)	$Q_p = 1.205(H_w V_w)^{0.48}$
MacDonald and Langridge-Monopolis (1984)	$Q_p = 3.85(H_w V_w)^{0.411}$
Froehlich (1995)	$Q_p = 0.607(H_w^{1.24} V_w^{0.295})^{0.411}$
BEF formula	$Q_p = 2.8(H_w)^{2.5}$
Froehlich (2008)	$Q_p = 3.1B_{avg} H_w^{1.5} (Y_Q / (Y_Q + t_f \sqrt{H_w}))^3$

### 2.3.2 New method for calculating the peak outflow discharge

The outflow hydrograph of embankment dams depends on parameters like type of the dam, dam failure time, water level in the reservoir and several other parameters. As it is not possible to consider all of these parameters in one relationship, some simplifications are made. Therefore one assumption is made by splitting the breach outflow hydrograph into the 3 primitive shapes as illustrated in Figure 2-2.

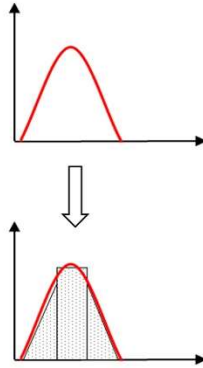


**Figure 2-2.** Convert hydrograph to simplified shapes

According to the Figure 2-2, these three primitive shapes are:

- Two similar triangular shapes
- One rectangular shape

It is assumed that the total areas of these three shapes are equal to the total area of the real outflow hydrograph. Therefore, any dam breach outflow hydrograph could be simplified into simple volume shapes which can be handled mathematically much easier.

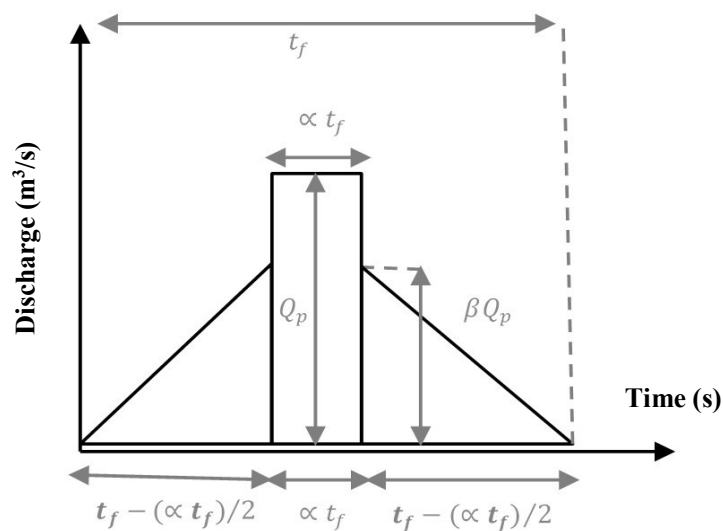


**Figure 2-3.** Simplified hydrograph

Figure 2-3 shows the concept of the simplification procedure where each outflow hydrograph is divided into simpler forms by using two triangular and one rectangular shapes.

Here, the height of the rectangular shape shows the maximum discharge of the breach outflow hydrograph ( $Q_p$ ) and the total width of the three shapes shows the duration of the hydrograph ( $t_f$ ).

In this new hydrograph, different shapes in the breach outflow hydrograph can be represented by changing in the height and width of the previously defined geometrical objects, as shown in the Figure 2-3 and Equations 2-5 to 2-8.

$$\text{Height of rectangle} = Q_p \quad 2-5$$

$$\text{Height of triangular shape} = \beta Q_p \quad 2-6$$

$$\text{Width of rectangular shape} = \alpha t_f \quad 2-7$$

$$\text{Width of triangular shape} = t_f - (\alpha t_f)/2 \quad 2-8$$

Here:

$\beta$  is the rate of change in the height of the outflow hydrograph ( $0 \leq \beta \leq 1.0$ )

$\alpha$  is the rate of change in the width of the outflow hydrograph ( $0 \leq \alpha \leq 1.0$ )

Furthermore, it is assumed that the area under the hydrograph is equal to the reservoir volume of the water behind the dam. This implies that the total sum areas under the new hydrograph (rectangular and triangular shapes) should be equal to the reservoir volume.

Therefore, the peak outflow discharge can be calculated based on the Equation 2-9.

$$Q_p = \frac{2V_w}{t_f(2\alpha + \beta - \alpha\beta)} \quad 2-9$$

In the Equation 2-9, known parameters are,  $V_w$  [ $m^3$ ] and  $t_f$  [s] while unknown parameters are  $Q_p$ ,  $\alpha$  and  $\beta$ .

To calculate  $\alpha$  and  $\beta$  parameters the calibration and sensitivity analysis are used based on the previous dam failures data. Here, the optimum value for these two parameters are given in the Table 2-8.

**Table 2-8.** Calibrate  $\alpha$  and  $\beta$  for the peak outflow discharge

Coefficient	Value	Suggested
$\alpha$	0.05-0.1	0.1
$\beta$	0.9-1.0	1.0

Based on the calibrated parameters which were mentioned in the Table 2-8, the final breach outflow hydrograph can be illustrated in the following figure.

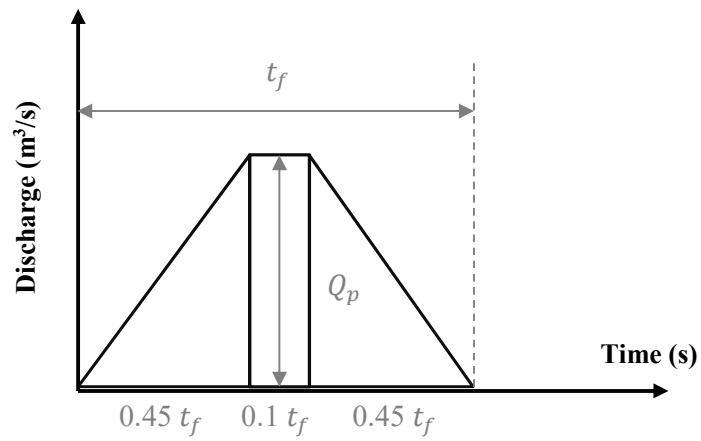


**Figure 2-4.** Simplified hydrograph based on the calibrated parameters

## 2.4 Validation of peak outflow discharge and failure time equations

The final step in this chapter is to validate the peak outflow discharge equation ( $Q_p$ ) and failure time equations ( $t_f$ ) for the same dam. The validation dataset for this step are taken from the IMPACT project (Morris et al. (2008)), the Chaq-Chaq dam (K.Abdulrahman (2014)) and the 12<sup>th</sup> International ICOLD Benchmark Workshop (Zenz et al. (2013)).

### 2.4.1 IMPACT project

The IMPACT project (Morris et al. (2008)) is one of the well-known large scale dam break projects which have been done in the Norway in 2002. In this project some dam failure parameters like outflow discharge, water level, pure pressure of water are measured and recorded during failure time. In this paper, Test # 2-2002 is selected for validation purposes. The parameters regarding this test are given in Tables 2-9 and 2-10.



**Figure 2-5:** A picture from the IMPACT project area

**Table 2-9.** Dam failure data for Test # 2-2002 dam

Name	Soil type	Storage volume [m <sup>3</sup> ]	H[m]
Test # 2-2002	Non-cohesive	0.09×10 <sup>6</sup>	5.0

**Table 2-10.** Measurement of failure parameter for Test # 2-2002

Name	$Q_p$ [m <sup>3</sup> /s]	$t_f$ [h]	$V_w/h_w$
Test # 2-2002	130	0.34	0.018

### 2.4.1.1 Calculate outflow hydrograph of IMPACT dam failure by using new relationship

Based on the information given in the Table 2-9, ( $V_w/H_w$ ) is equal 0.018, as shown in the following:

$$\frac{V_w}{H_w} = \frac{0.09}{5.0} = 0.018$$

The result of this ratio is less than 1, therefore Parameter  $\delta$  should be considered 1.0 (Table 2-6). Furthermore,  $\alpha$  and  $\beta$  parameters are equal to 0.1 and 1.0 respectively based on the Table 2-8.

Finally, the breach peak outflow discharge ( $Q_p$ ) and dam failure time ( $t_f$ ) are calculated based on the Equations 2-3 and 2-9 as shown in the following.

$$t_f = \delta \left( 0.1214 \ln \left( \frac{V_w}{H_w} \right) + 0.79 \right) = 1.0(0.1214 \ln(0.018) + 0.79) = 0.31 \text{ [Hour]}$$

$$Q_p = \frac{2V_w}{t_f(2\alpha + \beta - \alpha\beta)} = \frac{2 \times 90,000}{0.31 \times 3600 \times (1.1)} = 147 \left[ \frac{\text{m}^3}{\text{s}} \right]$$

The final results are shown in the Table 2-11.

**Table 2-11.** Calculated results for the IMPACT project using the new formulas

Name	$\delta$	$\alpha_{Q_p}$	$\beta_{Q_p}$	$t_f$ [h]	$Q_p$ [ $\frac{\text{m}^3}{\text{s}}$ ]
Test # 2-2002	1.0	0.1	1.0	0.31	147

It is additionally possible to draw the breach outflow hydrograph for the IMPACT test by using Equations 2-5 to 2-8, as shown in the Figure 2-6.

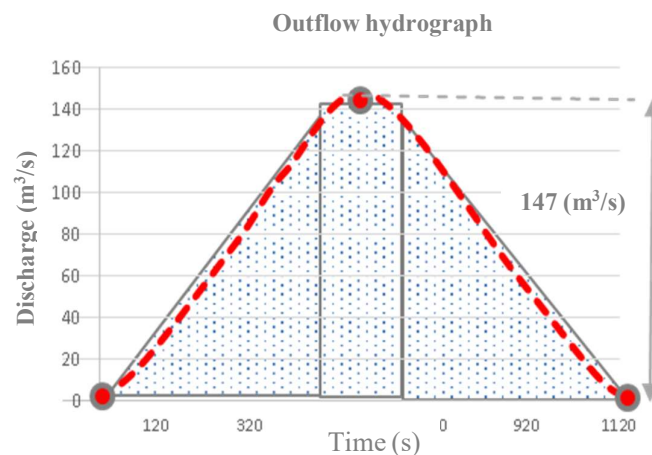


**Figure 2-6.** New formula result for the IMPACT test

### 2.4.1.2 Compare results of new relationships with other studies

For evaluating the accuracy of the new relationships, the final results are compared with the measurement results and result of six other relationships. This comparison and validation results are given in the Table 2-12.

**Table 2-12.** Compare results of new relationships with other studies for the IMPACT project

Name	$Q_p$ [m <sup>3</sup> /s]	$t_f$ [h]	$V_w$ [m <sup>3</sup> × 10 <sup>3</sup> ]
Measurement Results(IMPACT)	130	0.34	80.0
New Relationships_2015	147	0.31	90.0
Froehlich (2008)	146	0.34	89.0
MacDonald and Langridge-Monopolis(1984)	821	0.17	244.0
USBR(1982)	375	0.165	111.0
SCS (1981)	326	-	-
Froehlich (1995)	129	0.25	58.0
Von Thun and Gillette (1990)	-	0.1	
BEF formula	156	-	-

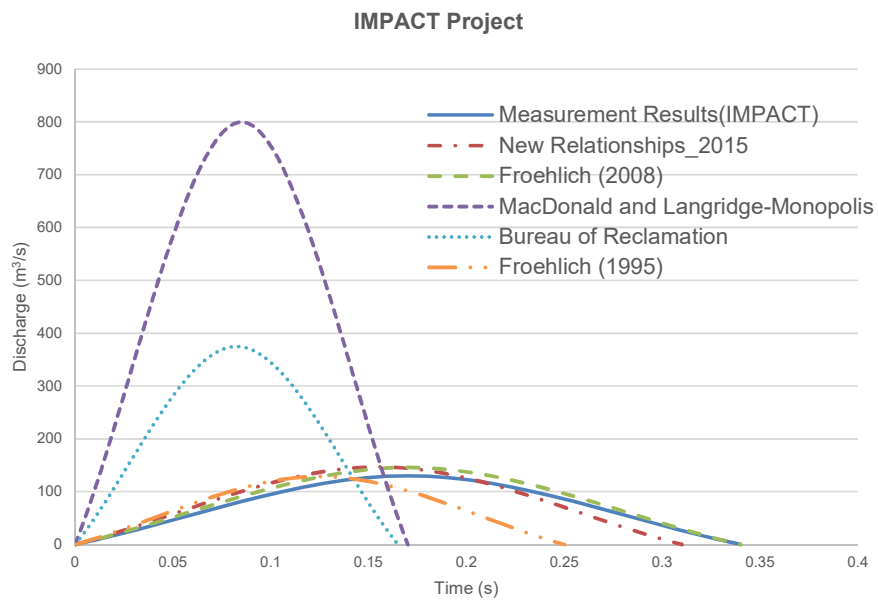


**Figure 2-7.** Comparison of gained results for the IMPACT project

Table 2-12 and Figure 2-7 show that the new relationships give good approximations in comparison to other relationships like Froehlich (2008) and (1995).

## 2.4.2 Chaq-Chaq Dam failure

The Chaq-Chaq dam (K.Abdulrahman. (2014)) is located in north east of Iraq. This dam is a zoned earth dam of central clay core with gravelly shell. This dam failed on 4<sup>th</sup> February 2006 due to overtopping flow, fortunately, this dam is located far from the populated area. Therefore, no person injured during this dam failure. The main reasons for the Chaq-Chaq dam failure were recognized as the spillway construction and low compaction in some part of this dam. Table 2-13 shows the general dam parameters and Table 2-14 shows measurement dam failure parameters.



**Figure 2-8.** Chaq-Chaq dam (K.Abdulrahman. (2014))

**Table 2-13.** Dam failure parameters for the Chaq-Chaq Dam

Name	Soil type	Storage volume [m <sup>3</sup> ]	H[m]
Chaq-Chaq	hard erosion	$2.55 \times 10^6$	14.5

**Table 2-14.** Measurement failure parameter for the Chaq-Chaq Dam

Name	$Q_p$ [m <sup>3</sup> /s]	$t_f$ [h]	$V_w/h_w$
Chaq-Chaq	930	1.0-1.3	0.175

### 2.4.2.1 Calculate outflow hydrograph of The Chaq-Chaq Dam failure by using new relationship

The breach outflow hydrograph by using the new formula are calculated. According to the data given in the Table 2-13, ( $V_w/H_w$ ) is equal to 0.175 and soil type is hard erosion which means that parameter  $\delta$  should be considered equal to 2.0 (Table 2-6). The  $\alpha$  and  $\beta$  parameters are equal to 0.1 and 1.0, respectively (Table 2-8). Based on these parameters, the breach peak outflow ( $Q_p$ ) and dam failure time ( $t_f$ ) are calculated and presented in the Table 2-15.

**Table 2-15.** Calculated result of new formula for Chaq-Chaq dam

Name	$\delta$	$\alpha_{Q_p}$	$\beta_{Q_p}$	$t_f$ [h]	$Q_p$ [ $\frac{m^3}{s}$ ]
Chaq-Chaq	2.0	0.1	1.0	1.16	1110

### 2.4.2.2 Compare results of new relationships with other studies

To evaluate the accuracy of the new relationships, the final results are compared against the measurement results and the results of six other relationships. Table 2-16 shows the results of this comparison.

**Table 2-16.** Compare results of the new relationships with other studies for the Chaq-Chaq dam

Name	$Q_p$ [m <sup>3</sup> /s]	$t_f$ [h]	$V_w$ [m <sup>3</sup> ×10 <sup>6</sup> ]
Measurement Results(Chaq-Chaq Dam)	930	1.0-1.3	2.1
New Relationships_2015	1110	1.16	2.55
Froehlich (2008)	-	0.61	-
MacDonald and Langridge-Monopolis(1984)	5051	0.51	4.6
USBR(1982)	2688	0.48	2.2
SCS (1981)	2336	-	-
Froehlich (1995)	1297	0.65	1.3
Von Thun and Gillette (1990)	-	0.54	-
BEF formula	2241	-	-

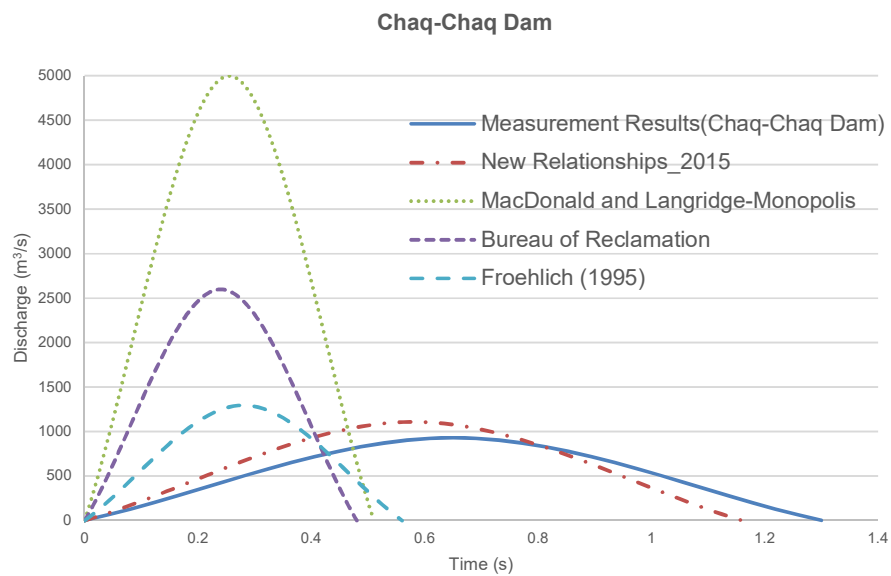


**Figure 2-9.** Comparison of gained results for the Chaq-Chaq dam

Table 2-16 and Figure 2-9 show that the new relationships give a higher accuracy and a better prediction in comparison to the other methods.

### 2.4.3 ICOLD Benchmark workshop

12<sup>th</sup> International ICOLD Benchmark Workshop (Zenz et al. (2013)) was held in Austria in 2013. In this workshop, homogeneous clay fill dam which was constructed in mountains was investigated (Table 2-17). This dam directly located above a highly populated area. They assumed overtopping failure taking place on this dam because of a heavy snowmelt. In this workshop, each participant should calculate the breach outflow hydrograph for this embankment dam failure. Table 2-17 and 2-18 show the dam failure parameters of this dam.

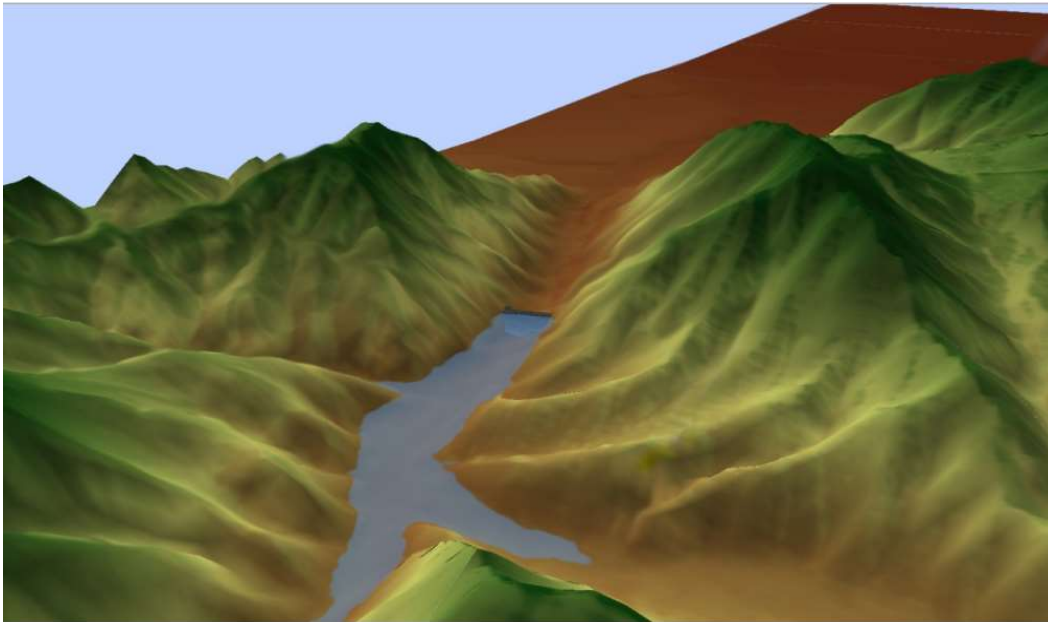


**Figure 2-10.** A hypothetical image of the dam given in the ICOLD Benchmark Workshop

**Table 2-17.** Dam failure data from ICOLD Benchmark Workshop

Name	Soil type	Storage volume [m <sup>3</sup> ]	H[m]
clay fill	hard erosion	38.0×10 <sup>6</sup>	61.0

**Table 2-18.** Failure parameter given by formulator for ICOLD Benchmark Workshop

Name	Q <sub>p</sub> [m <sup>3</sup> /s]	t <sub>f</sub> [h]	V <sub>w</sub> /h <sub>w</sub>
clay fill	11500	1.5	0.63

#### 2.4.3.1 Calculate outflow hydrograph of ICOLD Benchmark Workshop dam failure by using new relationship

The breach outflow hydrograph of this dam is calculated by using our new formula. According to the data given in the Table 2-17, ( $V_w/H_w$ ) can be considered 0.63. The soil type is hard erosion which means that parameter  $\delta$  should be considered equal to 2.0 (Table 2-6).  $\alpha$  and  $\beta$  Parameters are equal to 0.1 and 1.0, respectively (Table 2-8). Based on these parameters, the breach peak outflow ( $Q_p$ ) and dam failure time ( $t_f$ ) are calculated and presented in Table 2-19.

**Table 2-19.** Calculated result of new formula

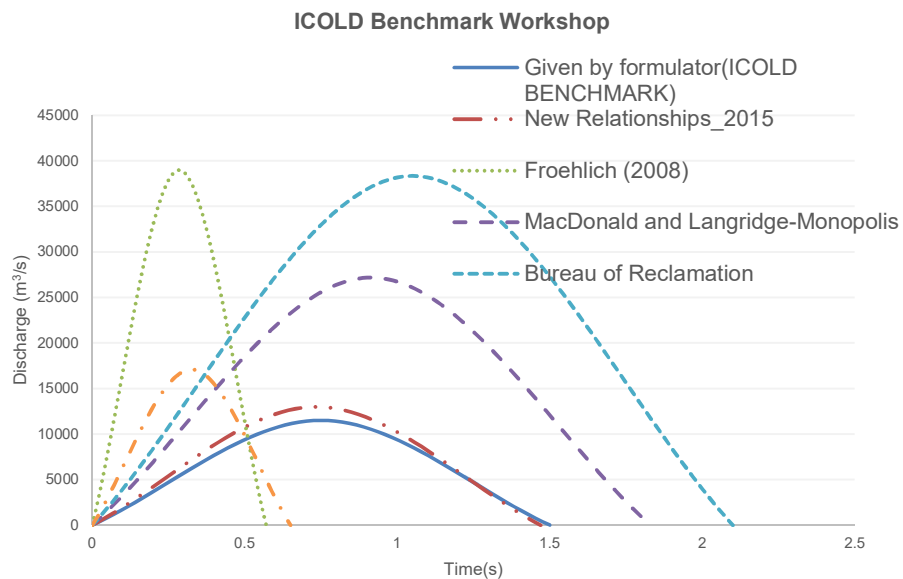
Name	$\delta$	$\alpha_{Q_p}$	$\beta_{Q_p}$	$t_f$ [h]	$Q_p$ [ $\frac{m^3}{s}$ ]
clay fill	2.0	0.1	1.0	1.47	13000

#### 2.4.3.2 Compare results of new relationships with other studies

For evaluating the accuracy of new the relationships, the final results are compared with the results of six other relationships. Table 2-20 shows all of these results against each other.

**Table 2-20.** Compare results of new relationships with other studies

Name	$Q_p$ [ $m^3/s$ ]	$t_f$ [h]	$V_w$ [ $m^3 \times 10^6$ ]
Given by formulator(ICOLD Benchmark Workshop)	11500	1.5	31.0
New Relationships_2015	13000	1.47	38.0
Froehlich (2008)	39000	0.57	40.0
MacDonald and Langridge-Monopolis	27789	1.83	89.0
USBR(1982)	38361	2.1	145.0
SCS (1981)	33340	-	-
Froehlich (1995)	17101	0.65	20.0
Von Thun and Gillette (1990)	-	1.47	-
BEF formula	81373	-	-

**Figure 2-11.** Comparison of gained results for ICOLD Benchmark Workshop

This table and figure (Table 2-20 and Figure 2-11) obviously show that our predicted values are very close to the formulator results.

### 2.4.4 Comparison all validation

In this part, in order to evaluate the accuracy of the new relationships all of the calculated results from the previous sections (sections 2.4.1, 2.4.2 and 2.4.3) are compared against the measurement relevant results. These comparisons are shown in the Figure 2-12.

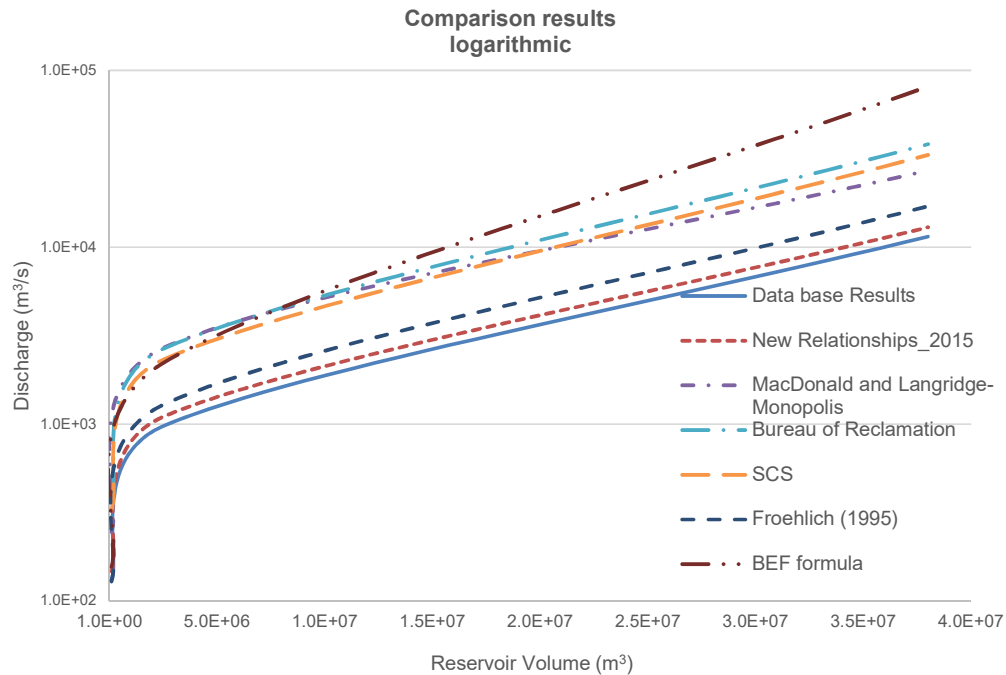


**Figure 2-12.** Comparison results of all equations

This figure shows that the new relationships give a higher accuracy and a better prediction in comparison to the other relationships.

In general, the most important reasons for increasing the accuracy of the new relationships in comparison to the previous relationships can be summarized as:

- In the new relationships, different type of fill material and different type of the dam are considered in the dam failure time equations through a parameter named  $\delta$ .
- In the new relationships, it is assumed that the whole reservoir volume becomes empty during dam failure time. This assumption control results in the peak outflow discharge equation given as below:

$$\sum_{i=1}^3 A_i = V_w$$

- In the new relationships, failure time is considered at the peak outflow equation (Equation 2-9). Therefore, the breach outflow hydrograph has to balance between peak outflow discharge and dam failure time. It means that by increasing failure time peak outflow discharge decrease and by decreasing failure time peak outflow discharge increase.

# Chapter 3

## Numerical modelling of dam overflow

---

### 3.1 Introduction

During the last decades, Computational Fluid Dynamics (CFD) have been developed rapidly and became the main procedure to model fluid flow in open channels or pressurized water flows. The main advantages of such methods compared to other methods like laboratory and experimental methods are:

- Reducing calculation time
- Reducing cost to build a model
- Handling complicate geometries
- Ability to analyze various boundary conditions

Computational Fluid Dynamics (CFD) are normally used to model fluid flow in open channels and pipes by solving governing equations like Navier-Stokes, shallow water or Saint-Venant with numerical algorithms. The first theory about CFD modelling has been suggested by John von Neumann in 1940 which contains novel ideas about modern CFD modelling. The first digital numerical modelling for the open channel flows was published in 1980 by U.S. Army Corp of Engineers (USACE). Afterwards, different software like ANSYS, DHI and TELEMAC were developed to calculate free-surface and pressurized flow for two and/or three dimensional modelling. In general, CFD methods follow four basic steps to model fluid flow in the open channels and pipes:

- Geometry specification
- Grid generation
- Algorithm to solve governing equations
- Post-processing and interpretation results

In these steps, first geometry is defined and then grids are generated to divide the geometry into individual nodes and elements. Furthermore, the governing equations are solved within the algorithm step. Finally, in the post-processing step the final results are displayed graphically as a chart or animation. In the next sections, the Saint-Venant equation along with finite difference methods are explained in more detail.

**Table 3-1.** Different equations and algorithms for modelling fluid behavior

Governing equations of fluid	Navier-Stokes (3- Dimensional)
	Shallow water (2- Dimensional)
	<b>Saint-Venant (1-Dimensional)</b>
Algorithms	Finite element (FEM)
	Finite volume (FVM)
	<b>Finite difference (FDM)</b>
	Method of characteristics (MOC)

### 3.1.1 Partial differential equation (PDE)

#### 3.1.1.1 Introduction

Differential equations are a set of relationships which contain unknown functions with their derivatives (rate of the function changes). They are normally divided into two groups based on their unknown variables:

- Ordinary differential equation (ODE)
- Partial differential equation (PDE)

Ordinary differential equations (ODEs) are referred to those differential equations which relate one independent variable (like X) to its derivative (dx) while partial differential equations (PDEs) are defined as equations with more than one variable (like X, Y...). These equations have a very wide range of application in science, and many natural laws can be modelled by using them. The general form of partial differential equations can be defined as:

$$A \frac{\partial^2 u}{\partial x^2} + B \frac{\partial^2 u}{\partial x \partial y} + C \frac{\partial^2 u}{\partial y^2} + f \left( u, x, y, \frac{\partial u}{\partial x}, \frac{\partial u}{\partial y} \right) = 0.0 \quad 3-1$$

According to Hoffman (2001), general form of PDEs can be classified into the three main categories based on the A, B and C values and their relationships:

- The first category is defined when these three variables satisfy the elliptic equation:

$$B^2 - 4AC < 0.0$$

Then Equation 3-1 can be written as:

$$\frac{\partial^2 u}{\partial x^2} + \frac{\partial^2 u}{\partial t^2} = 0.0 \quad 3-2$$

Which is the form of Laplace equation.

- Then the second form is parabolic equation if A, B and C satisfy below equation:

$$B^2 - 4AC = 0.0$$

Then the Equation 3-1 can be defined as:

$$\frac{\partial^2 u}{\partial x^2} = K \frac{\partial u}{\partial t} \quad 3-3$$

Which is similar to the heat equation or diffusion equation.

- Finally, if A, B and C satisfy hyperbolic equation then:

$$B^2 - 4AC > 0.0$$

And, Equation 3-1 can be written as:

$$\frac{\partial^2 u}{\partial x^2} = v^2 \frac{\partial^2 u}{\partial t^2} \quad 3-4$$

The last category is in the form of wave equation.

The Saint-Venant equation is written as a set of hyperbolic partial differential equation.

### 3.1.1.2 Solve partial differential equation

In general, there are two main approaches to solve partial differential equations:

- The mathematical approach
- The numerical approach

In the mathematical approach, a simple form of ordinary differential equations (ODEs) like linear equations with constant coefficients can be solved while in the numerical method, partial differential equations (PDEs) are solved based on an approximation value. It means that in this method by replacing the derivative function with the approximation value and changing partial differential equations to the simple form of differential equations (algebraic equations), the unknown parameters can be calculated.

The first numerical method is suggested and used by John von Neumann (1940) in order to solve partial differential equations. During the last sixty years, many numerical solutions are suggested for solving PDE, like finite difference, finite volume, finite element, etc.

In this research finite difference method (FDM) has been selected and used to solve the Saint-Venant equation for modelling embankment dam failure due to overtopping flow.

### 3.1.2 Finite difference method (FDM)

Finite difference method is one of the simplest and oldest numerical solutions to solve differential equations. It was proposed first by Peregrine (1966), for solving the regularized long wave (RLW) equation. Furthermore, other scientists like Vliegenthart (1971), Eilbeck (1975) and Greig (1976) did many investigations in this field and developed finite difference method.

Generally, finite difference method (FDM) solves partial differential equations by replacing the approximate differential values with derivatives in the PDE equations and change them into the simple form of equations like ODE equations or algebraic equations. Finite difference method (FDM) needs to discretize related topography into the points with equal distance as shown in the Figure 3-1. The main advantages of this kind of meshing are:

- Easy constructing
- Fast calculation along with higher accuracy

But the major disadvantage of this kind of mesh is related to modelling the complex geometries. Therefore, to model simple geometry like embankment dam, this type of mesh is an appropriate solution.

In this study, the finite difference method is employed to solve the one-dimensional Saint-Venant equation.

#### 3.1.2.1 Different schemes of the finite difference method

As mentioned in the previous part, to solve PDEs with FDM method, approximate parameters are substituted in PDEs to convert them into the algebraic equations. In the following some of these finite difference schemes are formulated based on time ( $\Delta t$ ) and location ( $\Delta X$ ):

Forward difference space and time scheme:

$$\frac{\partial U}{\partial X} = U_{X(\text{forward in space})} \quad \frac{U_{i+1}^j - U_i^j}{\Delta X} \quad 3-5$$

$$\frac{\partial U}{\partial t} = U_{t(\text{forward in time})} \quad \frac{U_i^{j+1} - U_i^j}{\Delta t} \quad 3-6$$

Backward difference space and time scheme:

$$\frac{\partial U}{\partial X} = U_{X(\text{backward in space})} \quad \frac{U_i^j - U_{i-1}^j}{\Delta X} \quad 3-7$$

$$\frac{\partial U}{\partial t} = U_{t(\text{backward in time})} \quad \frac{U_i^j - U_i^{j-1}}{\Delta t} \quad 3-8$$

Central difference space and time scheme:

$$\frac{\partial U}{\partial X} = U_{X(\text{central in space})} \quad \frac{U_{i+1}^j - U_{i-1}^j}{2\Delta X} \quad 3-9$$

$$\frac{\partial U}{\partial t} = U_{t(\text{central in time})} \quad \frac{U_i^{j+1} - U_i^{j-1}}{2\Delta t} \quad 3-10$$

The aforementioned schemes can solve simple differential equations like ordinary differential equations (ODEs) but complex differential equations like Saint-Venant equation cannot be solved by these schemes. Therefore, other advanced finite difference schemes, like Lax-Wendroff Scheme, Lax-Friedrich Scheme, Leap-Frog scheme, FTSC Scheme and MacCormack scheme have been developed to solve complex partial differential equations (as shown in Appendix–B). Among these methods, the MacCormack scheme has been selected to solve the Saint-Venant equation in this investigation. The main advantages of the MacCormack scheme in comparison to the other finite difference schemes are:

- The MacCormack scheme has two steps, predictor step and corrector step which is capable of capturing the discontinuities in the flows.
- This method has higher accuracy because of using two differential equations both in space and time.
- In the MacCormack scheme the primary results which are determined during the predictor part, are used during the corrector part as shown in Figure 3-7.

In the section 3.3.2, the MacCormack scheme will be explained in more detail.

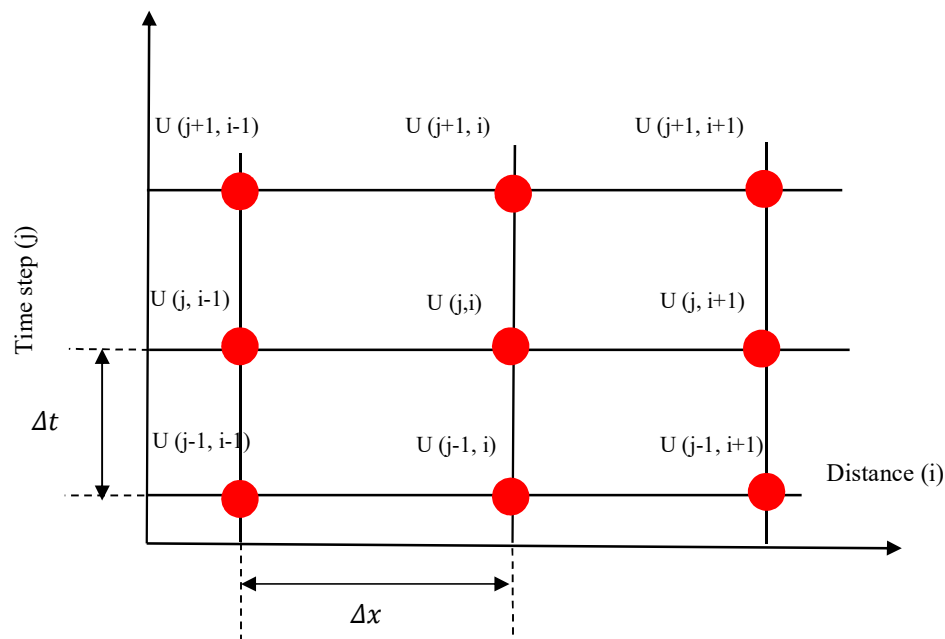


**Figure 3-1.** Finite difference mesh

## 3.2 Embankment dam failure modelling

### 3.2.1 Introduction

In this chapter, in order to achieve a better understanding of the failure mechanism in the non-cohesive embankment dams, two different numerical approaches are introduced and explained:

- In the first approach (section 3.3), the methodology of the one-dimensional program to model failure process in the embankment dams is introduced and discussed.
- In the second approach (section 3.4), the two-dimensional open-source TELEMAC software is modified to model bed load transport over the steep slopes. This modification is done by calibrating slope correction formulas in the sediment part of TELEMAC software (SISYPHE software).

In the following, the literature review related to the numerical modelling of embankment dam failure is presented.

### 3.2.2 Literature review

Modelling of embankment dam failure is one of the major problems for hydraulic engineers over the last decades. Embankment dam failure can be modelled in two ways:

- Laboratory model
- Numerical model

The laboratory model is not recommended because of high cost to build a real model, long time for dam construction, limitation in laboratory space and measurement tools, therefore, in recent years numerical modelling has been developed and became the best option for modelling embankment dam failure.

Table 3-2 shows the history of the numerical investigations that have already been done in this field during the last decades.

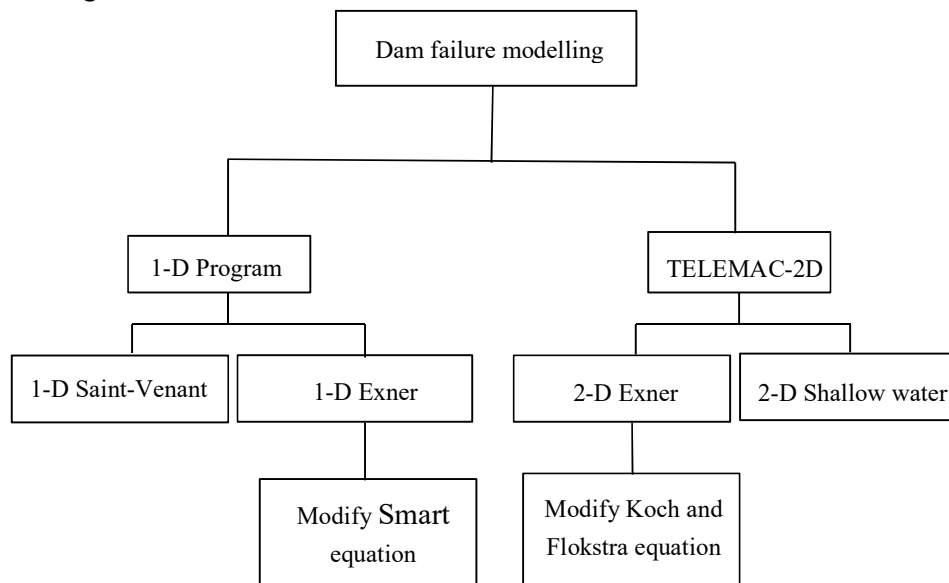


**Figure 3-2.** Different approaches for dam failure modelling

**Table 3-2.** Literature review for dam failure program

<b>Model</b>	<b>Sediment transport</b>	<b>Breach morphology</b>	<b>Year</b>
Cristofano	Empirical formula	Constant breach width	1965
BRDAM	Schoklitsch formula	Parabolic breach shape	1977
DAMBRK Fread	Linear predetermined erosion	Rectangular, triangular, or trapezoidal	1982
Lou; Ponce and Tsivoglou	Meyer-Peter and Müller formula	Regime type relation	1981
BEED	Scarlatos	Rectangular or trapezoidal	1987
BREACH	Meyer-Peter and Muller modified by Smart	Rectangular, triangular, or trapezoidal	1988
HR-BREACH	Empirical formula	Free formation of breach shape	2002
FIREBIRD BREACH	Meyer-Peter and Muller formula	Rectangular, triangular, or trapezoidal	2006
SIMBA	Empirical formula	Rectangular, or trapezoidal	2005

### 3.3 One-dimensional modelling

#### 3.3.1 Introduction

One-dimensional numerical modelling is used as the main solution to calculate the outflow hydrograph for embankment dam failure. Main advantages of one-dimensional numerical modelling are fast calculation time and reliable results.

Former investigations on the numerical modelling of the embankment dam failure show that the best approach to compute the embankment dam failure parameters can be obtained by solving the two main partial differential equations consequently.

- The Saint-Venant equation (Hydrodynamic part).
- Sediment continuity equation (Erosion part)

In the hydrodynamic part, flow parameters like height of the water and water velocity in the downstream of the dam are determined by solving the one-dimensional Saint-Venant equation.

In the erosion part by using calculated flow parameters, a bed elevation during dam failure process is calculated by solving the Exner sediment continuity equation.

In the following parts, these methods are explained in more detail.

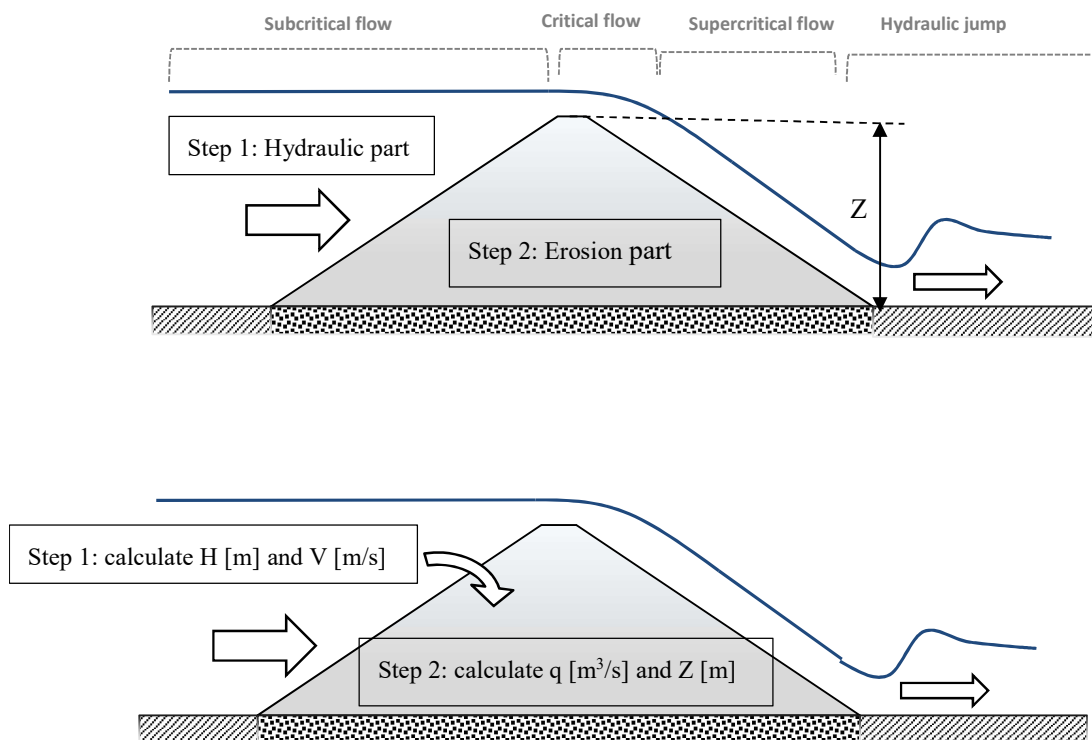


**Figure 3-3.** Embankment dam failure procedure

### 3.3.2 Hydrodynamic part

The hydrodynamic part in the numerical approach for dam failure modelling concerns on the flow parameters like height of the water and water velocity. These parameters can be determined by solving the governing equations like Navier-Stokes, shallow water or Saint-Venant equation. In this research the main investigation is focused on solving the one-dimensional Saint-Venant equation.

The one-dimensional Saint-Venant equation was suggested by Barre de Saint-Venant in 1870s to calculate flow parameters within a certain part of channels. This equation is derived from the continuity and momentum equations by using the following assumptions:

- The flow velocity and water depth change only in the direction of flow.
- Vertical acceleration is neglected and hydrostatic pressure is considered along the channel.
- The density of fluid is constant along the channel and fluid is incompressible.
- Slope of the channel is small.

In the following parts, these equations (continuity and momentum) are explained in more detail.

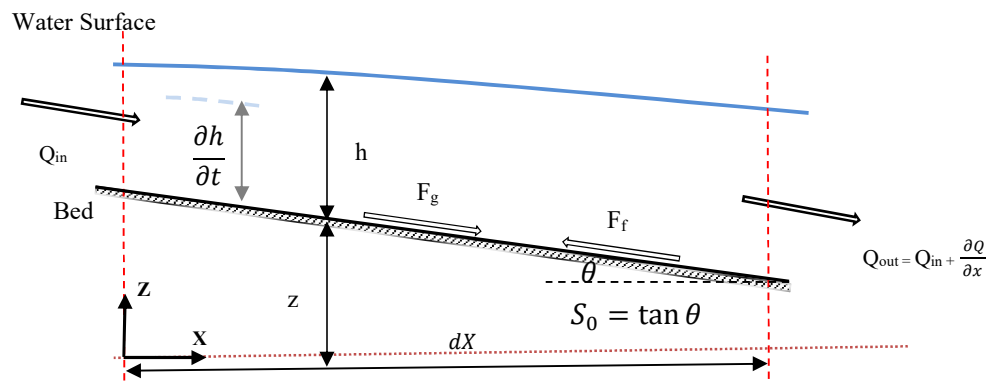


Figure 3-4. Control volume in the open channel

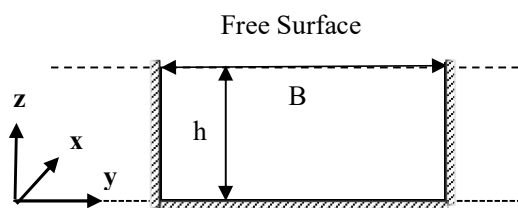


Figure 3-5. Cross section of channel

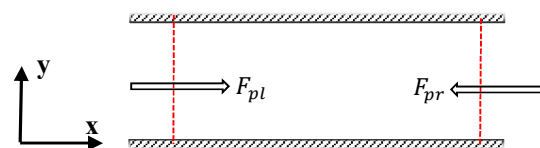


Figure 3-6. Forces in the rectangular channel

### - Continuity equation

According to the Figure 3-4, by assuming no lateral inflow, the continuity equation can be defined based on the mass conservation law (Popescu (2014)).

$$\left\{ \begin{array}{l} \text{Mass flow} = \dot{m} = (\rho_w Q) \left[ \frac{\text{kg}}{\text{s}} \right] \\ \text{Mass} = m = (\rho_w \forall) [\text{kg}] \end{array} \right. \quad \begin{array}{l} 3-11 \\ 3-12 \end{array}$$

Here,  $\forall$  is the volume of water in control volume [ $\text{m}^3$ ]

$$(\rho_w Q)_{\text{in}} - ((\rho_w Q)_{\text{in}} + (\rho_w \frac{\partial Q}{\partial x} dx))_{\text{out}} = \rho_w \frac{\partial A}{\partial t} dx \quad 3-13$$

$$\frac{\partial A}{\partial t} + \frac{\partial Q}{\partial x} = \mathbf{0.0} \quad 3-14$$

### - Momentum equation

Momentum equation is expressed based on the Newton's second law as shown in the Equation 3-15(Popescu (2014)).

$$\Sigma \vec{F} = \left[ \left( \frac{Q}{A} \right) \left( \rho_w \frac{\partial A}{\partial t} dx \right) - \left( \frac{Q}{A} \right) \left( (\rho_w Q)_{\text{in}} - ((\rho_w Q) + (\rho_w \frac{\partial Q}{\partial x} dx))_{\text{out}} \right) \right] \quad 3-15$$

$$\Sigma \vec{F} = \rho_w \left( \frac{\partial(Q^2/A)}{\partial x} + \frac{\partial Q}{\partial t} \right) dx \quad 3-16$$

In the left side of the Equation 3-16, three forces are considered. In the following these forces are explained in the more detail (Broich (1996) and Sabbagh et al. (2007)).

### - Gravity and friction forces along channel

These forces can be expressed as the following equations:

$$F_g = \rho_w g A dx S_0 \text{ (Gravity force)} \quad 3-17$$

$$F_f = -\rho_w g A S_f dx \text{ (Friction force)} \quad 3-18$$

### - Pressure force

$$F_p = -\rho_w g B h \left( \frac{\partial h}{\partial x} \right) dx \quad 3-19$$

$$\Sigma \vec{F} = \vec{F}_g + \vec{F}_f + \vec{F}_p \quad 3-20$$

By substituting Equations 3-17, 3-18 and 3-19 into the Equation 3-16 final momentum equation can be define as Equation 3-21.

$$-\rho_w g A S_f dx + \rho_w g A dx S_0 - \rho_w g A \left( \frac{\partial h}{\partial x} \right) dx = \rho_w \left( \frac{\partial Q}{\partial t} + \frac{\partial(Q^2/A)}{\partial x} \right) dx \quad 3-21$$

By simplify Equation 3-21, general form of the momentum equation can be written as:

$$\frac{1}{A} \frac{\partial Q}{\partial t} + \frac{1}{A} \frac{\partial}{\partial x} \left( \frac{Q^2}{A} \right) + \mathbf{g} \frac{\partial h}{\partial x} - \mathbf{g}(S_0 - S_f) = \mathbf{0.0} \quad 3-22$$

Here:

$$\frac{1}{A} \frac{\partial Q}{\partial t} \quad \text{A local acceleration term.}$$

$$\frac{1}{A} \frac{\partial}{\partial x} \left( \frac{Q^2}{A} \right) \quad \text{A convective acceleration term.}$$

$$\mathbf{g} \left( \frac{\partial h}{\partial x} \right) \quad \text{A pressure force term.}$$

$$\mathbf{g}(S_0 - S_f) \quad \text{A gravity and friction force term respectively.}$$

Furthermore, in the following the conservation form of the one-dimensional Saint-Venant equation is described based on Equations 3-14 and 3-22 (Athanasios et al. (2010)):

$$\frac{\partial U}{\partial t} + \frac{\partial F}{\partial x} = S \quad 3-23$$

$$U = \begin{pmatrix} A \\ Q \end{pmatrix} \quad F = \begin{pmatrix} Q \\ \frac{Q^2}{A} + gI_1 \end{pmatrix} \quad S = \begin{pmatrix} 0 \\ gA(S_0 - S_f) \end{pmatrix}$$

$I_1$  is the hydrostatic pressure force in the channel and by assuming a rectangular channel with constant width  $I_1$  can be written as Equation 3-24:

$$I_1 = \int_0^h (h - \eta) B d\eta = \frac{h^2 B}{2} = \frac{A^2}{2B} \quad 3-24$$

- **Solve the Saint-Venant equation by the MacCormack scheme**

As mentioned in the section 3.1.2, there are different numerical schemes available to solve the partial differential equations. One scheme is based on the P. Garcia-Navarro & J. M. Saviron (1992) and is known as the revised MacCormack scheme. This scheme has been selected for solving the Saint-Venant equation because of its advantages over the other methods.

In the MacCormack scheme, the Saint-Venant equation is solved in the two-steps:

- Predictor step
- Corrector step

- **Predictor step**

In the predictor step the forward finite difference scheme normally is used to calculate the primary flow parameters as shown in the Equations 3-25 and 3-26 (Athanasios et al. (2010)).

$$\tilde{A}_i = A_i^j - \frac{\Delta t}{\Delta x} (Q_{i+1}^j - Q_i^j) \quad 3-25$$

$$\tilde{Q}_i = Q_i^j - \frac{\Delta t}{\Delta x} \left( \left( \frac{Q_{i+1}^{j2}}{A_{i+1}^j} - \frac{Q_i^{j2}}{A_i^j} \right) + g(I_{1+1}^j - I_{1_i}^j) \right) + g\Delta t \left( A_i^j (S_{0_i}^j - S_{f_i}^j) \right) \quad 3-26$$

Here,  $S_0$  and  $S_f$  are source terms and are defined as the following equations:

$$S_{0_i}^j = (Z_i^j - Z_{i+1}^j) / \Delta x \quad 3-27$$

$$S_{f_i}^j = (n_i^2 Q_i^j |Q_i^j|) / (A_i^{j2} R_i^{j3}) \quad 3-28$$

- **Corrector step**

In the corrector step, by using the primary flow parameters and apply the backward finite difference scheme, the secondary flow parameters are calculated. This procedure is shown in the Equations 3-29 and 3-30 (Athanasios et al. (2010)).

$$\tilde{\tilde{A}}_i = A_i^j - \frac{\Delta t}{\Delta x} (\tilde{Q}_i^j - \tilde{Q}_{i-1}^j) \quad 3-29$$

$$\tilde{\tilde{Q}}_i = Q_i^j - \frac{\Delta t}{\Delta x} \left( \left( \frac{\tilde{Q}_i^{j2}}{A_i^j} - \frac{\tilde{Q}_{i-1}^{j2}}{A_{i-1}^j} \right) + g(\tilde{I}_{1_i}^j - \tilde{I}_{1_{i-1}}^j) \right) + g\Delta t \left( \tilde{A}_i^j (\tilde{S}_{0_i}^j - \tilde{S}_{f_i}^j) \right) \quad 3-30$$

Here,  $\tilde{S}_0$  and  $\tilde{S}_f$  are source terms and are defined as the following equations:

$$\tilde{S}_{0_i}^j = (Z_{i-1}^j - Z_i^j) / \Delta x \quad 3-31$$

$$\tilde{S}_{f_i}^j = (n_i^2 Q_i^j |Q_i^j|) / (A_i^{j2} R_i^{j3}) \quad 3-32$$

The final value for each hydraulic parameter is determined by averaging between the results from these two steps (predictor and corrector):

$$Q_i^{j+1} = \frac{1}{2} (\widetilde{Q}_i + \widetilde{\widetilde{Q}}_i) \quad 3-33$$

$$A_i^{j+1} = \frac{1}{2} (\widetilde{A}_i + \widetilde{\widetilde{A}}_i) \quad 3-34$$

The above methodology describes the procedure to solve the Saint-Venant equation by using the MacCormack scheme.

The stability of this calculation should be controlled by using the Courant-Friedrich-Lewy (CFL) formula. In general, calculation gets unstable when the CFL number become greater than 1.0. Therefore the value of the CFL number must be less than 1.0 to have stable calculation. The CFL number is expressed as the following equation:

$$CFL_{ni}^j = \frac{\Delta t}{\Delta x} (|U_i^j| + C_i^j) \leq 1.0 \quad 3-35$$

$$C_i^j = \sqrt{(gh_i^j)}$$

Here,  $C_i^j$  [m/s] is the wave velocity,  $U_i^j$  [m/s] is the flow velocity,  $A$  [m<sup>2</sup>] is the cross section area,  $Z$  [m] is the bed elevation,  $S_0$  is the bed slope and  $S_f$  is the friction slope and  $\eta$  [m] is the Vertical distance above the channel bottom.

Now, the only unknown parameters remaining in the Equations 3-33 and 3-34 are:

- The manning number ( $n_i$ )
- The boundary condition values

In the following sections these parameters are determined and explained in more detail.

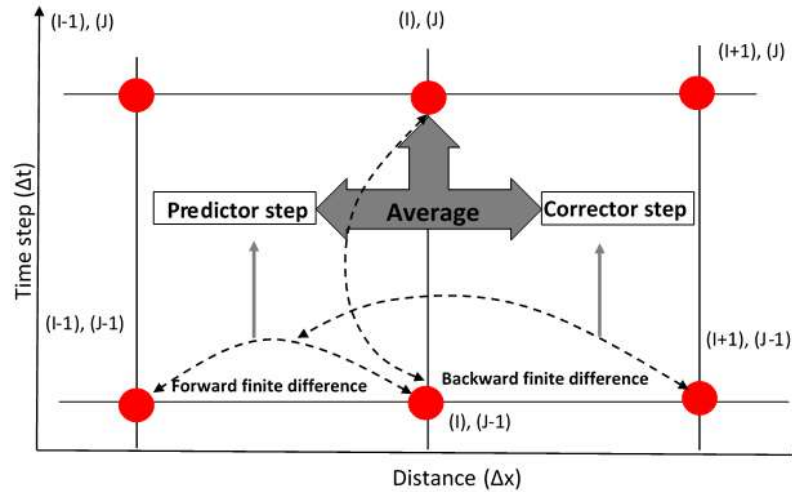


**Figure 3-7.** MacCormack method

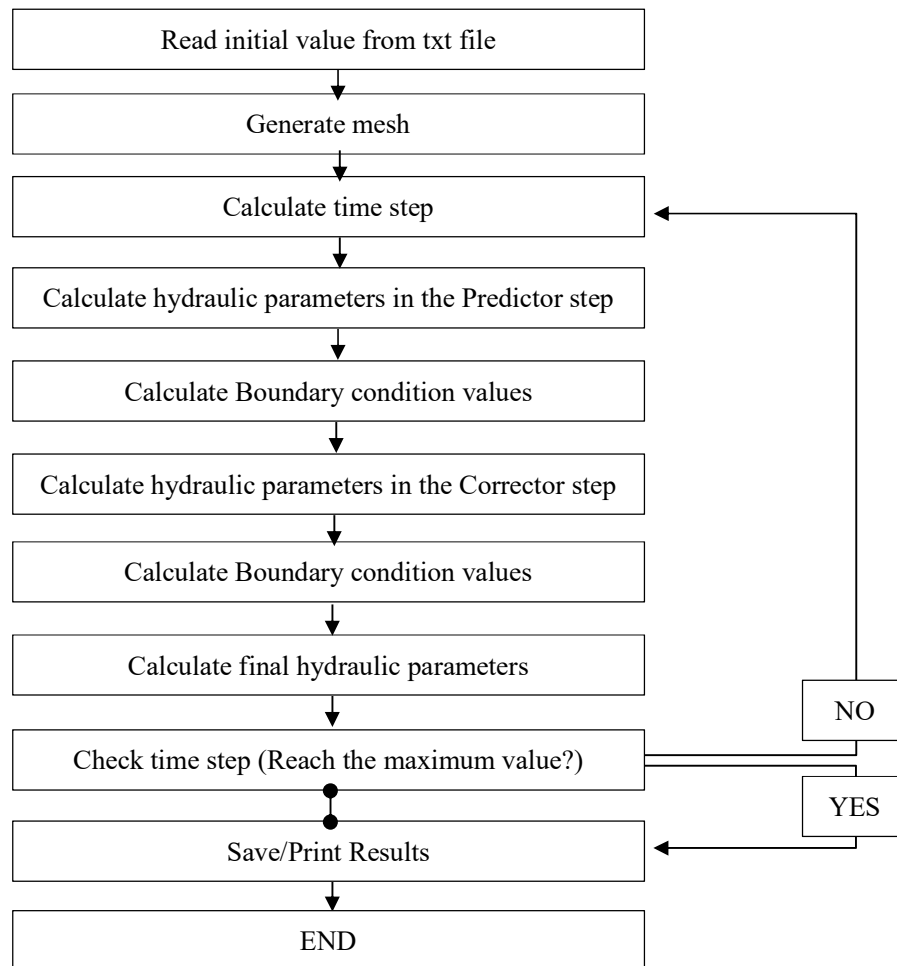


**Figure 3-8.** MacCormack procedure in 1-D program

### Roughness computation

In open channels, the total flow resistance results from interaction between different elements which are located on the bed of the channel. Among these elements, some of them have more influence on flow resistance like grain size, vegetation, bed slope, bed alignment and obstruction in the channel. In fact, roughness coefficient shows the effect of these parameters in stream flow. The importance of calculating roughness coefficient is related to define exact value for velocity in the Manning equation. Roughness coefficient can be obtained from the following methods:

- Experimental formula
- Prepared chart
- **Experimental formula**

In many open channels the particle size and bed slope have the most influence on the flow parameters. These influences can be measured and calculated by experimental equations which have been suggested by different researchers. Table 3-3 summarizes some of the most important relationships in this regard.

**Table 3-3.** Roughness equations

Name	Manning formula (n)
Strickler (1923)	$n = (d_{50}^{1/6}/21.1)$
Lane & Carlson (1953)	$n = (d_{75}^{1/6}/21.14)$
Meyer-Peter & Muller (1948)	$n = (d_{90}^{1/6}/26)$
Limerinos (1970)	$n = (0.113R^{1/6})/(0.35 + 2.0 \log(R/d_{50}))$
Bray (1979)	$n = (0.113H^{1/6})/(1.09 + 2.2 \log(H/d_{50}))$
Brownlie (1983)	$n = [1.893(R/d_{50})^{0.1374} S_0^{0.1112}](0.034d_{50}^{0.167})$
Bruschin (1985)	$n = (d_{50}^{1/6}/12.38)(R/d_{50} S_0)^{1/7.3}$
Ghani (2007)	$n = 4e10^{-8}(d_{50})^2 - 5e10^{-5}(H/d_{50}) + 0.0582$
Jarret (1984)	$n = 0.39S_f^{0.38}R^{-0.16}$

In this research the Ghani et al (2007) and Jarret (1984) equations are selected and used to calculate the friction slope in the MacCormack scheme.

- **Prepared chart**

If the above mentioned methods are not available, roughness coefficient can be defined by using prepared data as shown in the Table 3-4.

**Table 3-4.** Roughness coefficient for different surface

Surface type	Manning number (mean value)
Glass, copper, plastic, or other smooth surface	0.01
Smooth, unpainted steel, planed wood	0.012
Painted steel or coated cast iron	0.013
Smooth asphalt, common clay drainage tile, trowel-finished concrete, glazed brick	0.013
Uncoated cast iron, black wrought iron pipe, vitrified clay sewer tile	0.014
Brick in cement mortar, float-finished concrete, concrete pipe	0.015
Formed, unfinished concrete, spiral steel pipe	0.017
Smooth earth	0.018
Clean excavated earth	0.022
Corrugated metal storm drain	0.024
Natural channel with stones and weeds	0.03
Natural channel with light brush	0.05
Natural channel with tall grass and reeds	0.06
Natural channel with heavy brush	0.1

### Boundary condition

In the MacCormack method like other explicit methods, all computational nodes can be calculated except two nodes, the first node ( $n=1$ ) and the last node ( $n=N$ ). These nodes represent in total four unknown parameters which are related to the height of the water and water velocity at points 1 and N. In order to calculate these unknown parameters a new method has been used in this research. This method was suggested by P. Garcia-Navarro & J. M. Saviron (1992).

In this method unknown parameters are estimated by using characteristics and linear interpolation approaches.

The details of this method to calculate the unknown parameters are given in the Appendix-A.

### 3.3.3 Model verification (Modelling flow over bump)

In this part, in order to verify the accuracy and performance of the MacCormack scheme, the Goutal and Maurel (1997) test is employed. This test was carried out in a frictionless rectangular channel with 25 m length and 1.0 m width. In this channel one bump has been considered. The bed topography for this bump is illustrated in the Equations 3-36, 3-37 and 3-38. This test has been done in the three different flow situations:

- Subcritical Flow over bump
- Transcritical Flow over bump (supercritical with hydraulic jump)
- Transcritical Flow over bump (supercritical without hydraulic jump)

In this study, the model accuracy is demonstrated by using these three flow situations and the final results are compared against the analytical results.

In the following sections these comparisons are performed and explained in more detail.

Bed profile	{	$0.0$	$x < 8.0 \text{ m}$	3-36
		$0.2 - 0.05(x - 10)^2$	$8.0 \leq x \leq 12.0$	3-37
		$0.0$	$x > 12.0$	3-38

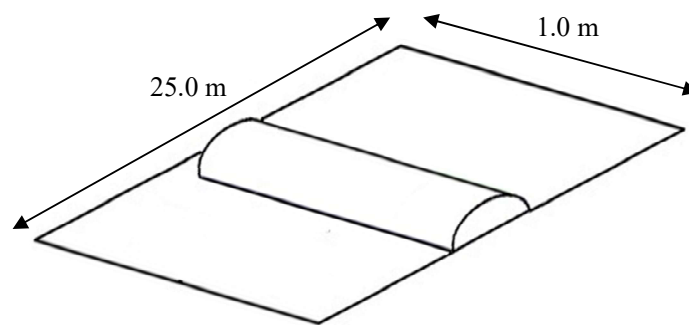
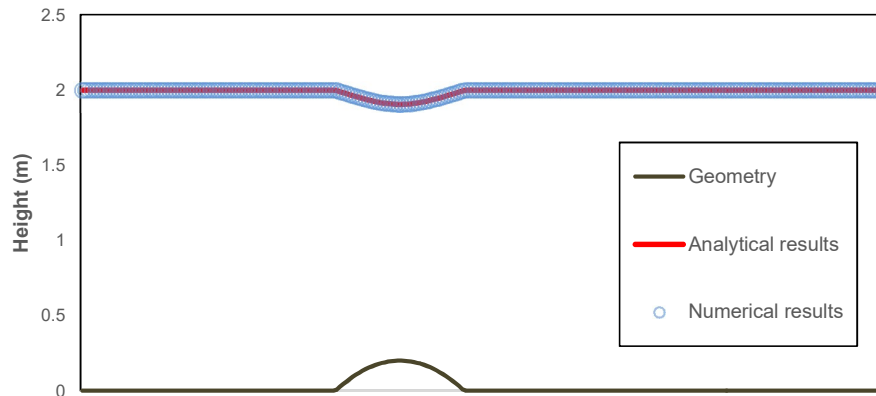


**Figure 3-9.** Geometry of the channel

### Subcritical Flow over bump

In this test the inflow discharge per unit width is kept constant at  $4.42 \text{ [m}^3/\text{s]} \text{ [1/m]}$  at the upstream boundary, while at the downstream boundary the water depth is kept constant at  $2.0 \text{ m}$ . The final results are shown in the Figure 3-10.

Comparison between analytical and numerical results



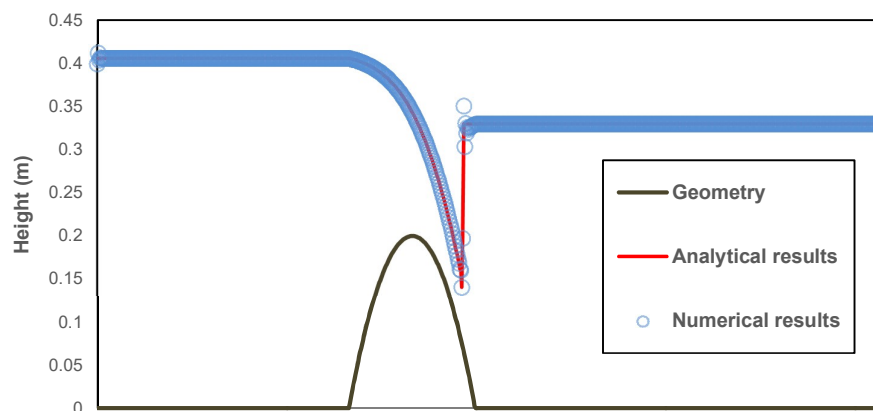
**Figure 3-10.** Subcritical Flow over bump

Figure 3-10, shows the MacCormack scheme has acceptable accuracy for modelling subcritical flow in the open channels.

### Transcritical Flow over bump (supercritical with hydraulic jump)

In this test the downstream water level is kept constant at  $0.33 \text{ m}$  and inflow discharge per unit width is kept constant at  $0.18 \text{ [m}^3/\text{s]} \text{ [1/m]}$ . In the Figure 3-11 the numerical result is compared against the analytical result.

Comparison between analytical and numerical results



**Figure 3-11.** Supercritical with hydraulic jump

Figure 3-11, shows the MacCormack scheme has acceptable accuracy for modelling the hydraulic jump in the open channels.

**Transcritical Flow over bump (supercritical without hydraulic jump)**

In this test the upstream inflow discharge is kept constant at  $1.53 \text{ [m}^3\text{/s]}/[1\text{/m}]$ . No boundary condition is specified at the downstream flow. In the Figure 3-12 the numerical result is compared against the analytical result.

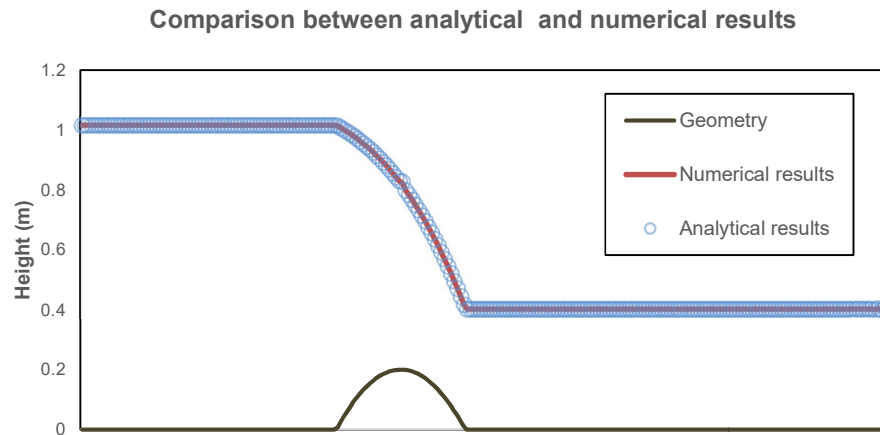


**Figure 3-12.** Supercritical without hydraulic jump

Figure 3-12, shows the MacCormack scheme has acceptable accuracy for modelling supercritical flow without shock in the open channels.

### 3.3.4 Erosion part

#### Literature review

The first numerical modelling for morphological modelling and sediment transports was introduced in 1992 as TIMOR software by Prof. U. Zanke in the Technical University of Darmstadt, Germany. After that many software have been developed and introduced such as HEC-RAS, MIKE, SOBEK, CCHE and SISYPHE. Table 3-5 shows the history of numerical investigations have already been done in this field during the last decades.

In the next part the major parameters which are needed to determine the bed evolution are introduced and explained in more detail.

**Table 3-5.** Literature review of Erosion modelling software

Name	Description	Institution	Year	Dimension
Mike 11	Open channel-Rivers-Sediment transport	DHI-Denmark	2009	1-D
HEC-RAS	Open channel-Rivers-Sediment transport-water quality	U.S.Army corps of engineers	2010	1-D
SOBEK	Flood forecasting-Sewers-River morphology	Delft Uni.Netherland	2009	1-D, 2-D
Mike 21	Open channel-Rivers-Sediment transport-Coastal areas	DHI-Denmark	2009	2-D
SISYPHE	Open channel-Rivers-Sediment transport	TELEMAC-France	2009	2-D
DELFT 3D	Hydrodynamic modelling-Sediment transport-water quality	Delft Uni.Netherland	2009	2-D, 3-D
CCHE2D/3D	Hydrodynamic modelling-Sediment transport-water quality-pollutant transport	Mississippi Uni.USA	2010	2-D, 3-D
SED2D	Sediment transport	U.S.Army corps	2006	2-D
ECOMSED	Sediment transport-Hydrodynamic modelling	Hydroqual-Inc-USA	2010	3-D
CH3d-SED3D	Simulate flow and sediment transport	Dr.Y.Peter Sheng since	-	3-D
MIKE 3D	Simulate flow and sediment transport	DHI-Denmark	2009	3-D

### Shear stress

In fluid dynamics shear stress in flow indicates two different forces.

- Force between two layers in flow.
- Force between fluid and solid boundary layers like bottom of the channel.

In this part the main investigation is focused on determining the bed shear forces.

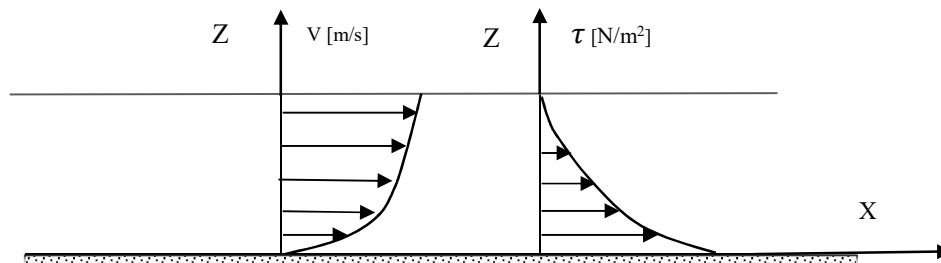


**Figure 3-13.** Velocity and Stress profile in the fluid

### Bed shear stress

In order to calculate shear stress on the bottom of the channel the following assumptions are considered:

- Flow is uniform
- Shear stress is calculated by considering block of water force on the bottom of the channel
- Bed slope is small

$$\sin \alpha \cong \tan \alpha \cong S_0$$

3-39

- Channel is wide and cross-section is a rectangular.

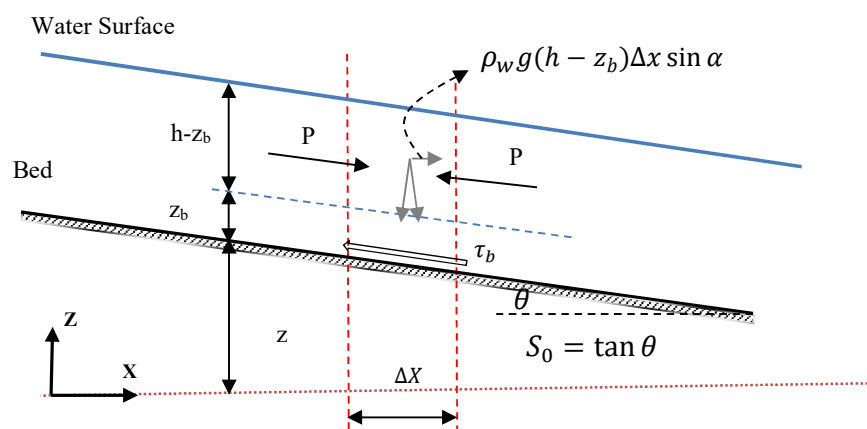


**Figure 3-14.** Forces in the fluid

Based on the above-mentioned assumptions, shear stress on the bottom of the channel can be expressed as the following equation:

$$\tau_b = \tau_{z=0} = \rho_w g h S_0 \quad 3-40$$

In a case of arbitrary cross-section, bottom shear stress is:

$$\tau_b = \rho_w g R S_0 \quad 3-41$$

### Friction Velocity

Often bottom shear stress can be expressed by friction velocity which is defined as:

$$u_* = \sqrt{\frac{\tau_b}{\rho_w}} = \sqrt{g R S_0} \quad \left[ \frac{m}{s} \right] \quad 3-42$$

### Sediment parameters

In the following the most important parameters of sediment are explained and discussed:

#### - Density

The density of the natural sediment ( $\rho_s$ ) is equal to  $2650 \left[ \frac{kg}{m^3} \right]$ . Therefore, the relative density can be expressed as the following equation:

$$s_{rel} = \frac{\rho_s}{\rho_w} = 2.65 \quad 3-43$$

#### - Grain size distribution

The grain size distribution chart is one of the best ways to characterize the sediment particles. This chart represents the particle cumulative volume in a given sample. This chart is illustrated in the Figure 3-15.

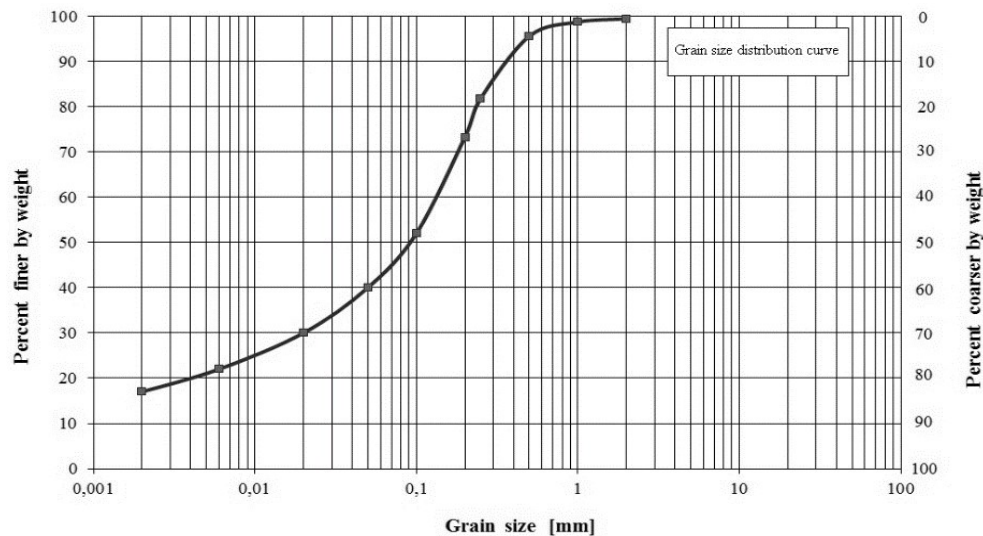


Figure 3-15. Grain distribution chart to characterize the sediments grain sizes

### - Threshold of sediment (Shield formula)

Threshold of sediments was suggested by A. Shields in 1936. Shields parameter is a non-dimensional parameter used to determine the initiation of motion of sediment in a fluid flow. It is a non-dimensional form of a shear stress, and is defined as the following equation.

$$\theta = \frac{u_*^2}{(s_{rel}-1)gd} \quad 3-44$$

Furthermore, critical shields parameter can be determined as:

$$\theta_c = \frac{u_{*c}^2}{(s_{rel}-1)gd} \quad 3-45$$

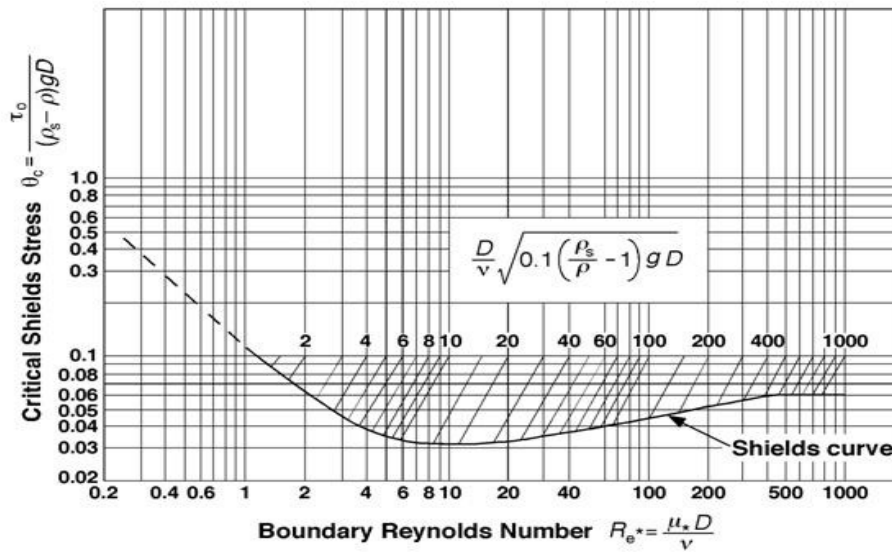


Figure 3-16. Shield diagram

### One-dimensional erosion modelling

The second step in the numerical modelling of the embankment dam failure is calculating the surface erosion. In this step the bed elevation is defined by solving the one-dimensional sediment continuity equation. The general form of the sediment continuity equation can be written as the Equation 3-46 (Kamal et al. (2009)):

$$\frac{\partial Q_s}{\partial x} + (1 - p) \frac{\partial A_b}{\partial t} + \frac{\partial (AC_s)}{\partial t} = 0.0 \quad 3-46$$

Here,  $Q_s$  [ $m^3/s$ ] is the volumetric sediment discharge,  $A_b$  [ $m^2$ ] is the cross sectional area of the bed,  $C_s$  is the section-averaged sediment concentration and  $p$  is the bed porosity.

In order to model the failure process in the non-cohesive embankment dams by using the one-dimensional sediment continuity equation, following assumption is considered:

Amount of the suspension load does not change significantly in comparison to bed elevation

$$\frac{\partial (AC_s)}{\partial t} \ll (1 - p) \frac{\partial A_b}{\partial t} \quad 3-47$$

Based on the mentioned assumption, this one-dimensional sediment continuity equation is written as the Equation 3-48:

$$(1 - p)(\partial z / \partial t) + (\partial q_b / \partial x) = 0.0 \quad 3-48$$

Equation 3-48 is known as the Exner (1925) equation.

The Exner equation can be discretized by using the Modified –Lax scheme (De Vries, M. (1987)) as shown in the follow equations:

$$\partial z / \partial t = 1 / \Delta t \left( z_i^{j+1} - \left( (1 - \alpha_{stab}) z_i^j + (\alpha_{stab} (z_{i+1}^j + z_{i-1}^j)) / 2 \right) \right) \quad 3-49$$

$$\partial q_b / \partial x = (q_{bi+1}^j - q_{bi-1}^j) / 2 \Delta x \quad 3-50$$

By substituting Equations 3-49 and 3-50 into the Equation 3-48, the bed elevation is determined as the following equation:

$$z_i^{j+1} = \left( (1 - \alpha_{stab}) z_i^j + (\alpha_{stab} (z_{i+1}^j + z_{i-1}^j)) / 2 \right) - (\Delta t / 2 (1 - p) \Delta x) (q_{bi+1}^j - q_{bi-1}^j) \quad 3-51$$

Here,  $\alpha_{stab}$  is the stability parameter and can be determined, based on the Vreugdenhil (1989) equation (Equation 3-52):

$$\alpha_{stab} = \mu^2 + 0.01, (0.0 < \alpha_{stab} < 1.0) \quad 3-52$$

Here,  $\mu$  is defined as Equation 3-53:

$$\mu = V((Q_s / Q) / (1 - Fr^2)) (\Delta t / \Delta x) \quad 3-53$$

### Sediment transport equation

Now, the only unknown parameter remaining in the Equation 3-51 is the bed load parameter ( $q_b$  [m<sup>3</sup>/s][1/m]).

This parameter has already been expressed through many experimental equations with different accuracy. In the Table 3-6 different equations to calculate the bed load parameter is presented.

**Table 3-6.** Different Bed-load transport formula

Name	Formula
M.Peter&Muller (1948)	$q_b = 8(\theta - \theta_c)^{1.5}(\sqrt{(s_{rel} - 1)gd^3})$
Wong and Parker (2006)	$q_b = 3.97(\theta - \theta_c)^{1.5}(\sqrt{(s_{rel} - 1)gd^3})$
Smart (1984)	$q_b = 4(d_{90}/d_{30})^{0.2}(V/(ghS_0)^{0.5})S_0^{0.6}\theta^{0.5}(\theta - \theta_c)(\sqrt{(s_{rel} - 1)gd^3})$
Abrahams (2003)	$q_b = \theta^{1.5}(V/(ghS_0)^{0.5})(\sqrt{(s_{rel} - 1)gd^3})$
Camenen & Larson (2005)	$q_b = [12\theta^{1.5}\exp(-4.5\theta/\theta_c)](\sqrt{(s_{rel} - 1)gd^3})$
Wu et al. (2000)	$q_b = 0.0053 \left( (n'/n)^{1.5}(\theta/\theta_c) - 1 \right)^{2.2} (\sqrt{(s_{rel} - 1)gd^3})$

Here,  $d$  [m] is the mean diameter,  $n$  [s/ (m<sup>1/3</sup>)] is the manning number,  $n'$  [s/ (m<sup>1/3</sup>)] is the global manning number,  $S_0$  is the bed slope and  $s_{rel}$  is the relative density

Generally, all available bed load equations are formulated for uniform flow with mild slopes. While in the embankment dam failure, flow regime is unsteady and the bed slope changes from steep to mild rapidly. Consequently, using these equations for modelling embankment dam failures may show excessive errors in the final results. In this study to overcome this deficiency the bed slope parameter in the sediment transport equation is calibrated. In the following, details of this calibration are explained.

### Choose proper sediment transport equation

In this research, proper sediment transport equation has been selected based on the Van Emelen (2013) test. In this test, uniform flow on various bed slopes with the following parameters are considered as:

$$S = S_0 = S_f, d = 2\text{mm}, n = 0.0168 \text{ s. m}^{-1/3}, q = 40 \text{ l/s/m}.$$

Six bed load transport equations were selected (Table 3-6) and the final results are compared to each other as shown in the Figure 3-17:

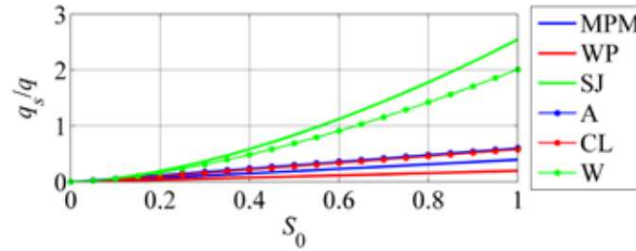


**Figure 3-17.** Choose proper sediment transport equation, Van Emelen (2013)

The final results show, the largest effect of the slope on the transport rate arises from the shear stress formulation in the Smart equation. Therefore in this research, the Smart (1984) equation is selected and calibrated to model slopes more than 20%. Furthermore, in order to reduce errors during the calculation different bed load equations were selected and applied for slopes less than 20%. The applied equations for different slopes are discussed briefly in the following:

#### - Zero slope

For this slope, original form of the Meyer-Peter & Muller (1948) equation is used

$$q_b = 8(\theta - \theta_c)^{1.5} [g(s_{rel} - 1)d^3]^{0.5} \quad 3-54$$

#### - Slopes up to 20%

To model this range of bed slope, the original form of the Smart (1984) equation is used

$$q_b = 4(d_{90}/d_{30})^{0.2} (V/(ghS_0)^{0.5}) S_0^{0.6} \theta^{0.5} (\theta - \theta_c) [g(s_{rel} - 1)d^3]^{0.5} \quad 3-55$$

#### - Slopes more than 20%

For this slope, the modified form of the Smart (1984) equation is used

$$q_b = 4(d_{90}/d_{30})^{0.2} (V/(ghS_0)^{0.5}) (S_0)^\omega \theta^{0.5} (\theta - \theta_c) [g(s_{rel} - 1)d^3]^{0.5} \quad 3-56$$

Here,  $S$  is the bed slope,  $\theta$  is the shield parameter,  $\theta_c$  is the critical shield parameter and  $\omega$  is the calibrated parameter.

In this investigation to calibrate  $\omega$  parameter, the Chinnarasri et al. (2003) dam failure tests are selected. The final value for  $\omega$  parameter is shown in the Table 3-7. The details of this calibration are given in the Appendix-G.

**Table 3-7.** Calibrated value for  $\omega$  parameter

Slope (%)	$\omega$
Between 1V:5H and 1V:4H (20%-25%)	0.6-0.9
Between 1V:4H and 1V:3H (25%-33%)	0.9-1.1
More than 1V:2H (33%)	1.1-2.8

### 3.3.5 Sliding

The last remaining part in this numerical program is checking the particle sliding during failure process. Generally, sliding happens when the bed slope ( $\varphi$ ) became greater than sediment response angles of the materials ( $\psi$ ). In this program, in order to check and calculate particle movement because of sliding the Guan et al. (2014) method is selected and applied. This method is expressed as the following equations:

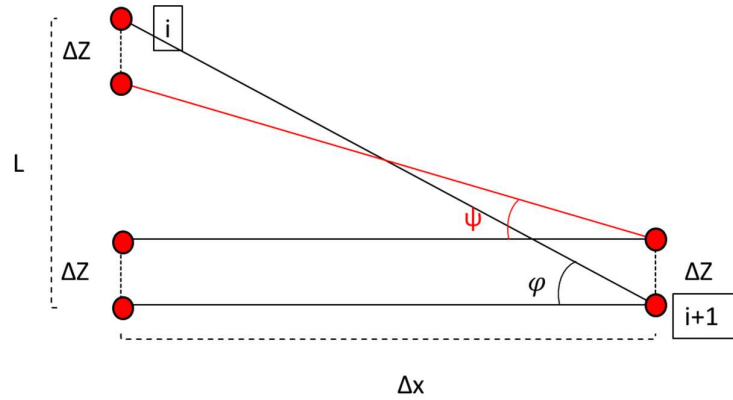


**Figure 3-18.** Sliding in 1-D numerical modelling

$$Z_{new,i+1} = Z_{i+1} + \Delta Z \quad 3-57$$

$$Z_{new,i} = Z_i - \Delta Z \quad 3-58$$

$$\Delta Z = +(\Delta x(\tan|\psi| - \tan \varphi))/2 \quad \text{If } \varphi > 0.0 \quad 3-59$$

$$\Delta Z = -(\Delta x(\tan|\psi| - \tan \varphi))/2 \quad \text{If } \varphi < 0.0 \quad 3-60$$

$$\Delta Z = 0.0 \quad \text{If } \varphi = 0.0 \quad 3-61$$

In the following the TELEMAC-MASCARET software is explained in more detail.

### 3.4 TELEMAC-MASCARET Software

The TELEMAC-MASCARET system has been developed by the Department Laboratoire National d'Hydraulique (LNH) at the Electric de France Direction des Etudes et Recherché (EDF-DER). The software system is owned by EDF-R&D and this software available as the open-source software which is designed for modelling free surface fluid, flood wave propagation, ground water flow and sediment transport in the open channels and rivers. The TELEMAC software is able to solve the Shallow Water equation for two dimensional modelling (TELEMAC-2D) and the Navier-Stokes equation for three dimensional modelling (TELEMAC-3D). For modelling erosion and sediment transport in the river the SISYPHE software is used in the TELEMAC system. In this chapter, the SISYPHE software is coupled with the TELEMAC-2D software to calculate the sediment transport during embankment dam failure. Figure 3-19 shows the different software which belong to the TELEMAC-MASCARET system.

In the following the TELEMAC-2D and SISYPHE software are discussed in more detail.

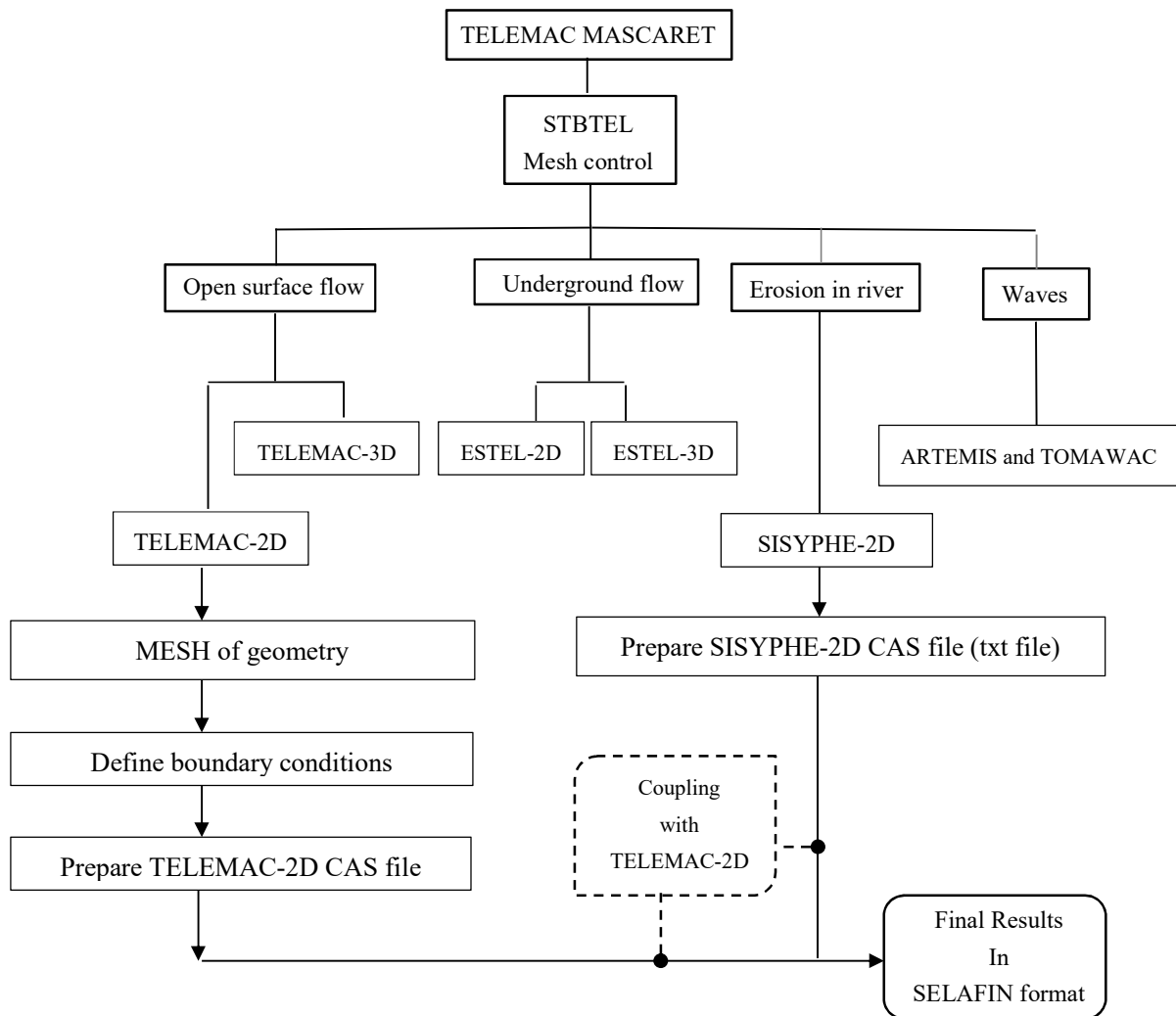


**Figure 3-19.** TELEMAC-MASCARET system

### 3.4.1 TELEMAC-2D software

TELEMAC-2D is a two dimensional software and belongs to the open-source TELEMAC - MASCARET system. This software is designed for modelling hydrodynamic flow in the open channels, rivers and marine fields. This software solves non-conservation form of shallow water equations with finite element or finite volume methods. Equations 3-62, 3-63 and 3-64 show the non-conservation form of the shallow water equations which are used in the TELEMAC-2D software (TELEMAC manual (2014)).

- Continuity equation

$$\frac{\partial h}{\partial t} + \vec{u}\vec{\nabla}(h) + h\text{div}(\vec{u}) = s_h \quad 3-62$$

- Momentum equations

$$\frac{\partial(u)}{\partial t} + \vec{u}\vec{\nabla}(u) = -g\frac{\partial z}{\partial x} + s_x + \frac{1}{h}\text{div}(h\nu_t\vec{\nabla}u) \quad 3-63$$

$$\frac{\partial(v)}{\partial t} + \vec{u}\vec{\nabla}(v) = -g\frac{\partial z}{\partial y} + s_y + \frac{1}{h}\text{div}(h\nu_t\vec{\nabla}v) \quad 3-64$$

Here,  $z$  [m] is the free surface elevation,  $h$  is the water height,  $\rho$  is the reference density,  $u$  and  $v$  [m/s] are the water velocity component in  $x$  and  $y$  direction respectively,  $s_x$  and  $s_y$  are source or sink terms in dynamic equations,  $s_h$  is the source or sink of fluid.

#### Instruction TELEMAC-2D software

In order to calculate and simulate flow parameters with the TELEMAC-2D software, the following steps have to be carried out (Figure 3-19):

- *Prepare boundary condition file*

This is a formatted file which is generated automatically by MATISSE, FUDAA-PREPRO, BLUE KENUE or STBTEL. It can be modified with a standard text editor. Each line of this file is dedicated to one point on the mesh boundary. Type and number of boundaries like open boundary or close boundary should be defined and located by the user on the related mesh during mesh generation.

- *Prepare liquid boundary file*

This text file enables the user to specify values for time-dependent boundary conditions (tracer flow rate, depth, velocity, and tracer concentration).

This file is optional, if the inflow to the boundaries is constant it is not necessary to prepare this file.

- *Prepare steering file (CAS\_TEL)*

This is a text file which is created by the FUDAA-PREPRO software. Generally, user starts from an already existing parameter file available in the TELEMAC structure. TELEMAC-2D reads the steering file at the beginning of the computation. The dictionary and steering files are read by a utility called DAMOCLES, which is included in TELEMAC-2D. Steering file is in FORTRAN language and containing the configuration of the computation.

- *Prepare geometry file*

This file contains all the information concerning the mesh, i.e. number of mesh points (NPOIN variable), number of elements (NELEM variable) and number of nodes per element (NDP variable). This file can also contain bottom topography information and/or friction coefficient at each mesh point.

TELEMAC-2D stores information on the geometry at the start of the results file. The geometry file can be prepared by using BLUE-KENUE software.

### 3.4.2 SISYPHE software

In order to model erosion process and sediment transport in river the SISYPHE software has been developed in the TELEMAC-MASCARET system. The SISYPHE software can simulate sediment transport and bed elevation in the complex morphology same as coastal, rivers, lakes and estuaries with the different discharge rate, different sediment grain size and different sediment transport equations. The SISYPHE software can be easily coupled with the TELEMAC-2D and TELEMAC-3D software. In this coupling, at each time step TELEMAC-2D or 3D send calculated Hydrodynamic parameters like height of the water (H) and water velocity (U, V) to the SISYPHE software.

The SISYPHE software model bed elevation by solving the two-dimensional sediment continuity equation which is called the Exner equation as shown in the Equation 3-65 (TASSI. P. (2014)):

$$(1 - p) \frac{\partial z}{\partial t} + \nabla(Q_b) = 0 \quad 3-65$$

Here,  $Q_b$  [ $m^3/s$ ] is the bed load transport,  $z$  [m] is the bed elevation and  $p$  is the bed porosity.

The SISYPHE software use four different equations to calculate bed load transport ( $Q_b$ ) as shown in Table 3-8.

**Table 3-8.** Different bed load equations in SISYPHE

Bed load formula	Mode of transport
Meyer-Peter	Bed load
Einstein-Brown	Bed load
Engelund-Hansen	Total load
Hunziker	Bed load

To improve the accuracy of the final results, the SISYPHE software uses two correction formula which are called Koch and Flokstra (1981) and Soulsby (1997) equations.

In this study, in order to model sediment transport over the steep slopes, the  $\beta_{Tel}$  parameter in the Koch and Flokstra (1981) formula is calibrated (Equation 3-66).

**Koch and Flokstra formula (1981)**

$$M_1 = 1 - \beta_{Tel}(\partial z / \partial x) \quad 3-66$$

$$Q_b = Q_{b0} \times M_1 \quad 3-67$$

Here,  $M_1$  is the correction formula,  $\beta_{Tel}$  is an empirical parameter,  $Q_{b0}$  [m<sup>3</sup>/s] is the bed load transport and  $Q_b$  [m<sup>3</sup>/s] is the corrected bed load transport.

In order to calibrate  $\beta_{Tel}$  parameter in the Equation 3-66, the Chinnarasri et al. (2003) Dam failure tests are employed. The final values for  $\beta_{Tel}$  parameter are shown in the Table 3-9. The details of this calibration are given in the Appendix-G

**Table 3-9.** Calibrated value for  $\beta_{Tel}$  parameter

Slope (%)	$\beta_{Tel}$
Less than 1V:4H (25%)	1.3
Between 1V:4H and 1V:3H (25%-33%)	2.0-3.5
More than 1V:2H (33%)	4.5-6.0

### 3.5 Validation of 1-D program and TELEMAC-2D software

In order to verify the accuracy and performance of the 1-D program and TELEMAC-2D software, two experimental tests are selected from the Schmocker et al. (2013) dam failure tests. These tests are carried out in a glass-side flume with 8.0 m length, 0.2 m width and 0.7 m height. The small scale dike is installed at 4.0 m distance from the channel intake with 0.2 m height and 0.1 m crest width. The upstream and downstream slopes of this dam are fixed at 1V:2H.

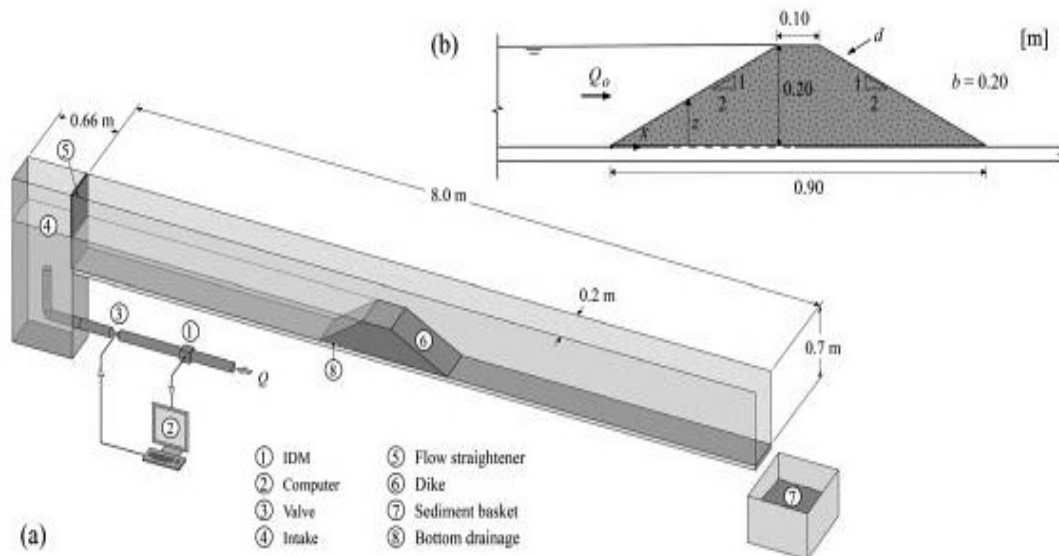


**Figure 3-20.** Schmocker et al. (2013) dam failure tests

Furthermore, these dam failure tests have been done based on two different dam materials:

- Homogeneous sand with mean sediment diameter 2.0mm.
- Homogeneous sand with mean sediment diameter 0.31mm.

In both materials the sediment is non-cohesive with density of  $2650 \text{ kg/m}^3$ . The inflow discharge was kept constant during failure process.

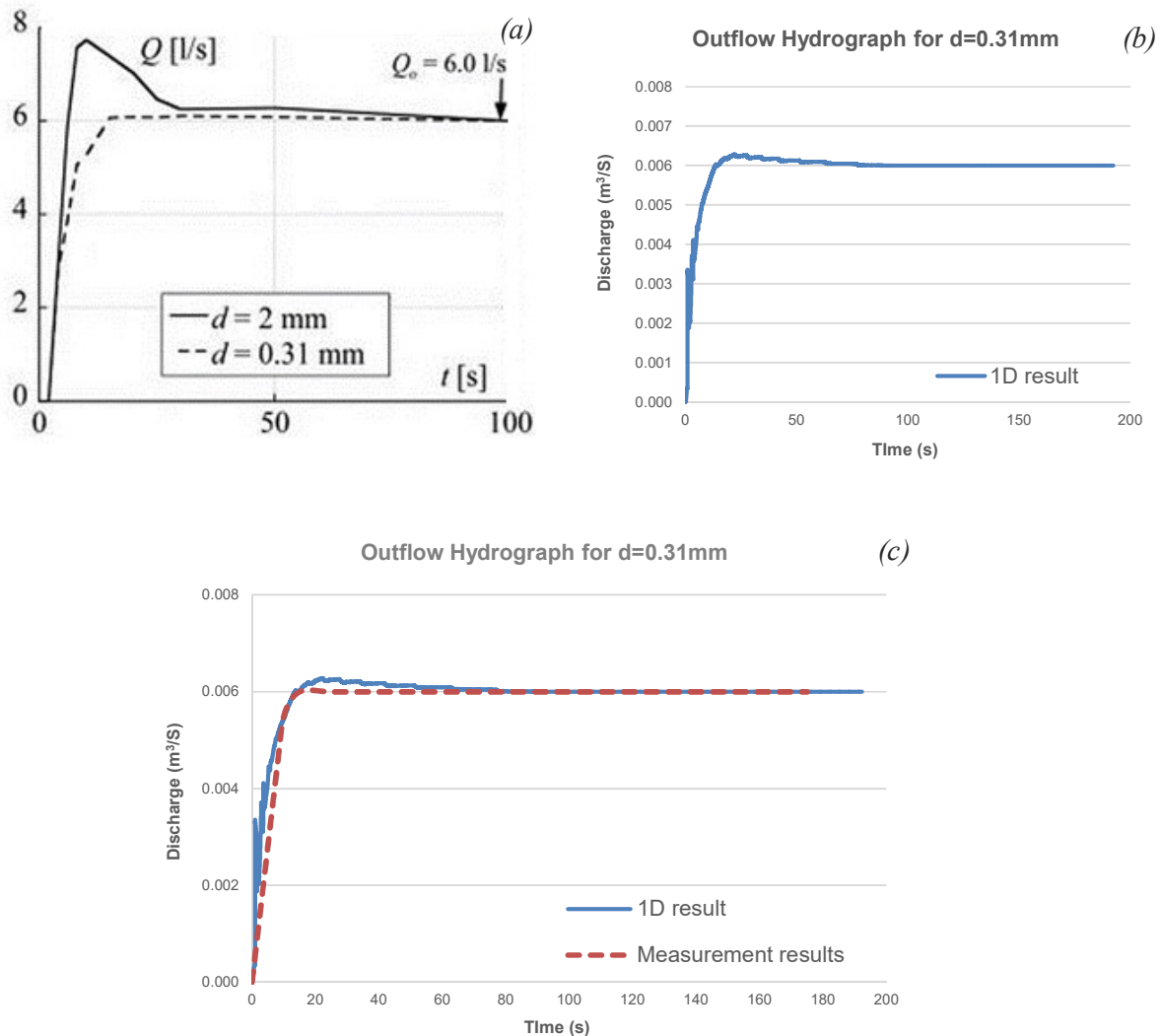
Table 3-10 shows the details about these dam failure tests.

**Table 3-10.** Details of the Schmocker et al. (2013) dam failure tests

Tests	One	Two
Sediment diameter	0.31 mm	2.0 mm
Inflow discharge	6.0 l/s	6.0 l/s
Density	$2650 \text{ kg/m}^3$	$2650 \text{ kg/m}^3$
Cohesion	0.0	0.0
Up and down stream slope	1V:2H	1V:2H

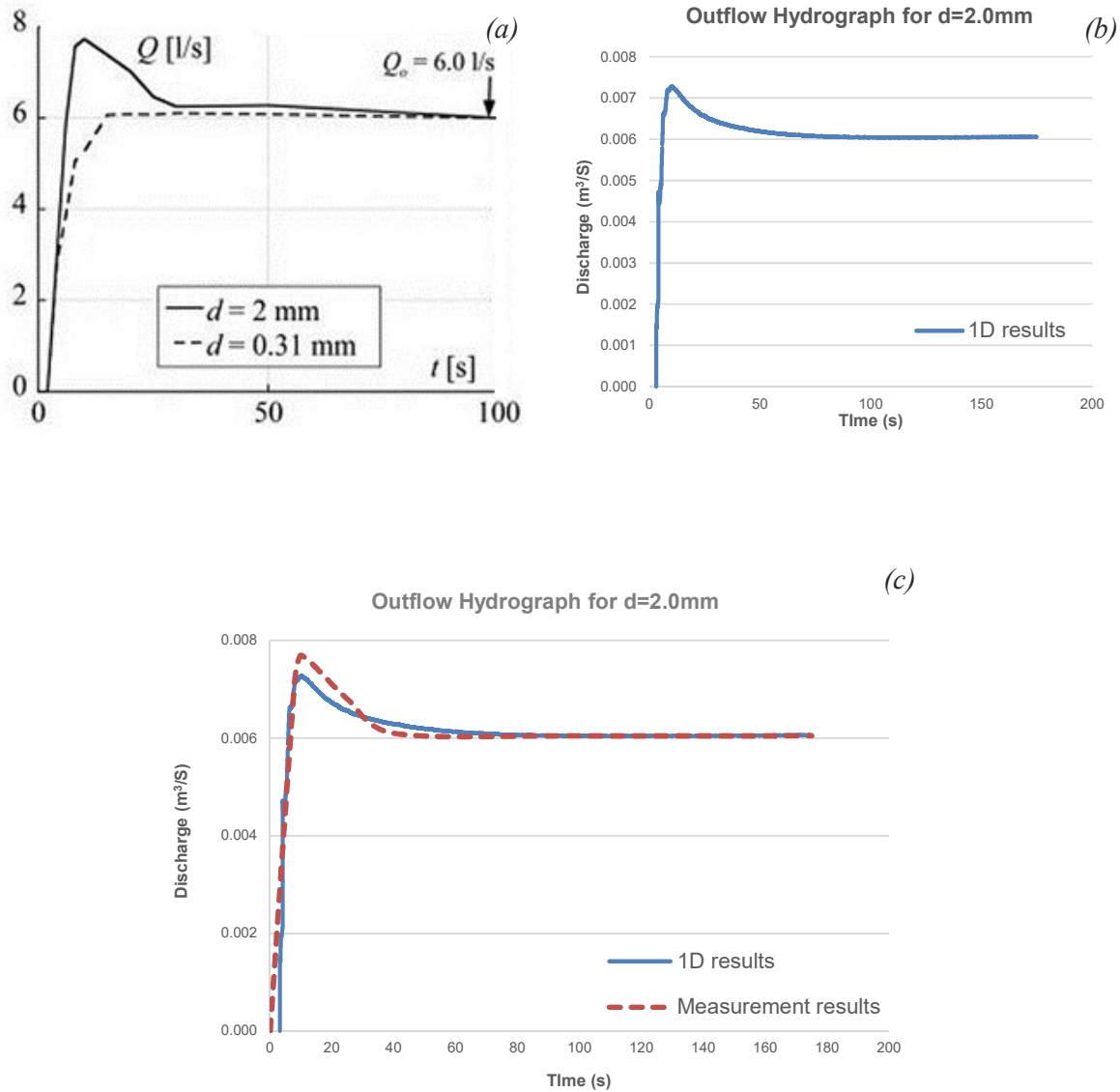
### 3.5.1 One-dimensional ( $d = 0.31$ mm)

In order to model the Schmocker et al. (2013) dam failure tests by using the 1-D program, a fixed spatial step  $\Delta x = 0.01$  m and constant time step  $\Delta t = 0.004$  s are considered. The channel is assumed to be rectangular with a fixed width 0.2 m. Furthermore, the inflow discharge is kept constant 6.0 l/s during failure process. After running the numerical simulation, the measurement hydrographs are compared against the modelled dam failure hydrographs as shown in the Figures 3-21 and 3-22.



**Figure 3-21.** Schmocker outflow hydrograph:(a) Measurement results, (b) 1-D results for  $d=0.31$  mm  
(c) Comparison between measurement and 1-D results

Figure 3-21c demonstrates, the applied calibration approach for the  $\omega$  parameter in the Smart equation has acceptable accuracy for modelling slope more than 20% and the best value is 2.7.

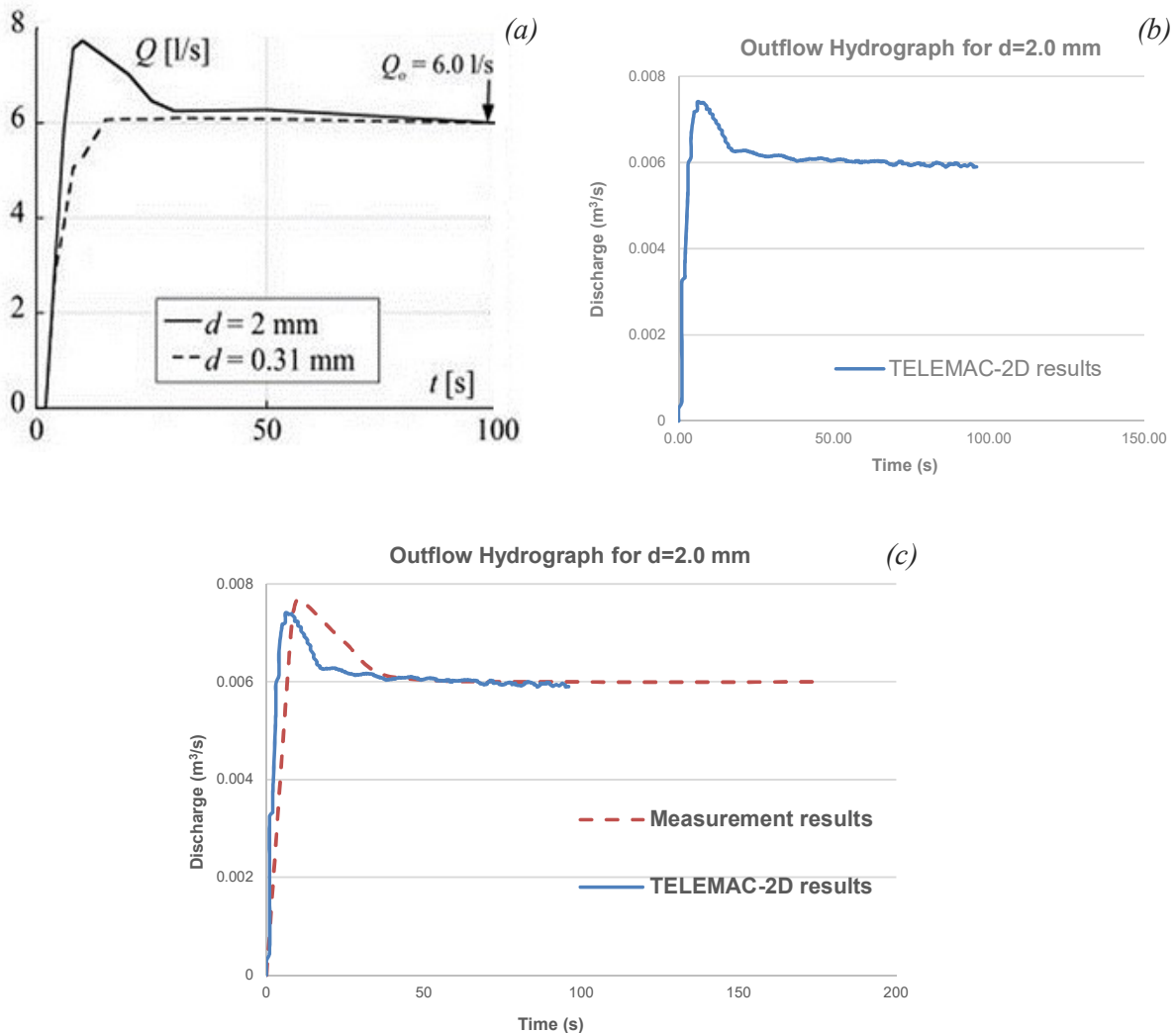
3.5.2 One-dimensional ( $d = 2.0$  mm)

**Figure 3-22.** Schmocker outflow hydrograph:(a) Measurement results, (b) 1-D results for  $d=2.0$  mm  
(c) Comparison between measurement and 1-D results

Figure 3-22c confirms that the applied calibration approach for the  $\omega$  parameter in the Smart equation has acceptable accuracy for modelling slope more than 20% and the best value is 1.2.

### 3.5.3 TELEMAC-2D ( $d = 2.0$ mm)

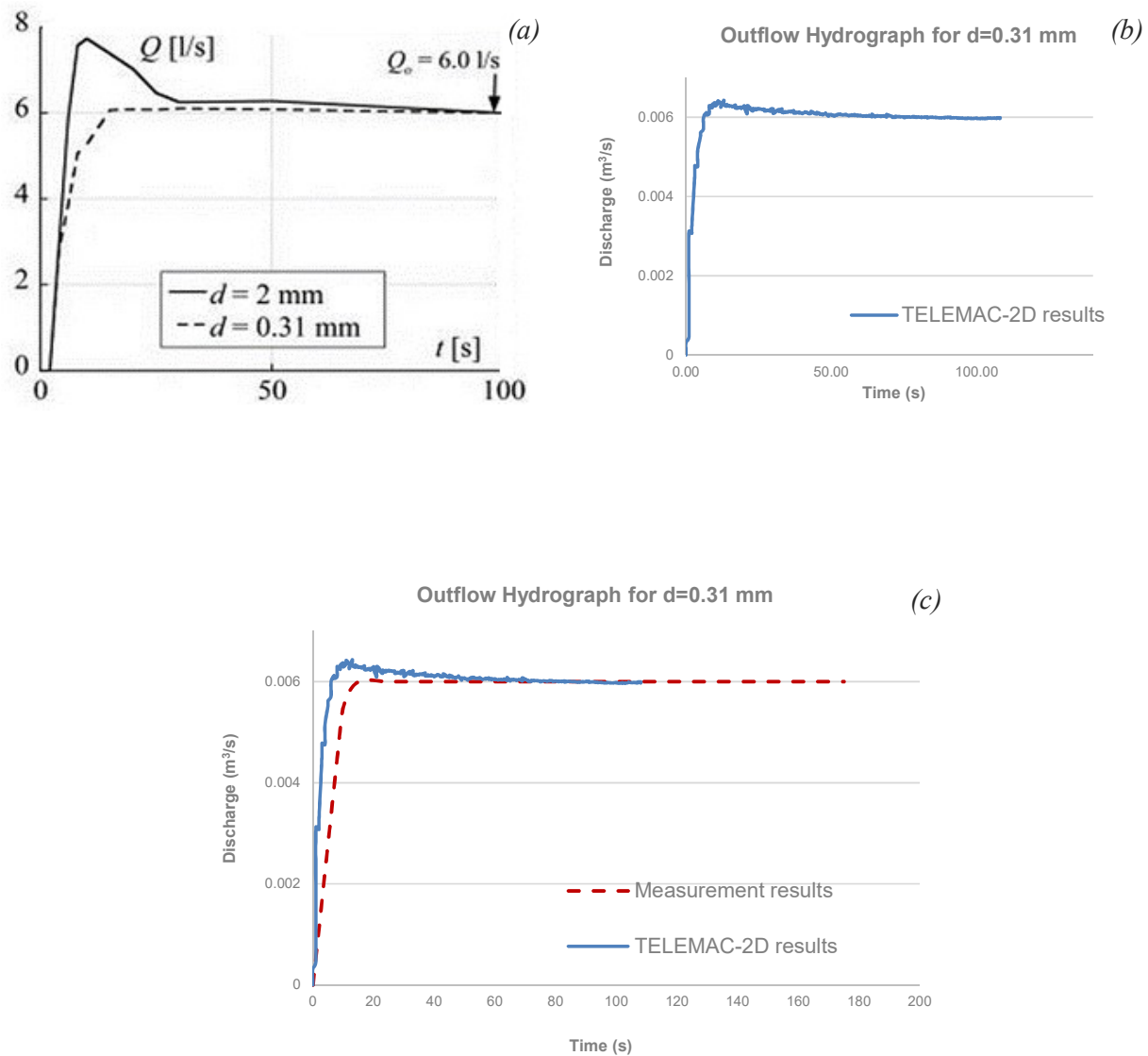
Two similar dams with a mean grain size of 0.31 mm and 2.0 mm are modelled by using TELEMAC-2D software. The experimental setup configuration for this software is represented by 4000 cells, which spatial step varies from 0.03 m for the reservoir and downstream, to 0.01 m for the dam. Furthermore, constant time step 0.05 s is considered throughout the calculation. After running the numerical simulation, the computational results are compared with measurement results as shown in the Figures 3-23 and 3-24.



**Figure 3-23.** Schmocker outflow hydrograph:(a) Measurement results, (b) TELEMAC- 2D results for  $d=2.0$  mm

(c) Comparison between measurement and TELEMAC- 2D results

Figure 3-23c shows that the applied calibration approach for the  $\beta_{tel}$  parameter in the Koch and Flokstra formula has acceptable accuracy for modelling slopes more than 20% and the best value is 4.5.

3.5.4 TELEMAC-2D ( $d = 0.31 \text{ mm}$ )

**Figure 3-24.** Schmocker outflow hydrograph:(a) Measurement results, (b) TELEMAC- 2D results for  $d=0.31 \text{ mm}$   
(c) Comparison between measurement and TELEMAC- 2D results

Figure 3-24c confirms that the applied calibration approach for the  $\beta_{\text{tel}}$  parameter in the Koch and Flokstra formula has acceptable accuracy for modelling slopes more than 20% and the best value is 6.5.

### 3.5.5 Comparison of 1-D program and TELEMAC-2D software

In this part, the modelling results of the one-dimensional program and the TELEMAC-2D software, are compared against the measurement results, these comparisons are shown in Figures 3-25a and 3-25b.

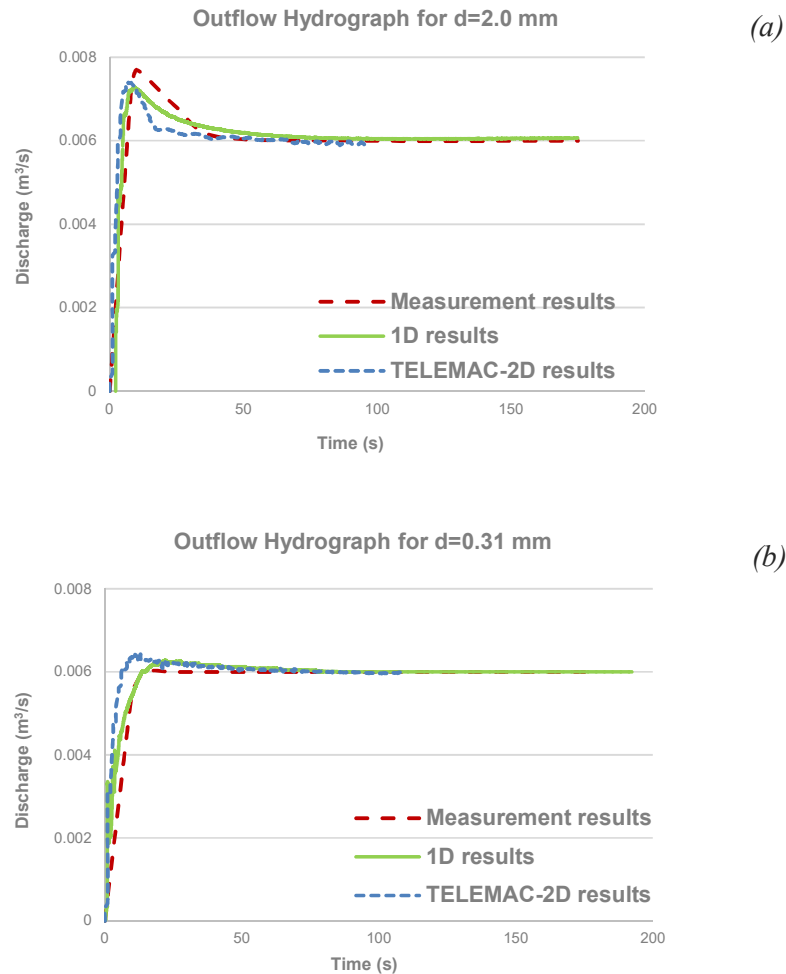


**Figure 3-25.** 1-D program, TELEMAC-2D software and measurement results: (a) For d=2.0 mm, (b) For d=0.31 mm

Based on the above- mentioned numerical results (Figures 3-25a and 3-25b), the following conclusions are achieved:

- Computational stability in the 1-D program is depending on the Courant number and the best result is obtained in the Courant number less than 1.0
- For modelling embankment dam failure with slopes less than 20%, no calibration is needed.
- In dams with slopes more than 20%, the best value for  $\beta$  parameter in the Koch and Flokstra formula is between 4.5- 6.0 and the best value for  $\omega$  parameter in the Smart equation is between 1.1- 2.8 .

---

# Chapter 4

## Influence of geometrical parameters on outflow hydrograph

---

### 4.1 Introduction

In the previous chapters, the main focus was on prediction and calculation of the breach outflow hydrograph in the embankment dams which are failed by overtopping flow. There, influence of the important parameters like different type of the soil and different sediment transport equations were investigated in order to increase the accuracy of the breach outflow hydrograph calculation.

In this chapter, the focus is mainly on the influence of dam's geometrical parameters on the breach outflow hydrograph during failure process. These geometrical parameters are:

- Upstream slope
- Downstream slope
- Crest width
- Initial breach

To achieve a better understanding of these influences, this chapter is divided into the two parts:

- In the first part, influence of the upstream slope, downstream slope and the crest width on the breach outflow hydrograph are investigated by using the Chinnarasri et al. (2003) dam failure test.
- In the second part, influence of the initial breach on the outflow hydrograph is investigated by using the Morris et al. (2008) dam failure test.

In the next sections (sections 4.2 and 4.3), these investigations are explained in more detail.

**Table 4-1.** List of modified geometrical parameters (Chinnarasri et al. (2003))

Test NO.	Upstream slope	Downstream slope	Crest width	Height of the dam
Test one	1V:2H	1V:2H - 5H	10 cm	80 cm
Test two	1V:2H - 5H	1V:2H	10 cm	80 cm
Test three	1V:2H - 5H	1V:2H - 5H	10 cm	80 cm
Test four	1V:2H	1V:2H	10cm – 50 cm	80 cm

## 4.2 Influence of geometrical parameters on the outflow hydrograph

In order to define which geometrical parameters have a more influence on the breach outflow hydrograph, the Chinnarasri et al. (2003) dam failure test is chosen. The details of this test is explained in the Appendix-G.

This dam failure test is numerically modelled by modifying shape parameters as expressed in the Table 4-1 by using TELEMAC-2D software. In all tests, the initial water level in the reservoir is kept constant at 0.83m and downstream water level is kept constant at 0.03m. The soil porosity is 0.35, soil density is  $2.65 \times 10^3 \text{ kg/m}^3$  and the sediment response angles is  $33^\circ$ .

In the following sections, these investigations and comparisons are discussed and explained in more detail.

### 4.2.1 Influence of downstream slope

First investigation concerns about the effects of changes in downstream slope on the breach outflow hydrograph and the crest elevation during failure process.

Herein, the downstream slope of the given dam (the Chinnarasri dam failure test) is changed from 1V:2H to 1V:5H as shown in Figure 4-1. Then, the influence of these modifications are numerically modelled using the TELEMAC-2D software and the final results are compared against each other. The final breach outflow hydrograph and crest elevation are shown in Figures 4-2 and 4-3.

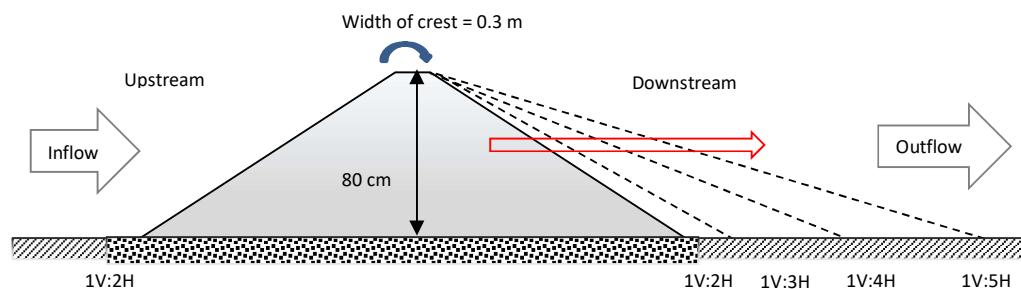


**Figure 4-1.** Downstream slopes variation

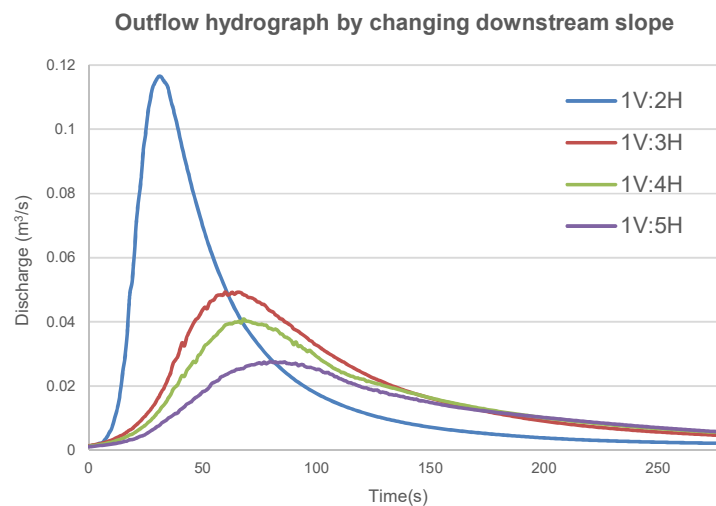


**Figure 4-2.** Influence of different downstream slope on the outflow hydrograph

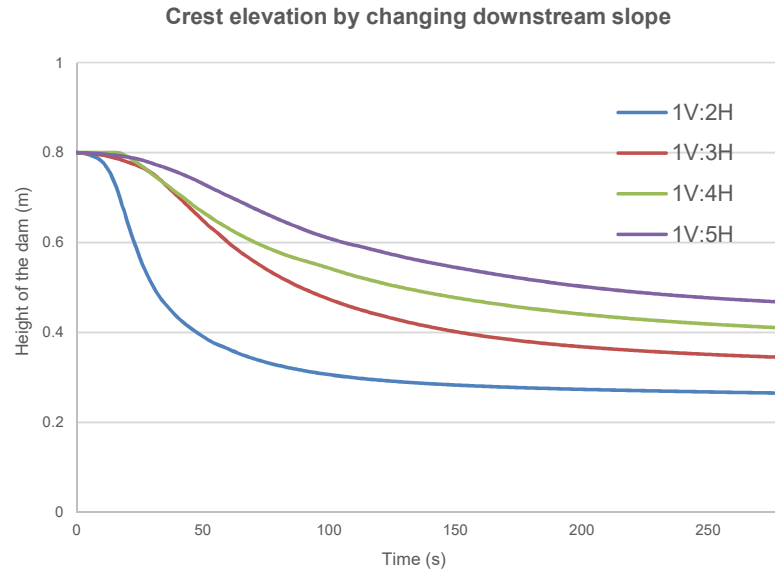


**Figure 4-3.** Influence of different downstream slope on the crest elevation (erosion rate)

The numerical modelling results are given in the Figures 4-2 and 4-3 can be interpreted as the following conclusions:

- By decreasing the downstream slope the peak outflow discharge is decreased and the dam failure time is increased.
- By decreasing the downstream slope the erosion of the dam's material is decreased. Therefore, less volume of water is released from the reservoir of the dam through the downstream valley.

#### 4.2.2 Influence of upstream slope

The next investigation is to model the effects of upstream slope changes on the breach outflow hydrograph. Same as the previous test, the upstream slopes is changed from 1V:2H to 1V:5H as shown in the Figure 4-4. Then, the effects of these changes are modelled numerically using the TELEMAC-2D software and the final results are compared to each other. The final breach outflow hydrograph and crest elevation are shown in Figures 4-5 and 4-6.

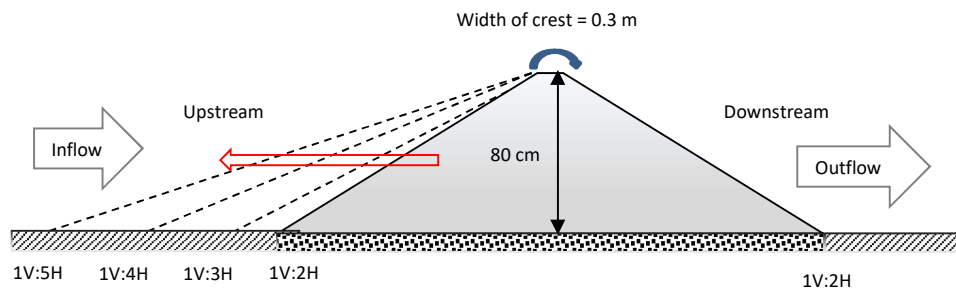


**Figure 4-4.** Upstream slopes variation

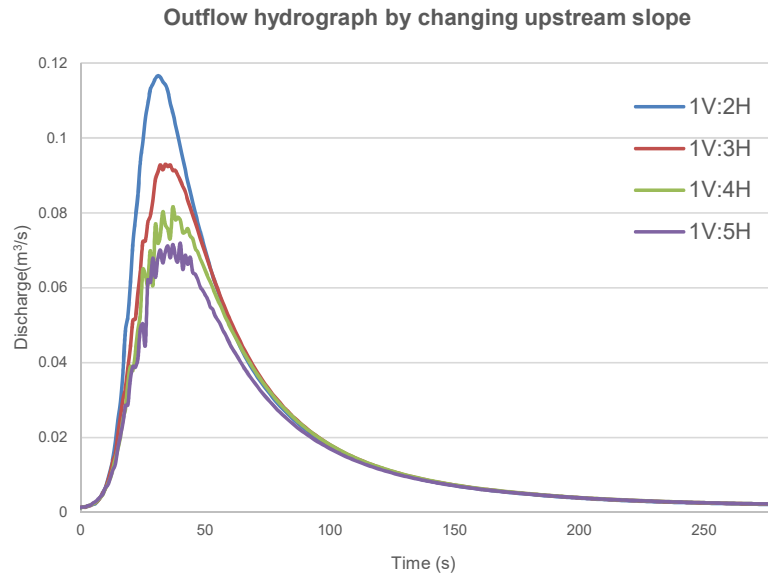


**Figure 4-5.** Influence of different upstream slope on outflow hydrograph

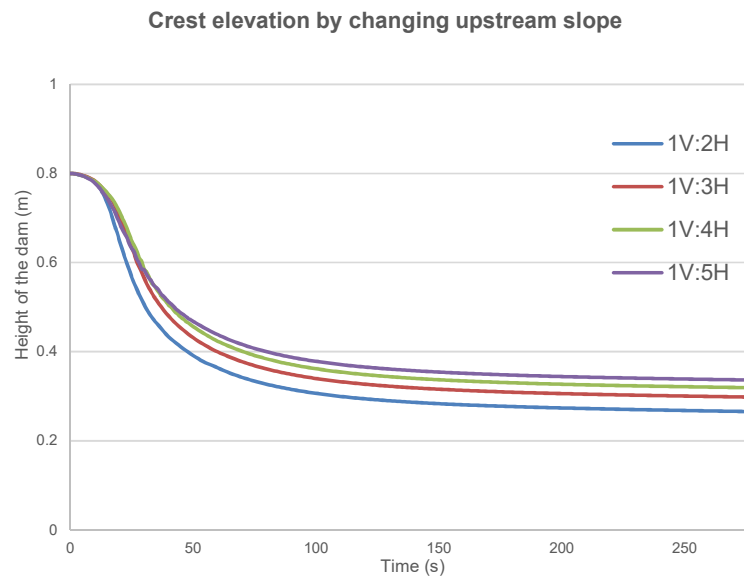


**Figure 4-6.** Influence of different upstream slope on crest elevation (erosion rate)

Figures 4-5 and 4-6 show that by decreasing upstream slope, the peak outflow discharge decreases, but the failure time and crest elevation do not change so much. This means that upstream slope has less influence on the outflow hydrograph in comparison to the downstream slope of a dam.

### 4.2.3 Influence of upstream and downstream slopes

In the previous tests influence of the upstream and downstream slopes on the breach outflow hydrograph in the embankment dam failure were modelled and compared to each other separately. In this section, the influence of the simultaneous changes in both upstream and downstream slopes on the breach outflow hydrograph are modelled using the TELEMAC-2D software. Figure 4-7 shows a schematic picture of the simultaneous change in upstream and downstream slopes of the given dam. The final results of this scenario are shown in the Figures 4-8 and 4-9.

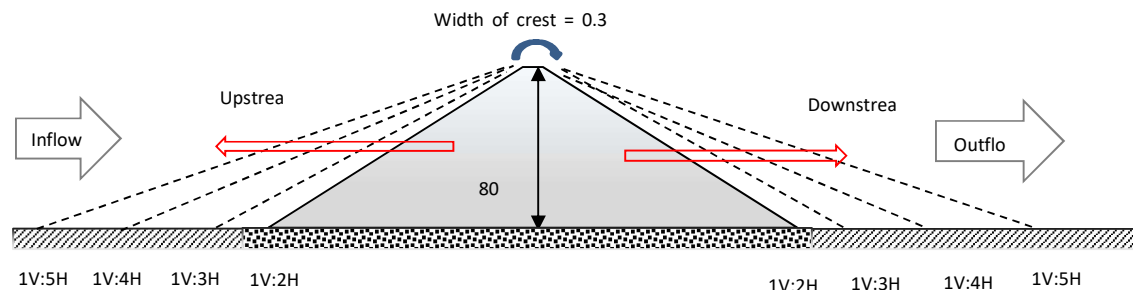


**Figure 4-7.** Change in both upstream and downstream slopes

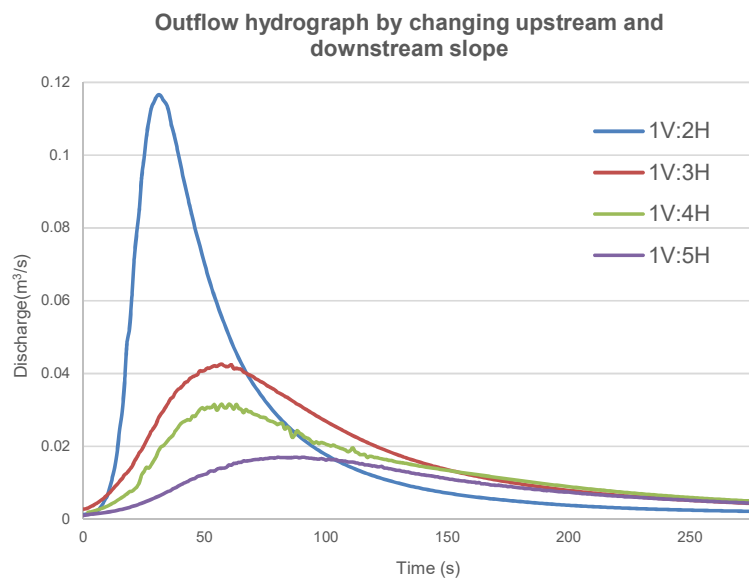


**Figure 4-8.** Influence of different upstream and downstream slope on outflow hydrograph

:

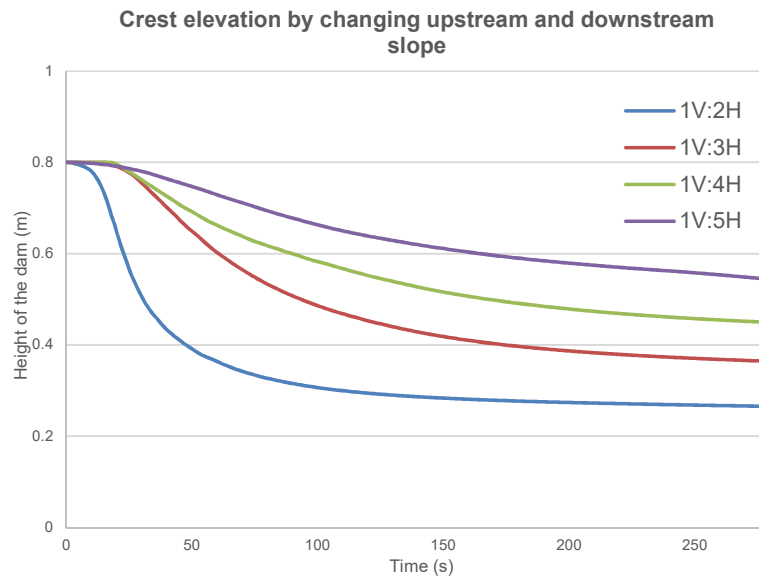


**Figure 4-9.** Influence of different upstream and downstream slope on crest elevation

The results which are shown in the Figures 4-8 and 4-9 follow the same trend which were observed in the Figures 4-2 and 4-3. These identical behaviors confirm that the upstream slopes do not have so much influence on the breach outflow hydrograph in comparison to the downstream slopes.

#### 4.2.4 Influence of crest width

The third important geometrical parameter to investigate is the crest width of the dam. This test can be setup very similar to the previous ones. The only difference here is the changes which are enforced during the modelling on width of the crest from 10cm to 60cm as being illustrated in the Figure 4-10. Here, the upstream slope and downstream slope are always kept constant at 1V:2H. Influences of these modifications on the breach outflow hydrograph and the crest elevation are modelled numerically using the TELEMAC-2D software. The final breach outflow hydrograph and the crest elevation are shown in Figures 4-11 and 4-12:

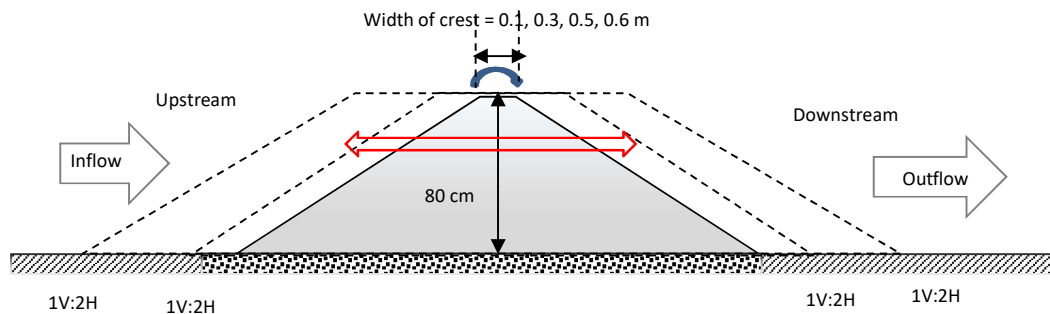


**Figure 4-10.** Change crest width

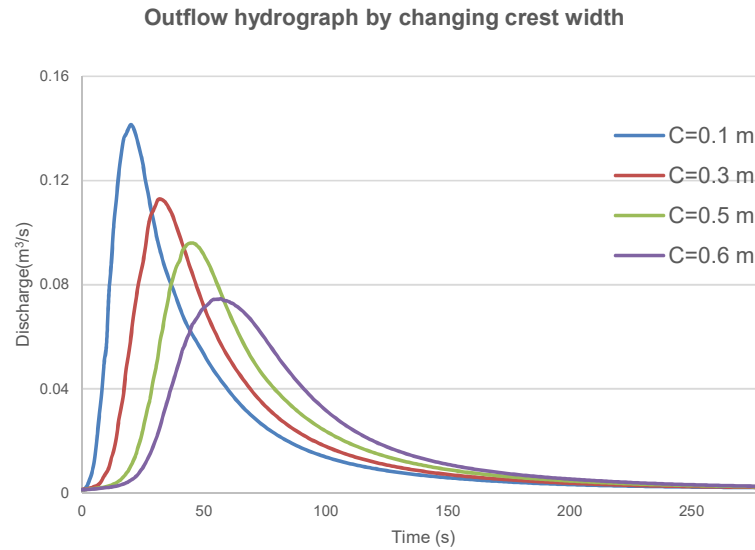


**Figure 4-11.** Influence of different width of the crest on outflow hydrograph

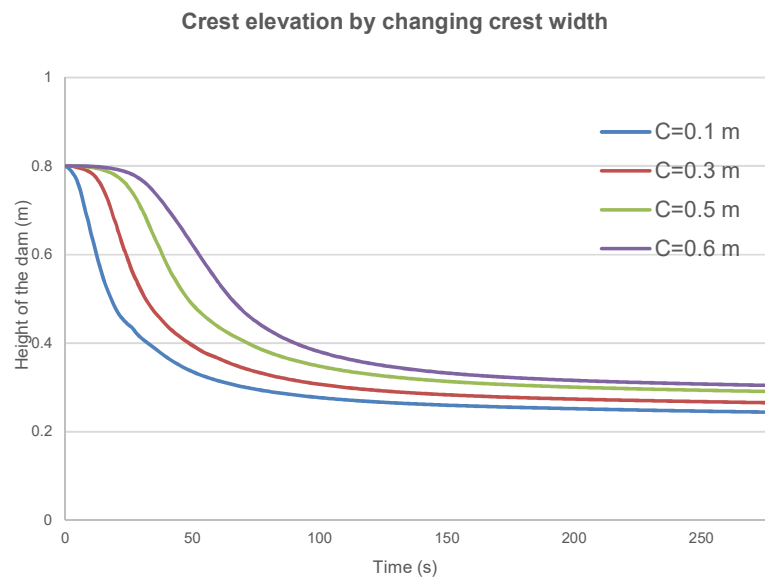


**Figure 4-12.** Influence of different width of the crest on crest elevation(erosion rate)

The modelling results are shown in the Figures 4-11 and 4-12 infer the following conclusions:

- Increase in the crest width will decrease the peak outflow discharge and increase in the failure time.
- Increase in the crest width will increase the lag time in the outflow hydrograph.

### 4.3 Influence of initial breach on outflow hydrograph

One of the major differences between one and two dimensional numerical modelling in embankment dam failure is consideration of the initial breach. In order to find the influence of the mentioned issue on the final results, two different scenarios have been made on the Morris et al. (2008) dam failure test.

- First scenario, initial breach is considered in the center of the crest.
- Second scenario, no initial breach is considered on the dam crest (Figure 4-13).

These scenarios are modelled numerically with the TELEMAC-2D software, 1-D program and empirical formulas and the final results are compared against each other.

In the following, these sections are explained in more detail.

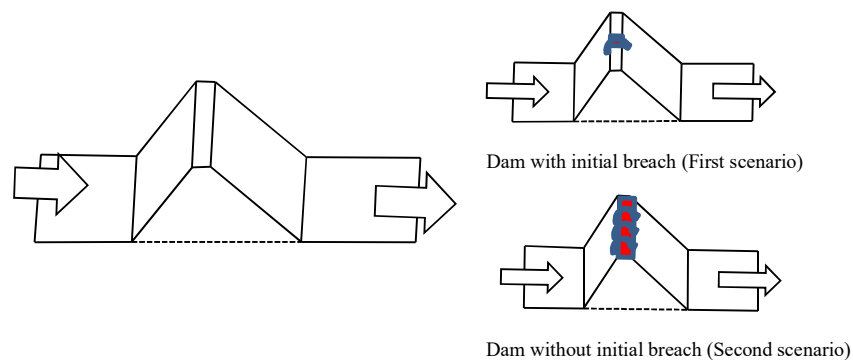


**Figure 4-13.** Influence of initial breach on the outflow hydrograph

#### 4.3.1 IMPACT project (Test No.2)

The IMPACT project (Morris et al. (2008)) is one of the well-known large scale dam-break projects which has been done in Norway in 2002. This embankment dam was built mainly from non-cohesive soil with  $d_{50}=4.75$  mm. The main purpose of this test was to have a better understanding of the failure mechanism in the homogeneous non-cohesive embankment dams which are failed by the overtopping flow. The parameters regarding this test are given in the Table 4-2.

**Table 4-2.** IMPACT project detail

Dam Height [m]	dam shoulder slopes	Initial breach depth [m]	Initial breach width [m]	Reservoir volume [m <sup>3</sup> ]	$d_{50}$ [mm]	Porosity	Cohesion [KN/m <sup>2</sup> ]	Inflow discharge [m <sup>3</sup> /s]
5.0	1V:1.7H	0.1	2.0	90000	4.75	0.22	0.0	< 5



**Figure 4-14.** The IMPACT project site picture

#### 4.3.2 Modelling IMPACT project by using TELEMAC-2D software

The TELEMAC-2D software is used to model the IMPACT project dam failure test (Morris et al. (2008)) with two different scenarios:

- Dam with initial breach.
- Dam without initial breach.

For this purpose, the domain (consisting of the reservoir, dam and downstream) is divided into 4000 cells. The spatial step varies from 1.5 m (for the reservoir and downstream) to 0.5 m (for the dam), and the time step is fixed at 0.05 s. Here, the Peter-Müller equation along with the Koch and Flokstra correction formula are applied to calculate sediment transport load during failure process. The details of the final mesh are shown in Figure 4-15 and the comparison between two scenarios are explained in the next sections.

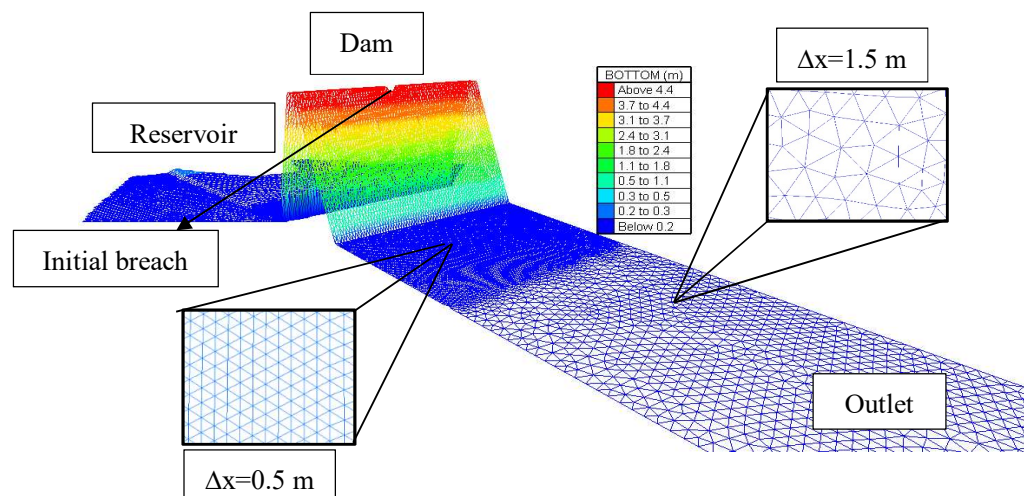


**Figure 4-15.** Modelling the IMPACT project using TELEMAC-2D software

#### 4.3.2.1 Comparison of the TELEMAC-2D and measurement results (First scenario)

The modelling hydrograph for the first scenario (dam with initial breach) is compared to the IMPACT measurement hydrograph and the final results are shown in Figure 4-16.

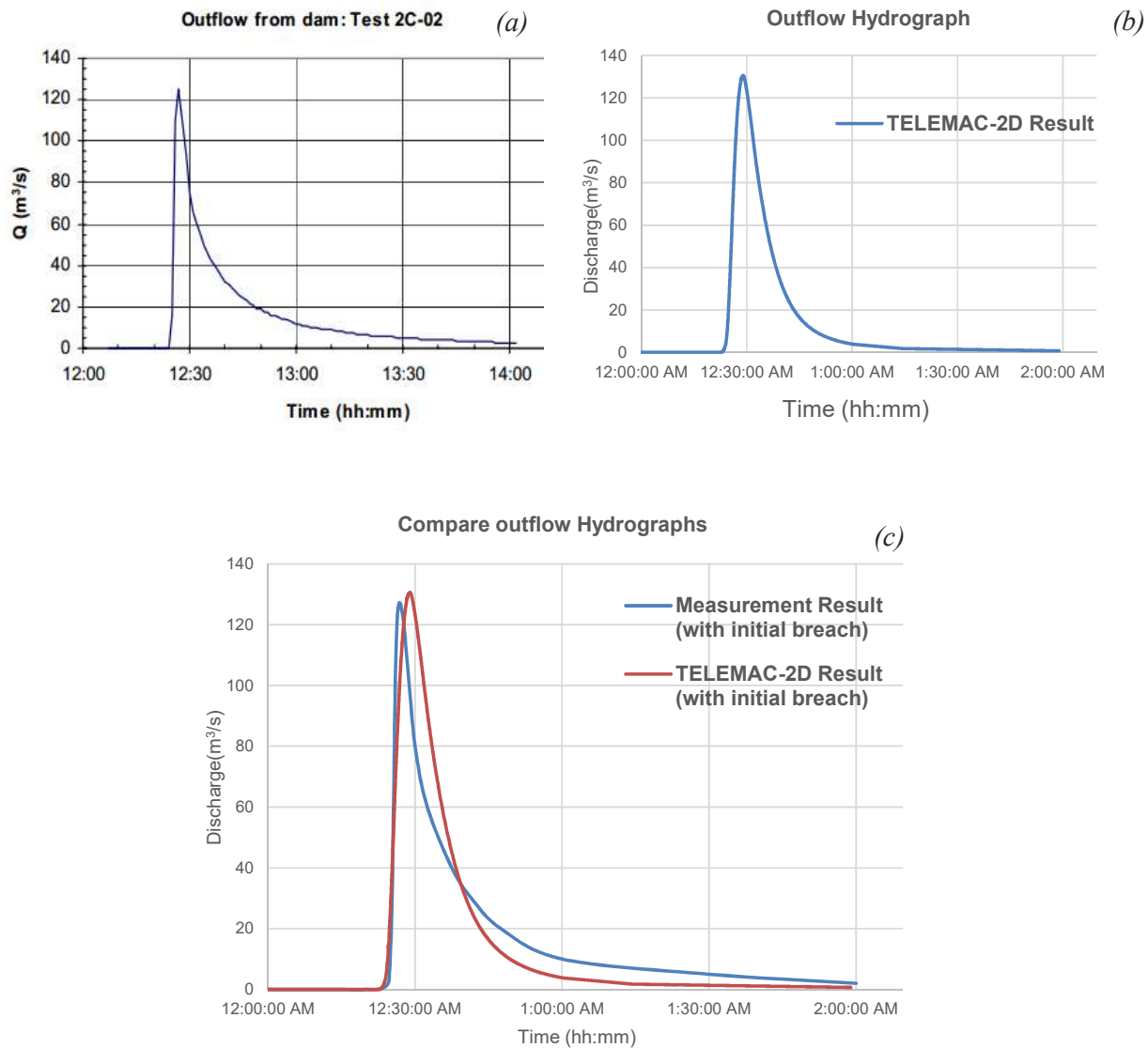


**Figure 4-16.** IMPACT outflow hydrograph: (a) Measurement results, (b) TELEMAC- 2D results (c) Comparison between measurement and TELEMAC- 2D results (First scenario)

The comparison results confirm that it is possible to model an embankment dam failure with the TELEMAC software in an appropriate manner. Additionally, this result confirms that the best value for  $\beta_{\text{Tel}}$  parameter in the Koch and Flokstra formula (Equation 3-66) is a value in the range of 4.5-6.0.

#### 4.3.2.2 Comparison of TELEMAC-2D and measurement results (Second scenario)

Herein, the second scenario (dam without initial breach) is numerically modelled by using the TELEMAC-2D software to find the influence of the initial breach on the outflow hydrograph. The final result is compared with the measurement result as shown in the Figure 4-17.

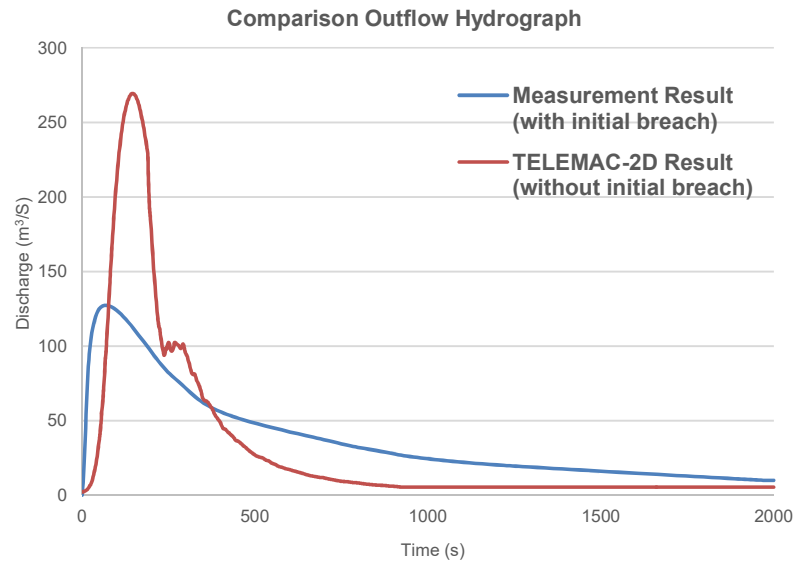


**Figure 4-17.** Influence of initial breach (Second scenario)

This figure shows that the calculated outflow hydrograph without initial breach gives the higher values in peak outflow discharge and lower values in the failure time compared with the actual measurements.

#### 4.3.3 Modelling IMPACT project by using 1-D program

In this part we will use the written 1-D program to model the IMPACT project. Two basic assumptions are considered within this 1-D procedure. These two assumptions are fundamental in the 1-D software:

- The initial breach is ignored or the whole length of the crest is eroded at the same time.
- The rectangular shape with constant width is considered to model the reservoir and downstream of the dam.

The details of these assumptions and the calculated outflow hydrograph are shown in Figures 4-18 and 4-19.



**Figure 4-18.** 1-D dam failure modelling assumptions

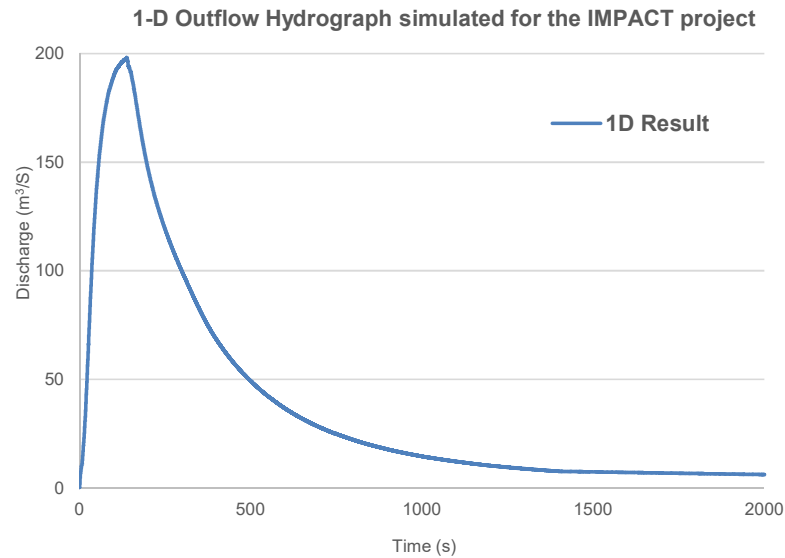


**Figure 4-19.** 1-D result for the IMPACT project

#### 4.3.4 Compare results of the 1-D program, TELEMAC-2D software and empirical formula

After modelling the IMPACT project by using the 1-D program and TELEMAC-2D software in the previous parts, the breach outflow hydrograph of this test is calculated and predicted by using the empirical formulas (Equations 2-3, 2-4 and 2-9). The final results of these methods are compared to the measured result as shown in the Figure 4-20.

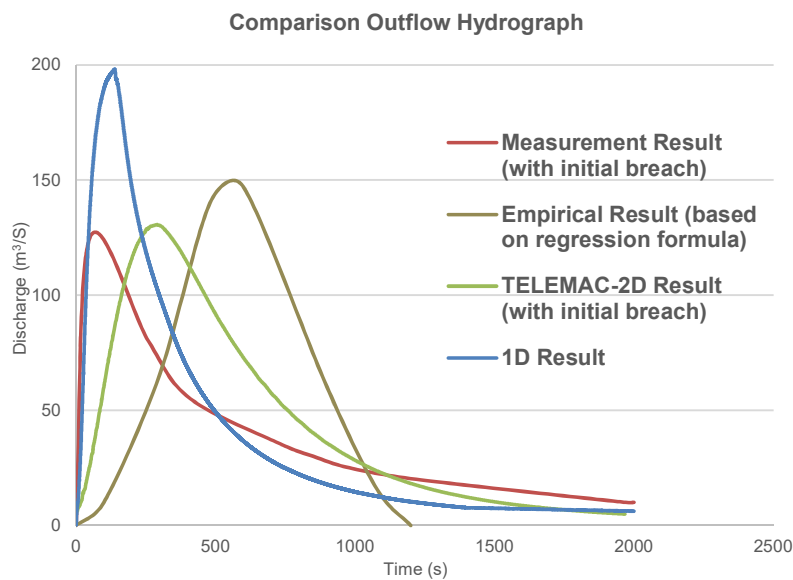


**Figure 4-20.** Compare results between 1-D program, TELEMAC-2D, empirical method and measurement result

Figures 4-16 and 4-20 show that the TELEMAC-2D software has good accuracy while the results of the empirical method and 1-D program have some difference with the measurement result. The main reasons for these differences are related to the basic assumptions which were used in each of them. These assumptions are:

- In the empirical formula, it was assumed that the outflow hydrograph is symmetric and the whole reservoir become empty during the failure time.
- In the one-dimensional numerical modelling, the reservoir's shape was assumed as the rectangular with constant width and the entire length of the crest is eroded simultaneously.

In general, Figures 4-16 and 4-20 reveal that these three methods based on their assumptions, give acceptable approximations for determining the breach outflow hydrograph in embankment dam failure modelling.

### 4.3.5 Influence of the sediment response angles on the outflow hydrograph

This investigation concerns about the effects of the sediment response angles on the breach outflow hydrograph during failure process.

Herein, the sediment response angle( $\psi$ ) and downstream slope of the given dam (Morris et al. (2008)) are changed from  $25^\circ$  to  $40^\circ$  and 1V:2H to 1V:5H respectively (Table 4-3). The influence of these modifications are numerically modelled using the TELEMAC-2D software and the final breach outflow hydrographs are shown in Figures 4-21 to 4-24.

**Table 4-3.** List of modified sediment response angles (Morris et al. (2008))

Upstream slope	Downstream slope	sediment response angles( $\psi$ )	Height of the dam	Reservoir volume
1V:1.7H	1V:1.7H - 5H	$30^\circ$ - $45^\circ$	5.0 m	90,000 m <sup>3</sup>

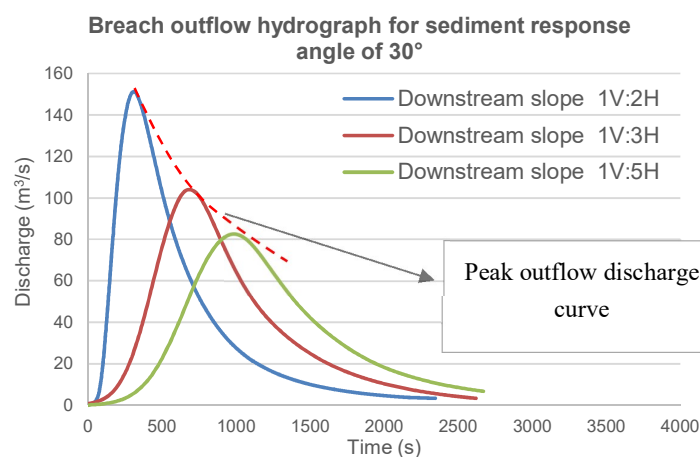


**Figure 4-21.** Influence of sediment response angle on outflow hydrograph( $\psi=30$ )

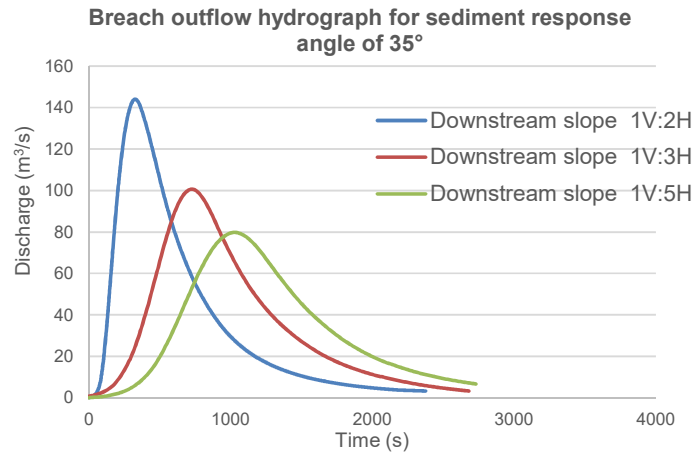


**Figure 4-22.** Influence of sediment response angle on outflow hydrograph( $\psi=35$ )

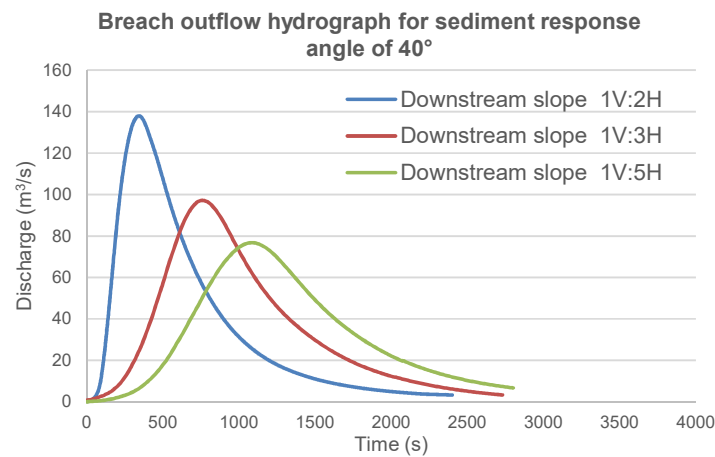


**Figure 4-23.** Influence of sediment response angle on outflow hydrograph( $\psi=40$ )

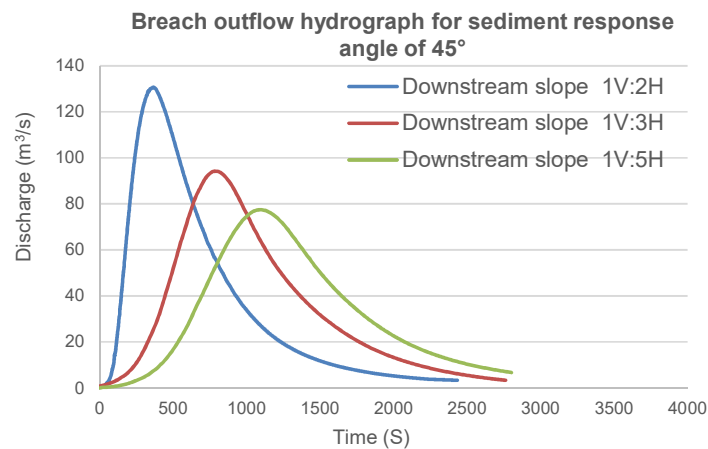


**Figure 4-24.** Influence of sediment response angle on outflow hydrograph( $\psi=45$ )

In order to illustrate influence of the sediment response angle on the breach outflow hydrograph the peak outflow discharge curves in the Figures 4-21, 4-22, 4-23 and 4-24 are compared against each other as shown in the Figure 4-25.

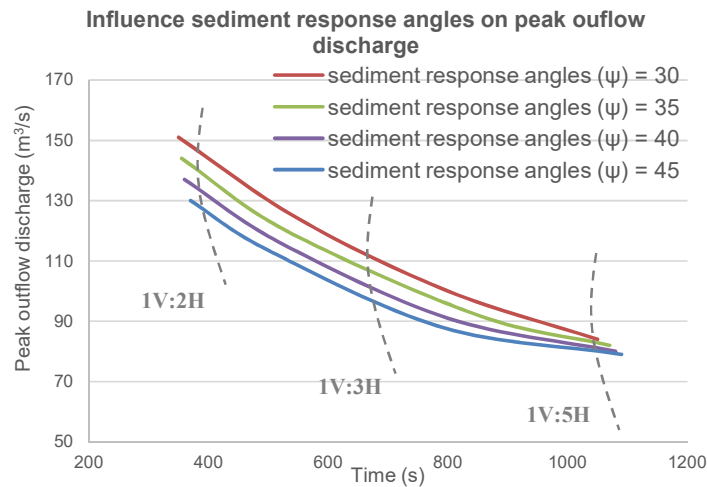


**Figure 4-25.** Compare all results

Figure 4-25 can be interpreted as the following conclusions:

- By increasing sediment response angle, the peak outflow discharge is reduced during failure process.
- By decreasing downstream slope influence of sediment response angle on the peak outflow discharge is decreased during failure process.

#### 4.3.6 Influence of the crest width on the outflow hydrograph

In this section influence of the crest width on the breach outflow hydrograph is investigated. Here in, width of the crest and height of the given dam (Morris et al. (2008)) are changed from 2.0 to 10.0 m and 5.0 to 50.0 m respectively (Table 4-4). In all tests, the upstream slope and downstream slope are always kept constant at 1V:1.7H, the soil porosity is 0.22 and soil density is  $2.12 \times 10^3 \text{ kg/m}^3$ . Influences of these modifications on the breach outflow hydrograph are modelled numerically using TELEMAC-2D software. The final breach outflow hydrographs are shown in Figures 4-26 and 4-27.

**Table 4-4.** List of modified crest width (Morris et al. (2008))

Upstream slope	Downstream slope	Crest width	Height of the dam	Reservoir volume
1V:1.7H	1V:1.7H	2.0-5.0-10.0 m	5.0	90,000 m <sup>3</sup>
1V:1.7H	1V:1.7H	2.0-5.0-10.0 m	50.0 m	2,000,000 m <sup>3</sup>

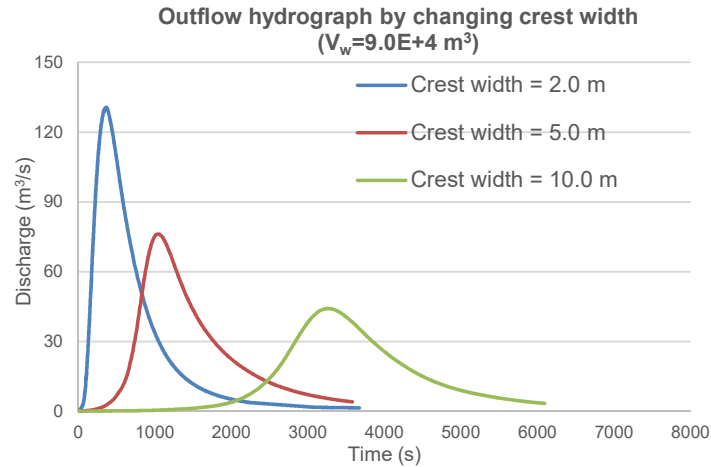


**Figure 4-26.** Influence of different width of the crest on outflow hydrograph ( $H_d = 5.0 \text{ m}$ )

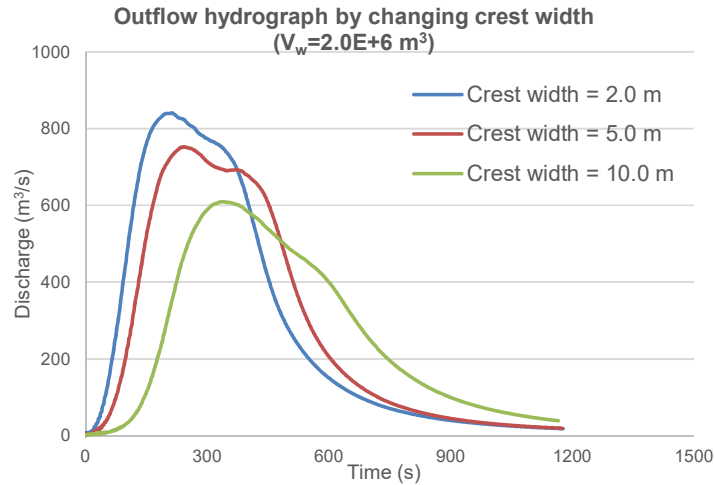


**Figure 4-27.** Influence of different width of the crest on outflow hydrograph ( $H_d = 50.0 \text{ m}$ )

Figures 4-26 and 4-27 reveal that by increasing width of the crest the peak outflow discharge decrease and failure time increased. Furthermore, increase in the crest width will increase the lag time in the breach outflow hydrograph.

# Chapter 5

## Flood wave propagation downstream of a dam

### 5.1 Introduction

In the previous chapters different methods to calculate the breach outflow hydrograph of the embankment dams were introduced and discussed.

In this chapter, the most important parameters of the dam-break flood at the downstream valley are determined. These parameters are:

- Maximum discharge
- Flood wave arrival time

In order to calculate these parameters, two relationships are introduced and examined.

- In the first relationship, an equation to calculate the peak outflow discharge curve is introduced by connecting the maximum value of the cross section hydrographs downstream of the dam. (Figure 5-2a)
- In the second relationship, an arrival time equation is calculated by assuming a linear equation for wave arrival time along the channel. (Figure 5-2b)

In the following sections, the relationships concerning the calculation of these two parameters are discussed in more detail.

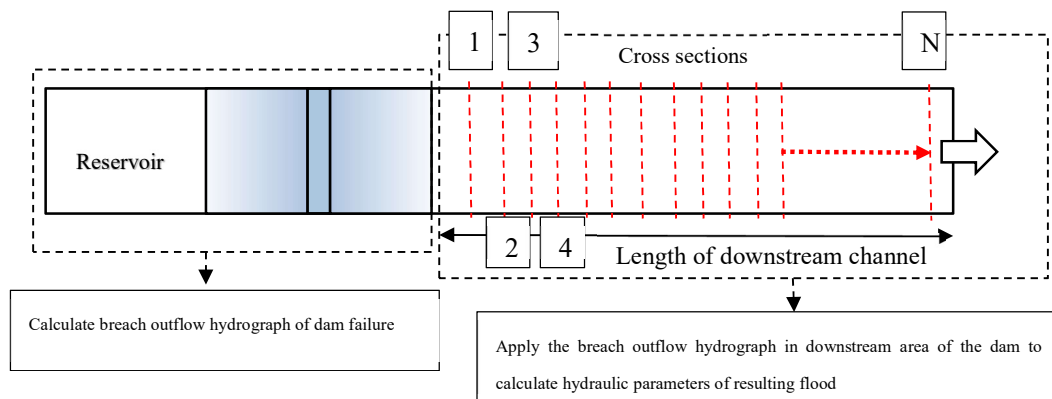


**Figure 5-1.** The plan view of a hypothetical dam along with the downstream area

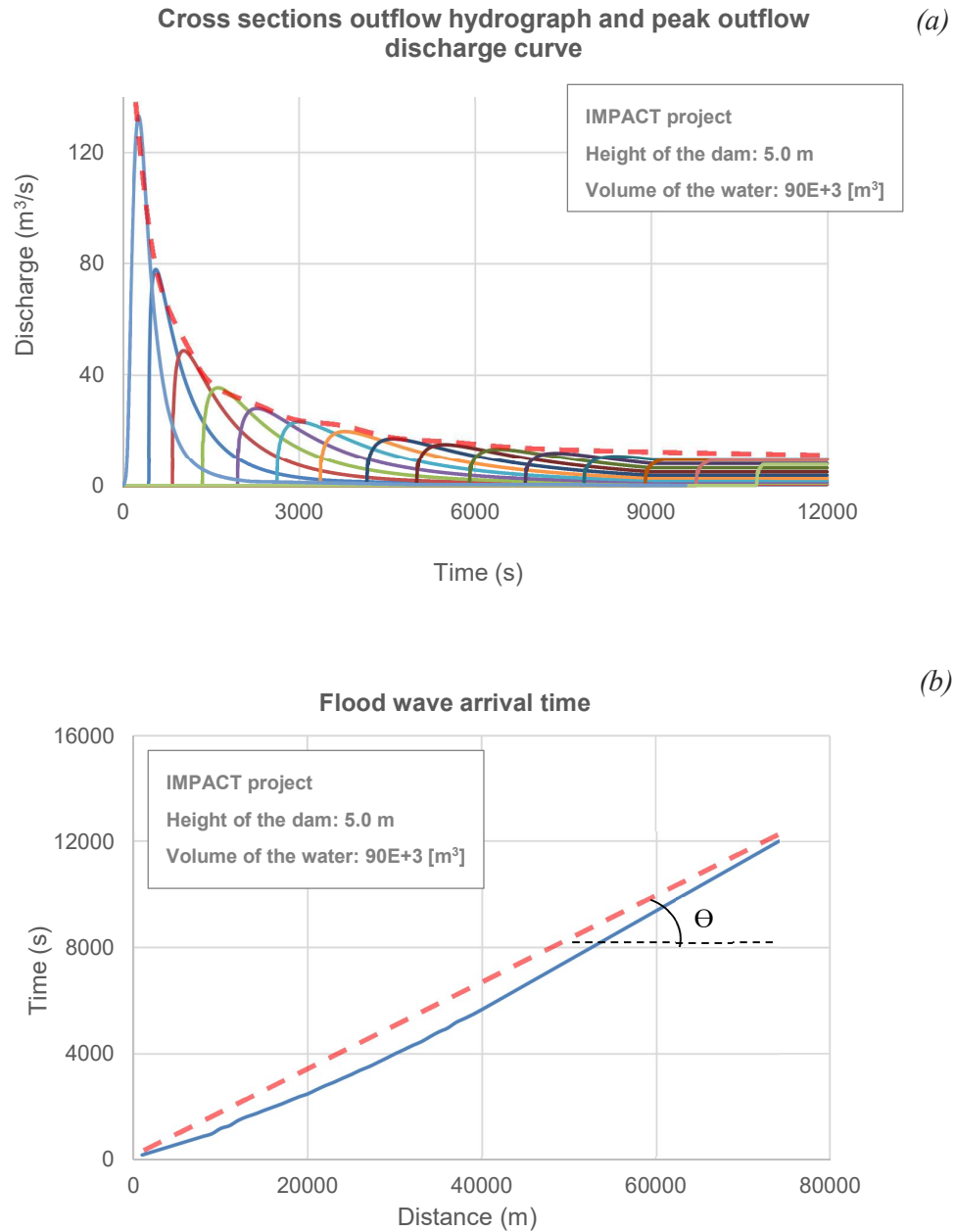


**Figure 5-2.** Dam-break flood wave parameters: (a) Peak outflow discharge curve (b) Arrival time line

Figures 5-2 (a) and (b) show the peak outflow discharge curve and wave arrival time line for the downstream side of the IMPACT dam failure project (Morris et al. (2008)). This dam failure test has been explained in the Sections 2.4.1 and 4.3.1.

## 5.2 Calculation of the peak outflow discharge and flood wave arrival time

### 5.2.1 Dataset collection and preparation

In order to find the best relationships for the peak outflow discharge and flood wave arrival time, 14 embankment dams and 57 channels are numerically modelled. Furthermore, these dams and channels are modelled by considering the following conditions:

#### All dams

- Have non-cohesive soil with same grain size ( $d_{50}=4.75$  mm) and same numerical configuration.
- Are numerically failed and modelled with TELEMAC-2D and SISYPHE software.
- Are failed by overtopping flow with initial breach in the middle of the crest.
- Have rectangular reservoir shapes.

#### All channels

- Have rectangular shape with 1%, 5% and 10% slope.
- Are numerically modelled with TELEMAC-2D software.
- Have 20 km length with 10, 20 and 30 Strickler Roughness coefficients.
- Are divided into 20 sections and cross-sections discharge are calculated for each of them.

The specific information related to each of these dams and channels are listed in Table 5-1. Furthermore, a numerical approach is used in order to calculate the peak outflow discharge and wave arrival time at the downstream of the dams. The details of these numerical modelling are given in the Appendix-D, E and F.

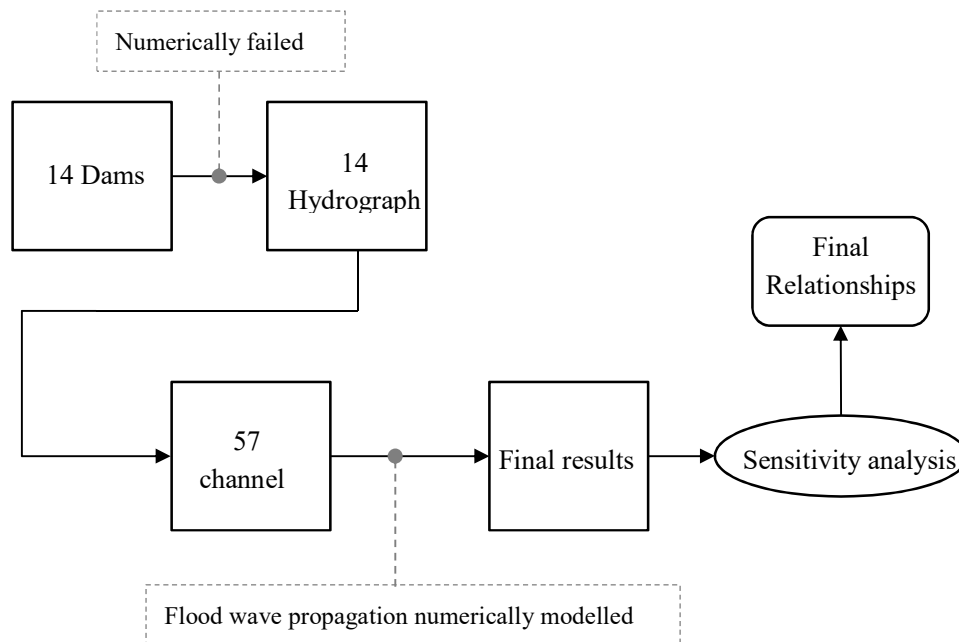


**Figure 5-3.** Procedure to find the peak outflow discharge and arrival time

**Table 5-1.** List of embankment dam failure

Height of the dam [m]	Width of the channel [m]	Reservoir volume [m <sup>3</sup> ]
50	36	2.0E+6
		12.0E+6
		40.0 E+6
50	250	2.0E+6
		12.0E+6
		40.0 E+6
50	500	2.0E+6
		12.0E+6
		40.0 E+6
80	36	2.0E+6
		2.0E+6
		12.0E+6
80	250	2.0E+6
		12.0E+6
		40.0 E+6
80	500	2.0E+6
		12.0E+6
		40.0 E+6

### 5.2.2 New approach to find the peak outflow discharge

The peak outflow discharge downstream of the dam mostly depends on the parameters like type of the dam, type of the failure, failure time, manning number and reservoir volume. In order to consider the influence of these parameters in one relationship, some simplifications needed to be made. One of the main simplification in this regard is the assumption of considering the peak outflow discharge curve instead of calculating different outflow hydrograph downstream of a dam. The peak outflow discharge curve is defined as a line which connects the maximum discharge value ( $Q_p$ ) of the cross section hydrographs downstream of a dam. This curve represents the magnitude of the breach outflow hydrograph at any locations within the downstream valley. A schematic picture of the peak outflow discharge curve is shown in Figure 5-4.

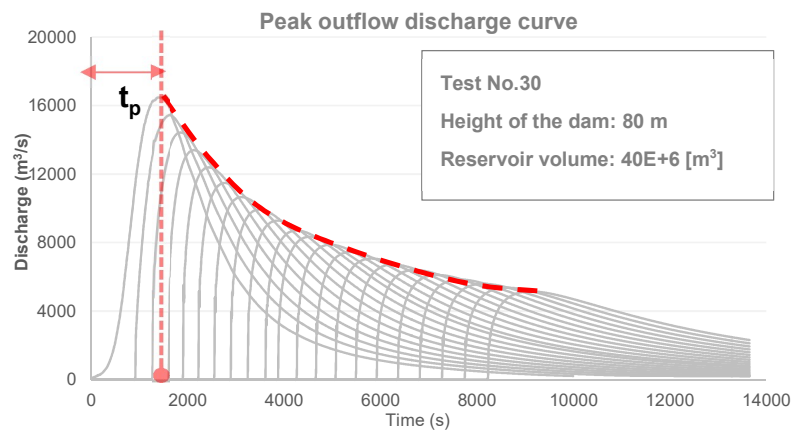


**Figure 5-4.** Peak outflow discharge curve (Test No.30)

In order to find the relationship to calculate the peak outflow discharge curve a sensitivity analysis was performed on the prepared dataset (Appendix-F). The final results of this sensitivity analysis are shown in the following:

- Each dam has a particular peak outflow discharge curve shape.
- In all dam failures the peak outflow discharge is reduced along the channel
- Shape of the peak outflow discharge curves directly depends on a so-called parameter ‘reduction value’ ( $\delta_R$ ) as illustrated in Figure 5-5.

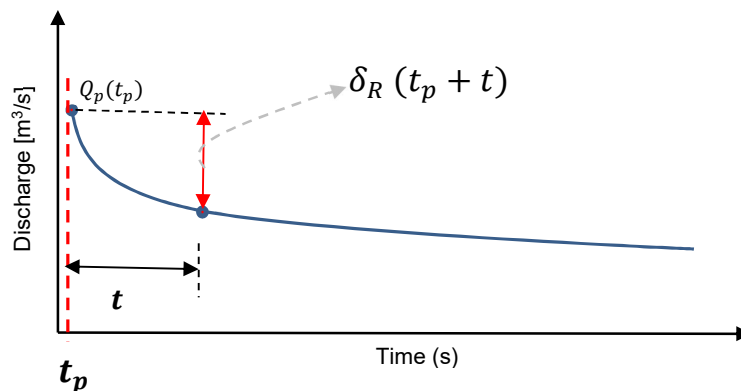


**Figure 5-5.** The ‘reduction value’ ( $\delta_R$ ) parameter on the peak outflow discharge curve

Based on the sensitivity analysis, it has been found that the ‘reduction value’ ( $\delta_R$ ) depends on the following parameters:

- Strickler roughness coefficient (Ks)
- Breach peak outflow hydrograph ( $Q_p$ )
- Time (t)

These parameters can be expressed in one equation as shown in the Equation 5-1.

$$\delta_R (t_{p+t}) = \frac{Q_p (t_p)}{Ks * \left(\frac{t_{p+t}}{3600}\right) * \ln\left(\frac{t_p}{300}\right)} \quad 5-1$$

Furthermore, results of our sensitivity analysis reveal that the accuracy of the Equation 5-1 can be improved significantly by using the time discretization (Equation 5-2).

$$t = i * \Delta t \quad 5-2$$

Here,  $\Delta t$  is the time step and  $i$  is the number of time step

By substituting Equation 5-2 into Equation 5-1, the final equation for the ‘reduction value’ ( $\delta_R$ ) can be expressed as the Equation 5-3. This procedure is illustrated in Figure 5-6.

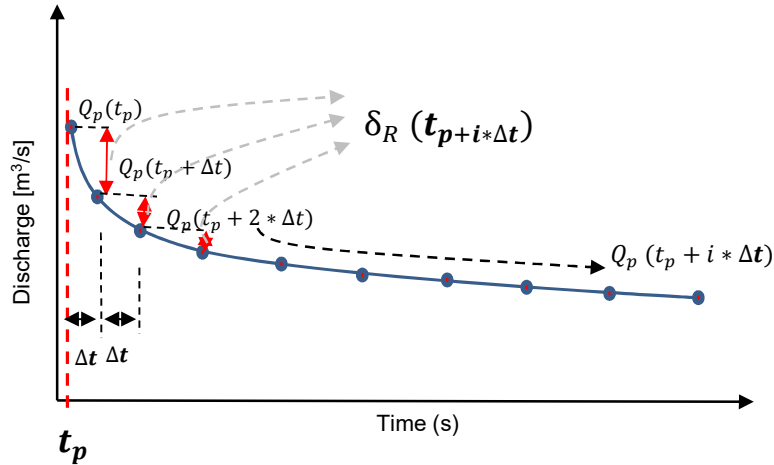


**Figure 5-6.** Time discretization (time steps) concept on the peak outflow discharge curve

$$\delta_R (t_{p+i*\Delta t}) = \frac{Q_p (t_{p+(i-1)\Delta t})}{Ks * \left(\frac{t_{p+i*\Delta t}}{3600}\right) * \ln\left(\frac{t_p}{300}\right)} \quad 5-3$$

After calculating reduction value ( $\delta_R$ ) from Equation 5-3, the peak outflow discharge curve can be calculated using Equation 5-4.

$$Q_p(t_p + (i)\Delta t) = Q_p(t_p + (i - 1)\Delta t) - \delta_R(t_{p+i\Delta t}) \quad 5-4$$

Here,  $t_p$  [s] is the time to reach peak outflow discharge and  $\Delta t$  [s] is the time step

In Equations 5-3 and 5-4, the known parameters are  $Q_p$ ,  $K_s$  and  $t_p$  while unknown parameter is  $\Delta t$ .

In order to calculate  $\Delta t$ , calibration and sensitivity analysis are used based on our prepared database. Here, this calibration is performed for a wide range of  $\Delta t$  parameter, and the calibration results are shown in the Table 5-2.

**Table 5-2.** Calibrated  $\Delta t$  value for calculating maximum discharge

Calibrated parameter	Value	Max. discharge range [ $\frac{m^3}{s} \times 10^3$ ]
$\Delta t$	100.0-120.0 (s)	0.6-16

### 5.2.3 New approach to find flood wave arrival time

In the previous part the relationship to calculate the peak outflow discharge curve was introduced (Equation 5-4). In this part a new relationship to calculate the flood wave arrival time is determined by considering the effective parameters on the wave arrival time. There are several parameters which have significant influence on the flood wave arrival time like type of the dam, kind of the failure, soil compaction, reservoir volume, height of the dam, manning number and width of the channel. Any change in either of these parameters can make sensible change in the arrival time calculation. In order to consider influence of these parameters in a single relationship, one assumption needed to be made by using the prepared dataset from different dam failures data (Appendix-E).

Based on our dataset, it is assumed that the flood wave arrival time is increased linearly along the channel as shown in Figure 5-7.

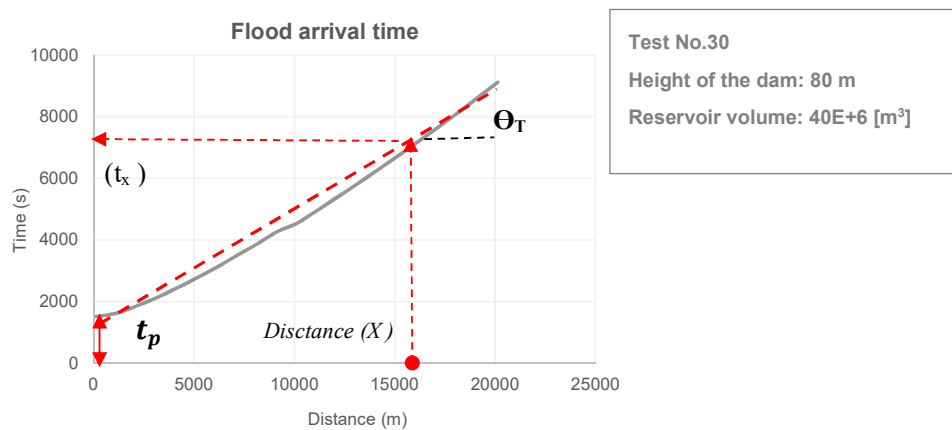


**Figure 5-7.** Flood arrival time assumption (Test No.30)

According to this assumption, the general equation for the wave arrival time can be written as the Equation 5-5.

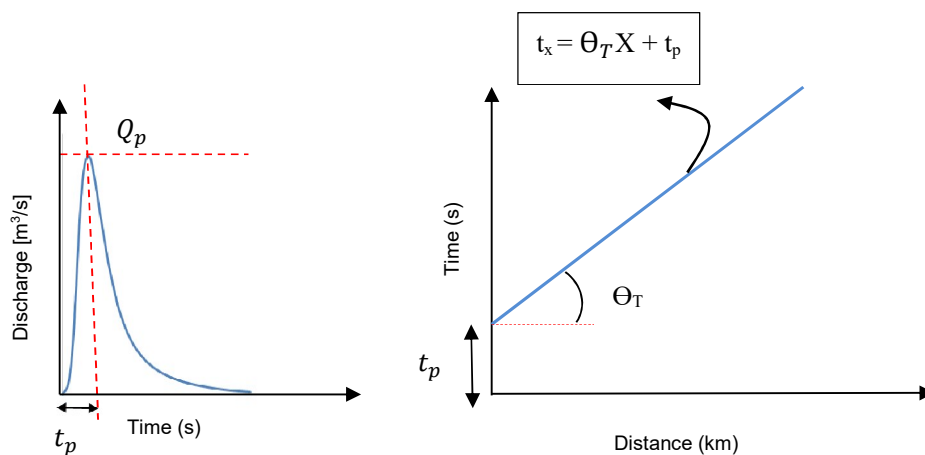


**Figure 5-8.** General form of wave arrival time line

$$t_x = \Theta_T X + t_p \quad 5-5$$

Here,  $X$  [m] is the arbitrary distance from dam,  $t_x$  [s] is the wave arrival time to the location of  $x$ ,  $t_p$  [s] is the time to reach the peak outflow discharge at dam location, and  $\Theta_T$  is the slope of the arrival time line.

In the Equation 5-5, all parameters are known except the slope of the arrival time line ( $\Theta_T$ ). In order to define this parameter, sensitivity analysis is employed.

Based on the sensitivity analysis results, slope of the arrival time line depends on the following parameters

- Strickler roughness coefficient ( $K_s$ )
- Width of the channel ( $W_c$ )
- Height of the dam ( $H_d$ )
- Peak outflow discharge at the dam location ( $Q_p$ )

All of these parameters can be expressed in a single relationship as shown in the Equation 5-6.

$$\Theta_T = \left( \frac{(H_d \cdot W_c)}{(K_s \cdot Q_p)} \right)^{0.71} \quad 5-6$$

Substituting Equation 5-6 into Equation 5-5, the arrival time equation can be calculated, and final equation can be written as:

$$t_x = \left( \frac{(H_d \cdot W_c)}{(K_s \cdot Q_p)} \right)^{0.71} X + t_p \quad 5-7$$

Here,  $H_d$  [m] is the height of the dam,  $W_c$  [m] is the width of the channel,  $K_s$  is the Strickler roughness coefficient and  $Q_p$  [ $m^3/s$ ] is the maximum peak outflow discharge.

In the next section the accuracy of these two relationships (Equations 5-4 and 5-7) are examined by using the ICOLD Benchmark Workshop dam failure test.

### 5.3 Validation of both relationships at same dam failure

#### 5.3.1 ICOLD Benchmark Workshop

The data of this dam are provided within the 12<sup>th</sup> International ICOLD Benchmark Workshop (Zenz et al. (2013)). In this workshop, a hypothetical clay fill dam was investigated in the surrounding mountains. This dam was directly located above a highly populated area, and it was assumed that the possible overtopping failure take place in this dam due to a heavy snowmelt. In this workshop, each participant should calculate the breach outflow hydrograph for this embankment dam failure along with the calculation of the flood wave propagation for the downstream of this dam after dam failure. Table 5-3 shows the failure parameters for this dam. Table 5-4 shows the location of the five given cross sections at downstream of this dam which participants should use for their calculation.

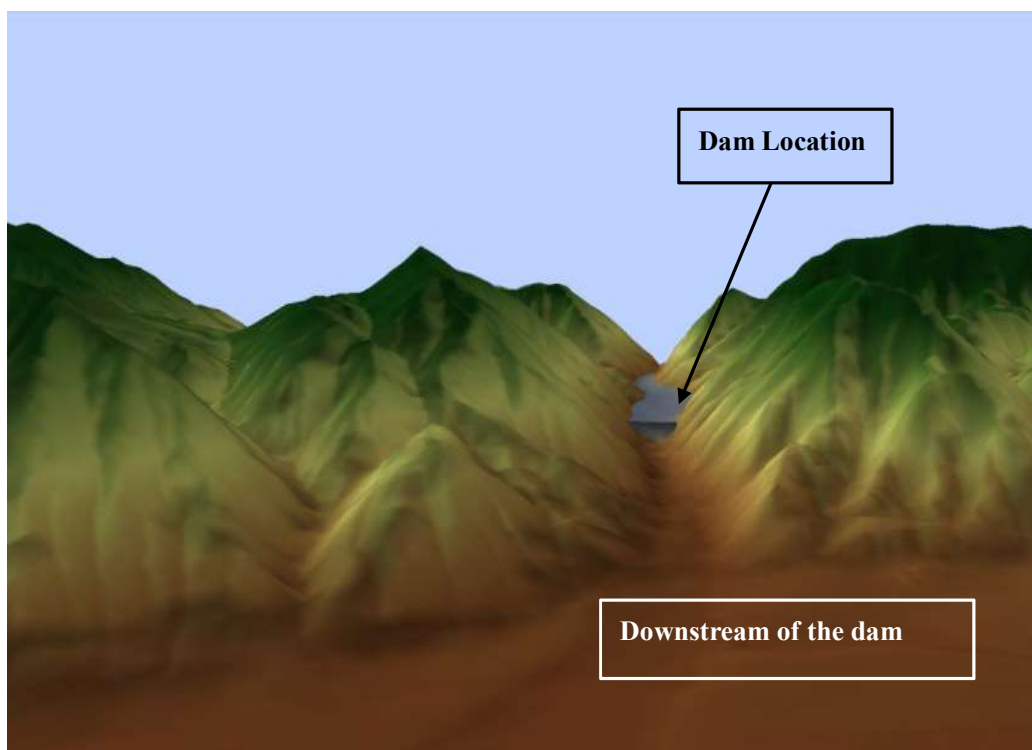


**Figure 5-9.** A schematic picture showing the ICOLD Benchmark Workshop dam and its downstream region.

**Table 5-3.** Dam data for ICOLD Benchmark Workshop

Name	Storage volume [m <sup>3</sup> ]	H [m]	Crest Length [m]	Peak outflow [m <sup>3</sup> /s]
clay fill	38.0×10 <sup>6</sup>	61.0	360	11500

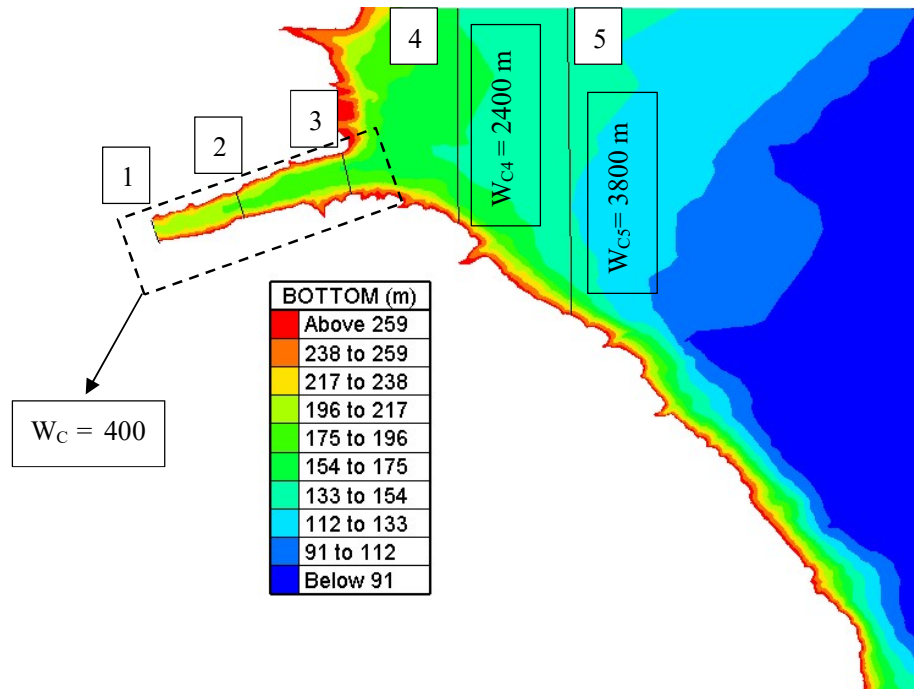


**Figure 5-10.** Plan view of ICOLD Benchmark Workshop downstream of the dam

**Table 5-4.** Cross sections at downstream of the dam

Cross section ID	X location [m]	Stickler Value	Given by formulator Peak outflow [m <sup>3</sup> /s]	Given by formulator Arrival time [s]
1	100	40	11500	1800
2	1300	40	11000	1850
3	2900	30	10300	2100
4	4500	30	10100	2600
5	6000	30	9800	3000

*5.3.1.1 Calculate outflow hydrograph of ICOLD Benchmark Workshop dam failure by using new relationship*

The introduced relationships in this study are applied on this dataset as the validation case study. The peak outflow and arrival time for section 1, 2 and 3, were calculated by using our new formula, and using the data given in the Tables 5-3 and 5-4.

**Table 5-5.** Calculated results by new formula for cross section 1, 2 and 3

Cross section ID	X location [m]	Calculated Results Peak outflow [m <sup>3</sup> /s]	Calculated Results Arrival time [s]
1	100	11500	1812
2	1300	11000	1962
3	2900	10600	2212

Because the width of the channel at sections 4 and 5 are changed, the average values are considered for these sections.

- Average width for section 4:

$$(\text{Width of the channel at section 3} + \text{width of the channel at section 4})/2 = 1400 \text{ m}$$

- Average width for section 5:

$$(\text{Width of the channel at section 4} + \text{width of the channel at section 5})/2 = 3100 \text{ m}$$

The final peak outflow and arrival time for section 3 and 4 are calculated by using our new formula, according to the data given in the Tables 5-3, 5-4.

**Table 5-6.** Calculated results by new formula for cross section 3 and 4

Cross section ID	X location [m]	Calculated Results Peak outflow [m <sup>3</sup> /s]	Calculated Results Arrival time [s]
4	4500	9600	2828
5	6000	8500	3932

#### 5.3.1.2 Compare results of new relationships with formulator results

For evaluating the accuracy of the new relationships, our final results are compared with the ICOLD Benchmark Workshop results.

**Table 5-7.** Compare results of new relationships with formulator results

Cross section ID	Peak outflow [m <sup>3</sup> /s] given by formulator	Arrival time [s] given by formulator	Calculated Results Peak outflow [m <sup>3</sup> /s]	Calculated Results Arrival time [s]
1	11500	1800	11500	1812
2	11000	1850	11000	1962
3	10300	2100	10600	2212
4	10100	2300	9600	2828
5	9800	3000	8500	3932

Table 5-7 shows all of these results against each other. This table confirms that the gained results from developed method provide a very good accuracy and the introduced relationships are validated successfully.

## 5.4 Excel sheet program

In the chapters two and five, four relationships were developed and introduced to calculate dam failure and flood wave parameters. These relationships are mainly derived to calculate the following parameters:

- Peak outflow discharge [ $\text{m}^3/\text{s}$ ]
- Dam failure time [s]
- Peak outflow discharge at downstream valley [ $\text{m}^3/\text{s}$ ]
- Wave arrival time [s]

In order to facilitate calculation of the dam failure and flood wave parameters an excel-sheet program is developed. This excel-sheet uses the following data as input in order to calculate the four aforementioned unknown parameters.

- Height of the dam [m]
- Reservoir volume [ $\text{m}^3/\text{s}$ ]
- Define type of the dam (homogeneous or non-homogeneous dam)
- Define type of the fill material (easy erosion or hard erosion)
- Peak out flow discharge [ $\text{m}^3/\text{s}$ ]
- Time to reach peak outflow discharge [s]
- Manning number along channel [-]
- Width of the channel [m]
- Height of the water behind dam at failure time [m]
- Distance of specific point in downstream of the dam [m]

This excel sheet program is explained in the Figures 5-11a and 5-11b.

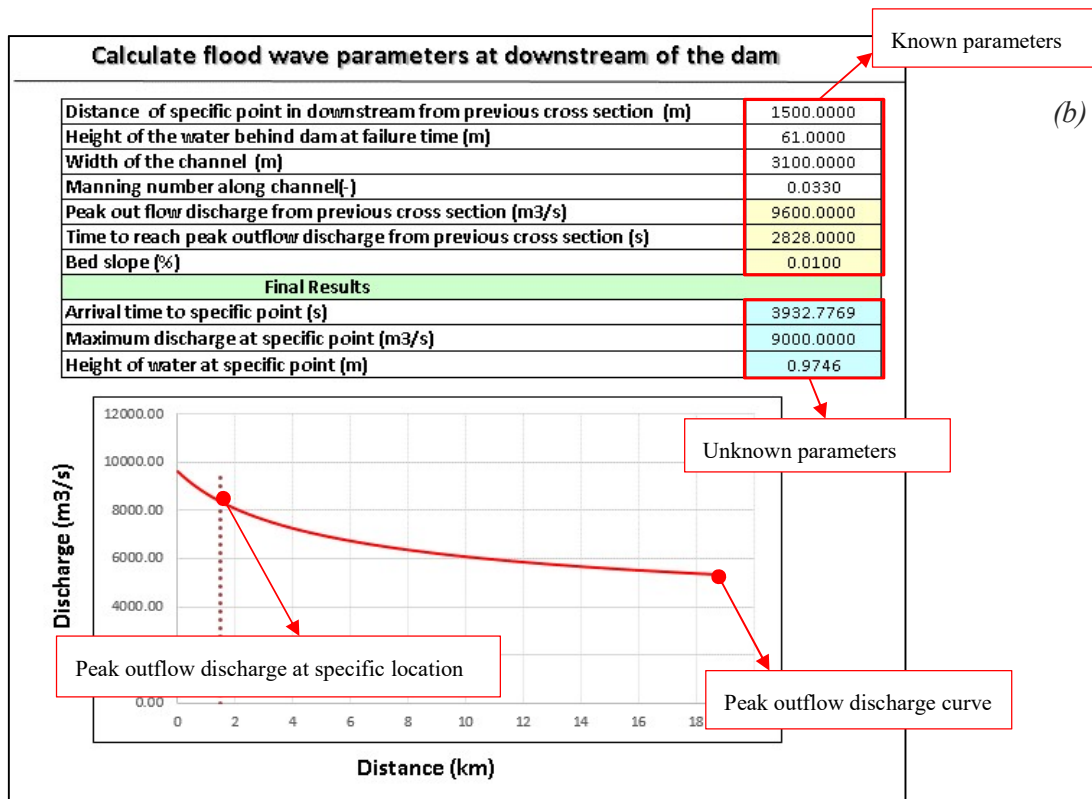
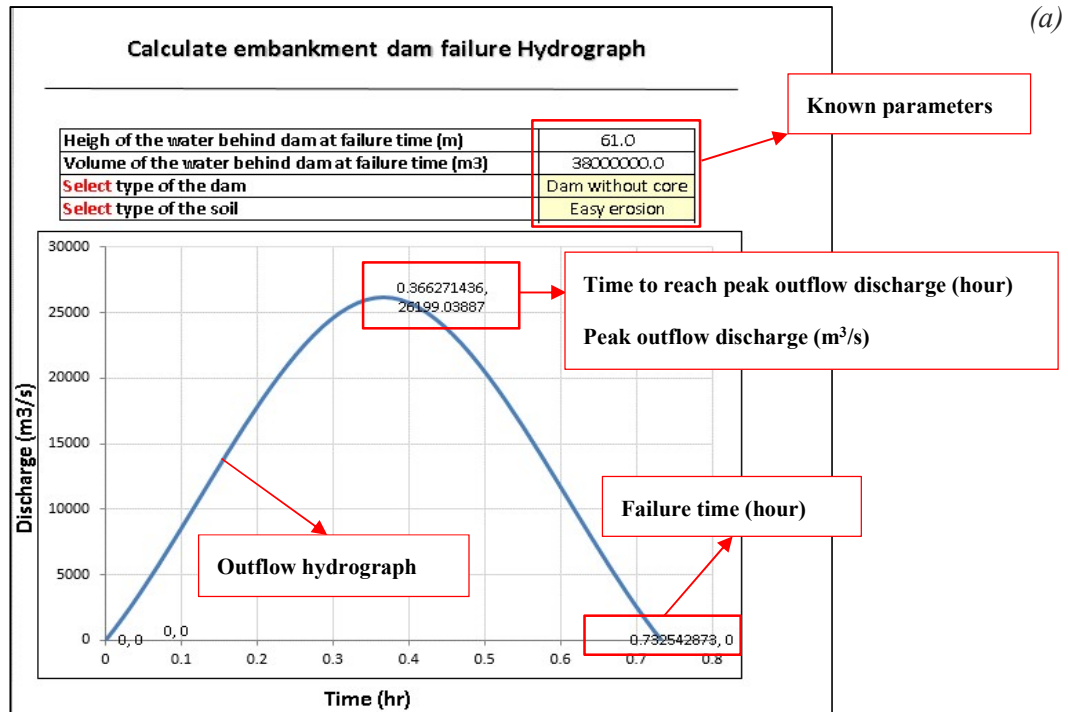


**Figure 5-11.** Excel sheet program: (a) Calculating dam failure parameters (b) Calculating flood wave parameters

---

# Chapter 6

## Conclusion

---

The main goal of this study is to introduce, develop and improve reliable methods to determine the breach outflow hydrograph of embankment dams which fail by overtopping flow. Furthermore, new methods are introduced to calculate flood wave parameters of the dam- break downstream of the dam. In this research, the empirical and the numerical methods were introduced, developed, improved, calibrated and validated against each other. The overall results show that the new methods have acceptable accuracy in comparison with the measurement results. The following approaches were tested during this study and relevant conclusions are made based on each part.

### 6.1 Empirical formula

The failure time relationships were obtained by using non-linear regression analysis on published histories of dam failures around the world. In all of these case studies failure time ( $t_f$ ), reservoir volume ( $V_w$ ) and height of the water behind dam ( $H_w$ ) are known. Among them, 45% of the dams have known soil types while 55% of the dams have known breach peak outflows ( $Q_p$ ).

To derive the peak outflow discharge, non-linear regression analysis was applied to obtain an appropriate relationship. However, the final results reveal that the applied regression analysis is not a proper solution. Therefore, a new method is employed. In this method the area under the outflow hydrograph is split into three shape of primitives (one rectangle and two triangles). The peak outflow discharge is calculated from the sum of the areas of these three shapes. The following conclusions can be made based on this work:

- Based on our database, it is found that dam erosion has a significant influence on the failure time. This means that the accuracy of the failure time relationships can be improved significantly by considering soil and construction type of the dam in the regression formula.
- Failure time relationships ( $t_f$ ) show some errors for small dams ( $V_w < 1.0$  million  $m^3$ ). This error is mainly related to the lack of information for our regression analysis.
- In the peak outflow discharge relationship, it is assumed that the whole reservoir volume becomes empty during the dam failure time. This assumption control results in the peak outflow discharge equation.

- In the peak outflow discharge relationship, it has been assumed, the breach outflow hydrograph is symmetric, therefore, time to reach peak outflow discharge is always constant and equal to  $t_f/2$  .

## 6.2 Numerical modelling

A 1-D program is developed by using the Saint-Venant equation as the governing equation for characterizing the water flow on embankment dams. The bed evolution is determined by using the one-dimensional sediment continuity equation (Exner equation). The modified MacCormack methods is employed to discretize the Saint-Venant equation and determine flow parameter. The Modified-Lax scheme is applied to discretize sediment continuity equation. Finally, the calibrated Smart (1984) equation is applied to calculate the sediment transport and outflow hydrograph during failure process.

The following conclusions can be made based on this work:

- Computational stability in 1-D program is sensitive to the Courant number and best result can be reached if the Courant number is less than 1.0.
- In 1-D program two basic assumptions are considered. The first assumption is that the initial breach is not considered. In the second assumption, rectangular shape with constant width is considered to model the reservoir of a dam.
- A 1-D program cannot model a variety in width of the channel like breach propagation, while in 2-D software like TELEMAC-2D breach propagation can be modelled during the failure time.

## 6.3 Change of geometrical parameters

In this investigation, the focus is mainly on the influence of dam's geometrical parameters like upstream slope, downstream slope, crest width and initial breach on the outflow hydrograph during failure process. The influence of these parameters are numerically modelled by using TELEMAC-2D software and the final results are compared against each other.

The following conclusions can be made based on this work results:

- The change of downstream slope in embankment dam failure has a high influence on the breach outflow hydrograph compared to the other geometrical parameters.
- The change of upstream slope in embankment dam failure has less influence on the breach outflow hydrograph.
- Outflow hydrograph without initial breach gives higher values in peak outflow discharge but lower values in failure time compared with the outflow hydrograph with initial breach.

## 6.4 Flood Wave propagation

In this investigation two new relationships are introduced to calculate the most important flood wave parameters in the valley downstream. These relationships are obtained and modelled by using sensitivity analysis on 71 dam failures and channels. Among them, 14 cases are related to the embankment dams which are failed numerically by overtopping flow while 57 cases are related to the rectangular channels which flood wave propagation are numerically modelled inside them.

In all of these case studies the length of the channel, soil parameters, reservoir and channel shapes are kept constant. To improve the accuracy of the final relationships several variations have been done on the following parameters:

Reservoir volume, height of the dam, channel width, channel slope and manning number.

Finally, two main assumptions are made to calculate these two relationships:

- In the first assumption, the peak outflow discharge curve is considered instead of calculating different outflow hydrograph downstream of the dam.
- In the second assumption, linear equation is considered for calculating the wave arrival time. Therefore, by calculating the slope of this line, the arrival time can be calculated at any location in the downstream valley.

The following conclusions can be made based on the results of this work:

- Each dam has a particular peak outflow discharge curve shape.
- Width of the channel is not influenced on the peak outflow discharge curve shape.
- Accuracy of the peak outflow discharge equation can be improved significantly by using time discretization in the reduction relationship.
- The manning number, reservoir volume, channel slope and the breach outflow hydrograph has the main influence on the peak outflow discharge and wave arrival time downstream.

## 6.5 Recommendations for Future Work

Based on the results of this work, the following recommendations are suggested for further studies.

- More full-scale dam failure tests need to be performed to determine the effects of scaling on laboratory dam failure tests.
- Many dam failure software have been developed and introduced during the last decades. But all of them are closed-source programs and it is very difficult for other researchers to validate or evaluate the software's accuracy and performance. Therefore, it is suggested that future researchers and developers publish dam failure modelling as an open-source program.

---

# Chapter 7

## Reference

---

**Abrahams A.** Bed-Load Transport Equation for Sheet Flow [Journal] // Journal of Hydraulic Engineering. - 2003.

**Athanasios N. Papanicolaou, John T. Sanford, Dimitrios C. Dermisand and Gabriel A. Mancilla** 1-D morphodynamic model for rill erosion [Journal] // Water resource research. - 2010.

**Azinfar Hossein** Flow Resistance and Associated Backwater Effect Due To Spur Dikes In Open Channel [Bericht]. - [s.l.] : University of Saskatchewan (P.h.D Thesis), 2010.

**Barker m and Holroyde D** Risk and Standards Based Riprap Design for Grahamstown Dam [Bericht]. - [s.l.] : GHD, 2000.

**Bellos, C., and Hrissanthou, V.** Numerical Simulation of Morphological Changes in Rivers and Reservoirs [Journal] // computers and mathematics with applications. - 2003. - S. 453-464.

**Bray D.I.** Estimating average velocity in gravel-bed rivers [Journal] // Journal of the Hydraulics Division. - 1979. - S. 1103-1122.

**Briaud J. L.** Case histories in soil and rock erosion [Journal] // Journal of Geotechnical and Geoenvironmental Engineering. - 2008. - S. 1425–1447.

**Broich K.** Computergestützte Analyse des Damerosionsbruchs [Bericht]. - [s.l.] : Universität der bundeswehr münchen institut für wasserwesen (P.h.D Thesis), 1996.

**Brown, R J. and Rogers, D. C.** BRDAM User's Manual [Bericht]. - Denver : Water and Power, 1977.

**Brownlie W.** Flow Depth in Sand-Bed Channels. [Journal] // Journal of Hydraulic Engineering. - 1983. - S. 959-990.

**Bruschin J.** Flow Depth in Sand-bed Channels [Journal] // Journal of Hydraulic Engineering. - 1985. - S. 736-739.

- Camenen B. and Larson, M.** A general formula for non-cohesive bed load sediment transport [Bericht]. - [s.l.] : Estuarine Coastal Shelf Sci, 2005.
- Chanson Hubert** Embankment overtopping protection systems [Journal] // Springer-Verlag Berlin Heidelberg. - 2013. - S. 305-318.
- Chinnarasri,C. and Tingsanchali,T. and WeesakuliS. and Wongwises,S.** Flow patterns and damage of dike overtopping [Journal] // International Journal of Sediment Research. - 2003. - S. 301-309.
- Costa J. E.** Floods from dam failures [Bericht]. - Denver : U. S. Geological Survey Open-File Report 85 560, 1985.
- Cunge, J. A.,Holly, F. M., Verwey, A.** Practical Aspects of Computational River [Buch]. - London : Pitman Publishing Ltd, 1980.
- De Vries M** Morphological computations [Bericht]. - Delft, The Netherlands : Faculty of Civil Engineering, Delft University of Technology, 1987.
- Duricic door Jasna** Dam Safety Concepts [Bericht]. - Delft : Technische Universiteit Delft (PhD thesis), 2004. - S. 12.
- Eilbeck, J. C., and G. R. McGuire** Numerical study of the regularized long wave equation [Journal] // Journal of computational physics. - 1975. - S. 43–57.
- Einstein H. A.** The bed-load function for sediment transportation in open channel flows. [Bericht]. - Washington : USDA Soil Conservation Service, Technical Bulletin No. 1026 , 1950.
- Evans S. G.** The maximum discharge of outburst floods caused by the breaching of man-made and natural dams [Journal] // Canadian Geotechnical Journal. - 1986. - S. 23, August.
- Exner** Über die Wechselwirkung zwischen Wasser und [Bericht]. - [s.l.] : Gedruckt mit Unterstützung aus dem Jerome und Margaret Stonborough-Fonds, 1925.
- Fread D. L.** A Breach Erosion Model for Earthen Dams [Bericht]. - [s.l.] : National Weather Service (NWS), 1984.
- Froehlich D. C.** Embankment dam breach parameters and their uncertainties [Journal] // Journal of Hydraulic Engineering. - 2008. - S. 1708-1721.
- Froehlich D. C.** Embankment dam breach parameters revisited [Konferenz] // Proc., Water Resources Engineering, 1995 ASCE Conf. on Water Resources Engineering. - NY, 887–891 : [s.n.], 1995.
- Froehlich D. C.** Peak outflow from breached embankment dam [Journal] // Journal of Water Resources Planning and Management. - 1995. - S. 90-97.

- Garcia N., Alcrudo F., and Saviron J. M.** 1-D Open Channel Flow Simulation Using TVD-MacCormack Scheme [Journal] // Journal of Hydraulic Engineering. - 1992. - S. 1359-1372.
- Garcia-Navarro,P. and Saviron,J. M.** MacCormack's method for the numerical simulation of one dimensional discontinuous unsteady open channel flow [Journal] // Journal of Hydraulic Research. - 2010. - S. 95-105.
- Ghani A. A. B., Zakaria, N. A., Kiat, C. C., Ariffin, J., Hasan, Z. A., and Ghaffar, A. B. A.** Revised equations for Manning's coefficient for sand-bed rivers [Journal] // International Journal of River Basin Management. - 2007. - S. 329-346.
- Gordienko P.I.** Reinforced-Concrete-Earth Overflow Dams [Bericht]. - Moscow : Dams and Spillways, Collection of Works No. 61, 1978.
- Goutal, N. and Maurel, F** Proceeding of the second workshop on dam-break wave simulation [Bericht]. - France : Laboratoire National d'Hydraulique Chatou, Electricité de France, 1997.
- Greig, L. S. and Morris, J. L. L** A hopscotch method for the Korteweg-de Vries equation [Journal] // Journal of computational physics. - 1976. - S. 20, 64-80.
- Guan M.,Wright,NG., and Sleight,PA.** A multi-mode morphodynamic model for sediment-laden flows and geomorphic impacts [Journal] // Journal of Hydraulic Engineering. - 2014.
- H. Tennekes and J. L. Lumley** A first course in turbulence [Buch]. - [s.l.] : 6th Edition, MIT Press, 1972.
- H. Weilbeer and J. A. Jankowski** A Three-Dimensional Non-Hydrostatic Model for Free Surface Flows [Journal] // Journal of Hydraulic Engineering. - 2000. - S. 162-177.
- Hagen V. K.** Re-evaluation of design floods and dam safety [Konferenz] // Proceedings, 14th Congress of International Commission on Large Dams, Rio de Janeiro. - 1982.
- Harris, G. W. and Wagner** Outflow From Breached Earth Dams [Bericht]. - [s.l.] : University of Utah, Salt Lake City.
- Hervouet J. and E. Razafindrakoto** The wave equation applied to the solution of Navier-Stokes equations in finite elements [Buch]. - London : WIT press, 2005.
- Hoffman Joe D. , Steven Frankel** Numerical Methods for Engineers and Scientists [Buchabschnitt]. - New York : Marcel Dekker, 2001.
- Holton James R.** An Introduction to Dynamic Meteorology, Volume 1 [Buch]. - California, USA : Elsevier Academic Press, 2004.
- ICOLD** Dam Failure Statistical Analysis. [Bericht]. - [s.l.] : Bulletin 99, 1995.
- Jarret R.D.** Hydraulics of high-gradient streams [Journal] // American Society of Civil Engineers, Journal of Hydraulic Engineering. - 1984. - S. 1519-1539.

**John von Neumann and Richtmyer, R. D.** A Method for the Numerical Calculation of Hydrodynamic Shocks [Journal] // Journal of Applied Physics. - March 1940.

**K.Abdulrahman** Case Study of the Chaq-Chaq Dam Failure: Parameter Estimation and Evaluation of Dam Breach Prediction Models [Journal] // Int. Journal of Engineering Research and Applications. - 2014. - S. 109-116.

**Kabir M. R. and Nasir ahmad** Bed Shear Stress for Sediment Transport in The River JAMUNA [Journal] // Journal of civil engineering. - 1996.

**Kamal El kadi Abderrezzak and Andre´ Paquier** One-dimensional numerical modeling of sediment transport and bed deformation in open channels [Journal] // Water resource research. - 2009.

**Kirkpatrick G. W.** Evaluation guidelines for spillway adequacy [Konferenz] // American Society of Civil Engineers, Engineering Foundation Conference. - Pacific Grove, CA : [s.n.], 1977. - S. 395-414.

**Koch, F.G. and Flokstra, C.** Bed level computations for curved alluvial channels [Journal] // XIXth Congress of the International Association for Hydraulic Research, New Delhi India. - 1981.

**Lane, E.W and Carlson, E.J** some factor affecting the stability of channels constructed in coarse granular materials [Journal] // International Hydraulics convention. - 1953.

**Lax, P,D, and Wendroff, B.** Difference schemes for hyperbolic equations with high order of accuracy [Journal] // Applied mathematics committee. - 1964.

**Limerinos J.T.** Determination of the Manning coefficient from measured bed roughness in natural channels [Journal] // U.S. Geological Survey Water-Supply Paper 1898-B. - 1970. - S. 47.

**MacCormack R.W.** The Effect of Viscosity in Hypervelocity Impact Cratering [Journal] // AIAA Paper. - 1969. - S. 354.

**MacDonald, T. C., and Langridge-Monopolis, J.** Breaching characteristics of dam failures [Journal] // journal of hydraulic engineering. - 1984. - S. 567–586.

**Mackay G.R.** Design of Minimum Energy Culverts. [Bericht]. - Brisbane, Australia : Dept of Civil Eng., Univ. of Queensland, 1971.

**Meyer-Peter, E. and R. Müller** Formulas for bed load transport [Journal] // paper presented at 2nd Meeting, International Association for Hydraulics research. - 1948. - S. 39-64.

**Morris Mark** IMPACT Project Field Tests Data Analysis [Bericht]. - London : HR Wallingford, 2008.

**Nielsen P.** Coastal bottom boundary layers and sediment transport [Journal] // Advanced Series on Ocean Engineering . - 1992.

- Ouillon, S and Dartus, D.** Three-dimensional computation of flow around groyne [Journal] // Journal of Hydraulic Engineering. - 1997. - S. 962-970.
- Parker, G., and Paola, C., and Leclair, S.** Probabilistic Exner Sediment Continuity Equation for Mixtures with No Active Layer [Journal] // Journal of Hydraulic Engineering. - 2000. - S. 818-826.
- Peregrine D.H.** Calculations of the development of an undular bore [Journal] // J. Fluid Mechanics. - 1966. - S. 321–330.
- Popescu Ioana** Computational Hydraulics: Numerical methods and modelling [Bericht]. - London : IWA publishing, 2014.
- Ralston D. C.** Mechanics of embankment erosion during overflow [Konferenz] // Proc., 1987 ASCE National Conf. on Hydraulic Engineering. - NY : [s.n.], 1987. - S. 733–738.
- Sabbagh-Yazdi S. R., Mastorakis, E. N., and Zounemat-Kermani, M.** Velocity profile over spillway by finite volume solution of slopping depth averaged flow. [Konferenz] // 2nd IASME/WSEAS Int. Conf. on Continuum Mechanics, World Scientific and Engineering Academy and Society (WSEAS). - 2007.
- Saberi O. Dorfmann C., Zenz G.** 2-D hydraulic modelling of a dam break scenario [Konferenz] // 12th international ICOLD. - Graz-Austria : [s.n.], 2013.
- Saberi O., Zenz G.** Numerical Investigation on 1D and 2D Embankment [Journal]. - [s.l.] : International Journal of Hydraulic Engineering, 2016.
- Saberi O., Zenz G.** Empirical Relationship for Calculate Outflow [Journal]. - [s.l.] : International Journal of Hydraulic Engineering, 2015.
- Scarlatos, P. D. and Singh, V. P.** Mud Flows and Sedimentation Problems Associated With a Dam Break Event [Journal] // River Sedimentation. - 1987. - S. 1063-1068.
- Schmocker, L. r, Hager, W.** Plane dike-breach due to overtopping: effects of sediment, dike height and [Journal] // IAHR. - 2013. - S. 576-587.
- Schoklitsch A.** Der Geschieletrieb Und die Geschielefracht [Journal] // Wasserkraft und Wasserwirtschaft. - 1934. - S. 37.
- SCS** Simplified dam-breach routing procedure [Bericht]. - [s.l.] : Soil Conservation Service , December 1981. - S. 39 .
- Şentürk Fuat** Hydraulics of Dams and Reservoirs [Buch]. - Ankara-Turkey : Water Resources Publication, 1994.
- Shields A** Application of similarity principle and turbulence research to bed load movement [Journal] // Mitteilungen der Preussischen Versuchsanstalt für Nassexbau und Schiffbau. - 1936.

**Silveira J.F.A (ICOLD-2011)** Small Dams Design, Surveillance and Rehabilitation [Journal] // International Committee on Large Dams. - 2011. - S. 30-34.

**Singh K. P., and Snorrason, A** Sensitivity of outflow peaks and flood stages to the selection of dam breach parameters and simulation models [Bericht]. - Illinois : State Water Survey (SWS) Contract Report 288, Illinois Department of Energy and Natural Resources, 1982.

**Singh V. P.** Dam breach modeling technology [Buch]. - Boston Rouge : Louisiana State University, 1998.

**Smart G.** Sediment Transport Formula For Steep Channels [Journal] // Journal of Hydraulic Engineering. - 1984. - S. 267-276.

**Soulsby R.** Dynamics of Marine Sands [Buch]. - London : Thomas Thelford Edition, 1997.

**Strickler A.** Some Contributions to the Problem of the Velocity Formula and Roughness Factors for Rivers Canals and Closed Conduits [Journal] // Mitteilungen des Eidgenossischen Amtes für Wasserwirtschaft, Bern Switzerland. - 1923.

**Swartenbroekx C, Van Emelen, S., Zech, Y., and Soares-Frazaõ, S** Numerical modelling of the breaching process in an earthen dike [Konferenz] // Fifth International Conference on Advanced computational Methods in Engineering. - 2010.

**Tassi Pablo** Sisyphé v6.3 User's Manual [Bericht]. - [s.l.] : EDF R&D, 2014.

**Tawatchai T., and Chaiyuth, C.** Numerical modelling of dam failure due to flow overtopping [Journal] // Hydrological Sciences. - 2001. - S. 113-130.

**TELEMAC-2D DESOMBRE, Jonathan** Reference manual [Bericht]. - [s.l.] : EDF-DRD, 2013.

**TELEMAC-3D** User's Manual, Release 6.2 [Journal]. - March 2013.

**U.S Army Corps of Engineers** National Inventory of Dams [Online] // National Inventory of Dams. - April 2015. - <http://nid.usace.army.mil/>.

**U.S Army Corps of Engineers** Shore Protection Manual [Bericht]. - Washington, DC : [s.n.], 1984.

**USBR 2012a.** Calculations for Quarterly Report, Q4-2012 [Bericht]. - [s.l.] : US Bureau of Reclamation, February 8, 2013, 2012a.

**USBR** Appurtenant Structures for Dams (Spillways and Outlet Works) [Bericht]. - [s.l.] : US Bureau of Reclamation, 2012.

**USBR** Downstream hazard classification guidelines [Bericht]. - Denver : Rep. No. 11, U.S. Dept. of the Interior, Bureau of Reclamation, 1988.

**USBR** Freeboard Criteria and Guidelines for Computing Freeboard Allowances for Storage Dams [Bericht]. - [s.l.] : US Bureau of Reclamation, 1992.

**USBR** Guidelines for defining inundated areas downstream [Bericht]. - Denver : Bureau of Reclamation, 1988. - S. 11-82.

**USBR** Guidelines for defining inundated areas downstream from Bureau of Reclamation dams. [Bericht]. - [s.l.] : US Bureau of Reclamation, 1982.

**USBR** Roller-Compacted Concrete [Bericht]. - Denver, Colorado : U.S.Bureau of Reclamation, 2005.

**Van Emelen Sylvie** Erosion Modeling over a Steep Slope: Application to a Dike Overtopping Test Case [Artikel] // Proceedings of 2013 IAHR World Congress. - 2013.

**Van Rijn L.C.** Sediment Transport, Part I: Bed Load Transport [Journal] // Journal of Hydraulic Engineering. - 1984a.

**Van Rijn L.C.** Sediment Transport, Part II: Suspended Load Transport [Journal] // Journal of Hydraulic Engineering. - 1984b.

**Vliegenthart A.C** On finite-difference method for the Korteweg de Vries equation [Journal] // Journal of Engineering Mathematics. - 1971. - S. 137-55.

**Volz C., Rousselot, P., Vetsch, D., and Faeh, R** Numerical modelling of non-cohesive embankment breach [Journal] // Journal of Hydraulic Research. - 2012. - S. 587-598.

**Von Thun J. L & Gillette, D. R.** Guidance on breach parameters [Bericht]. - Internal Memorandum Rep. Prepared for U.S. Dept. of the interior : Bureau of Reclamation, 1990.

**Vreugdenhil, C. B. and Wijnbenga, J. H. A.** Computation of flow patterns in rivers [Journal] // Journal of Hydraulic Engineering. - 1989. - S. 87-90.

**Wan, C. F., and Fell, R.** Investigation of rate of erosion of soils in embankment dams [Journal] // Journal of Geotechnical and Geoenvironmental Engineering. - 2004. - S. 373–380.

**Wong M., Parker, G.** Reanalysis and correction of bed-load relation of Meyer-Peter and Müller using their [Journal] // Journal of Hydraulic Engineering. - 1161–1168 : Journal of Hydraulic Engineering, 132(11), 2006. - S. 1161-1168.

**Wu W. and Wang, S.S.Y.** One-dimensional explicit finite-volume model for sediment transport with transient [Journal] // Journal of Hydraulic Engineering. - [s.l.] : Journal of Hydraulic Engineering, 46(1), 87–98, 2008.

**Wuthrich D., and Chanson, H.** Air entrainment and energy dissipation on gabion stepped weirs [Artikel] // 5th International Symposium on Hydraulic Structures. - 25-27. 6 2014.

**Xin, L., Abdolmajid, M., and Julio, A.** One dimensional numerical simulation of bed changes in irrigation channels using finite volume method [Journal] // Irrigation & Drainage Systems Engineering. - 2012. - S. 1-6.

**Xu, Y., and Zhang, L. M.** Breaching parameters for earth and rockfill dams [Journal] // Journal of Hydraulic Engineering. - 2009. - S. 1957-1970.

**Yarde A J [et al.]** Reservoir dams : wave conditions, wave overtopping and slab protection [Buch]. - [s.l.] : Wallingford, Oxon : HR Wallingford, 1996.

**Zenz,G., and Goldgruber, M.** Numerical analysis of dams [Konferenz] // 12th International Benchmark Workshop. - Graz : Austrian National Committee on Large Dams, 2013. - S. 195-322.

**Zhou Liu** Sediment transport [Bericht]. - [s.l.] : Instituttet for Vand, Jord og Miljøteknikk, 2001.

# Chapter 8

## Appendix

### 8.1 Appendix-A

#### Boundary condition

In the MacCormack method like other explicit methods, all computational nodes can be calculated except two nodes, the first node ( $n=1$ ) and the last node ( $n=N$ ). These nodes represent in total four unknown parameters related to the height of the water and water velocity at points 1 and  $N$ . In order to calculate these unknown parameters a new method has been used in this research. This method was suggested by P. Garcia-Navarro & J. M. Saviron (1992).

In the following this method is explained in more detail.

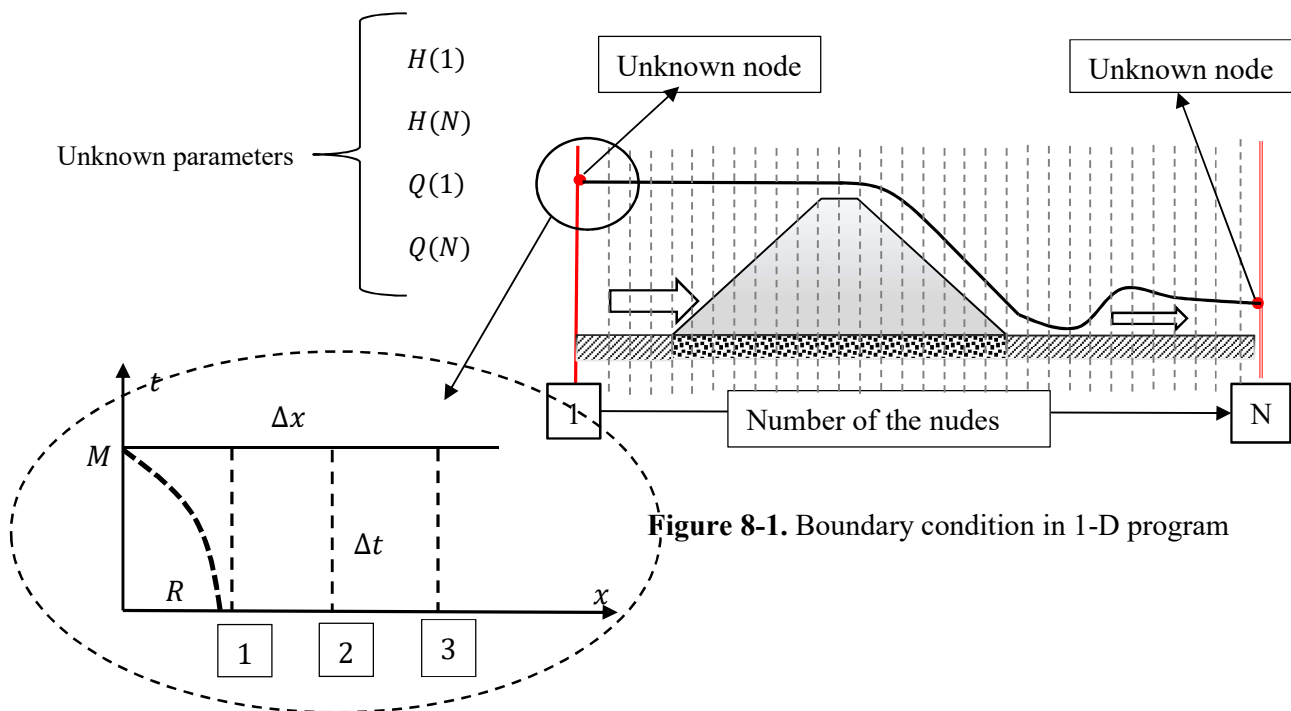


Figure 8-1. Boundary condition in 1-D program

Figure 8-2. P. Garcia-Navarro & J. M. Saviron (1992) method

**Step one (Predictor step)**

Find the best location for point R:

$$x_R = x_M - \left( \frac{Q}{A} - \sqrt{gy} \right) \Delta t \quad 8-1$$

Find the best hydraulic parameters of the point R:

$$Q_R = Q_2 - (Q_2 - Q_1) \left( \frac{x_2 - x_R}{\Delta x} \right) \quad 8-2$$

$$H_R = H_2 - (H_2 - H_1) \left( \frac{x_2 - x_R}{\Delta x} \right) \quad 8-3$$

**Step two**

First guess for the point M:

$$H_M = \left( Q_M - \left( Q_R + H_R \left( -\frac{QB}{A} - B\sqrt{gH} \right)_R + g\Delta t \left( A(S_0 - S_f) \right)_R \right) \right) / \left( \frac{QB}{A} + B\sqrt{gH} \right)_R \quad 8-4$$

**Step three (Correction step)**

Find R location based on predictor step:

$$x_R = x_M - \left( \left( \frac{Q}{A} - \sqrt{gy} \right)_M + \left( \frac{Q}{A} - \sqrt{gy} \right)_R \right) \frac{\Delta t}{2} \quad 8-5$$

Find the best hydraulic parameters for the point R based on predictor step:

$$Q_R = Q_2 - (Q_2 - Q_1) \left( \frac{x_2 - x_R}{\Delta x} \right) \quad 8-6$$

$$H_R = H_2 - (H_2 - H_1) \left( \frac{x_2 - x_R}{\Delta x} \right) \quad 8-7$$

**Step four**

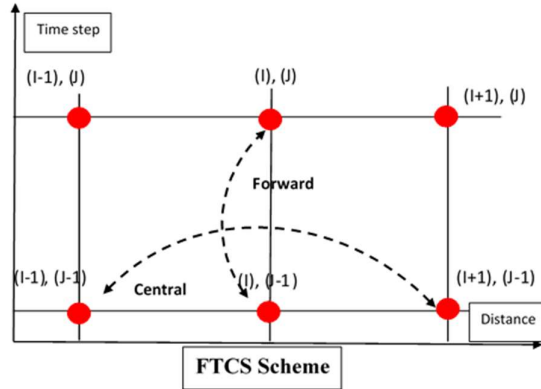
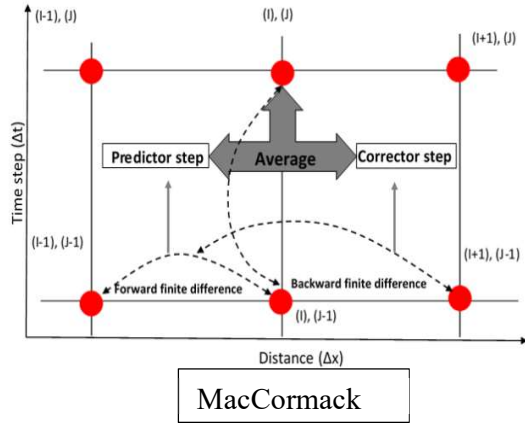
Second guess for the point M:

$$\begin{aligned} Q_M - Q_R + \frac{(H_M + H_R)}{2} \left( \left( -\frac{QB}{A} - B\sqrt{gH} \right)_R + \left( -\frac{QB}{A} - B\sqrt{gH} \right)_M \right) \\ = \frac{\Delta t}{2} \left( \left( gA(S_0 - S_f) \right)_R + \left( gA(S_0 - S_f) \right)_M \right) \end{aligned} \quad 8-8$$

This procedure has to be repeated (step one to step four), till the best value is calculated.

## 8.2 Appendix-B

### Different scheme of finite difference method (FDM)



$$\left(\frac{\partial u}{\partial x}\right)_{P_{i,j}} = (u_{i+1}^{j-1} - u_{i-1}^{j-1}) / \Delta x \quad 8-9$$

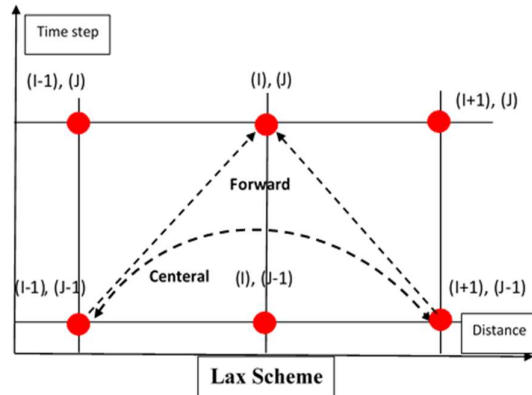
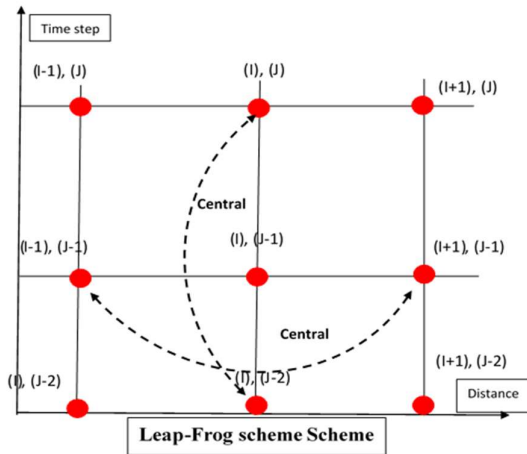
$$\left(\frac{\partial u}{\partial t}\right)_{P_{i,j}} = (u_i^j - u_i^{j-1}) / \Delta t \quad 8-10$$

$$\left(\frac{\partial u}{\partial x}\right)_{C_{i,j}} = ((u_i^j)P - u_{i-1}^{j-1}) / \Delta x \quad 8-11$$

$$\left(\frac{\partial u}{\partial t}\right)_{C_{i,j}} = (u_i^j - u_i^{j-1}) / \Delta t \quad 8-12$$

$$\left(\frac{\partial u}{\partial t}\right) = (u_i^j - u_i^{j-1}) / \Delta t \quad 8-13$$

$$\left(\frac{\partial u}{\partial x}\right) = (u_{i+1}^j - u_{i-1}^j) / 2\Delta x \quad 8-14$$



$$\left(\frac{\partial u}{\partial t}\right) = (u_i^{j+1} - u_i^{j-1}) / 2\Delta t \quad 8-15$$

$$\left(\frac{\partial u}{\partial x}\right) = (u_{i+1}^j - u_{i-1}^j) / 2\Delta x \quad 8-16$$

$$\left(\frac{\partial u}{\partial t}\right) = ((u_i^j - u_{i-1}^{j-1}) + (u_i^j - u_{i+1}^{j-1})) / 2\Delta t \quad 8-17$$

$$\left(\frac{\partial u}{\partial x}\right) = (u_{i+1}^j - u_{i-1}^j) / 2\Delta x \quad 8-18$$

### 8.3 Appendix-C

#### 1-D program for modelling embankment dam failure.

- This program is written in the FORTRAN 90.
- The Saint-Venant equation is used as the governing equation for the water flow on embankment dams.
- The modified MacCormack method is employed to discretize the Saint-Venant equation and determine flow parameter.
- The bed evolution is determined by using the one-dimensional sediment continuity equation (Exner equation).
- The Modified-Lax scheme is applied to discretize sediment continuity equation.
- The calibrated Smart (1984) equation is applied to calculate the breach outflow hydrograph during failure process.

In the following this 1-D program is explain in more detail.

**MacCormack method start time steps**-----

Do it = 1, nt

**Predictor step (forward method)** -----

**Area of flow**-----

$$Ap(2:nx-1) = A(2:nx-1) - (dt/dx) * (Q(3:nx) - Q(2:nx-1))$$

**Radius hydraulic**-----

$$Rp(1:nx) = (A(1:nx) / (B(1:nx) + 2 * H(1:nx)))$$

**Energy slope method**-----

$$Sfp(2:nx-1) = ((Nm(2:nx-1) ** 2) *$$

$$& (((Q(2:nx-1)) * ABS((Q(2:nx-1)))))) /$$

$$& (((A(2:nx-1)) ** 2) * ((Rp(2:nx-1)) ** (4/3)))$$

**Discharge**-----

$$Qp(2:nx-1) = Q(2:nx-1) - (dt/dx) *$$

$$& (((Q(3:nx) ** 2) / A(3:nx)) - ((Q(2:nx-1) ** 2) / A(2:nx-1))) +$$

$$& (g * ((0.5 * (A(3:nx) * A(3:nx)) / B(3:nx)) -$$

$$& (0.5 * (A(2:nx-1) * A(2:nx-1)) / B(2:nx-1)))) +$$

$$& (g * dt * (A(2:nx-1) *$$

$$& (S0p(2:nx-1) - Sfp(2:nx-1))))$$

**Height of water**-----

$$H_p(2:nx-1) = A_p(2:nx-1)/B(2:nx-1)$$

**Corrector step (backward method)**-----**Hydraulic radius**-----

$$R_c(1:nx) = (A_p(1:nx)/(B(1:nx) + 2 * H_p(1:nx)))$$

**Energy slopes**-----

$$\begin{aligned} S_{fc}(2:nx-1) &= ((N_m(2:nx-1) ** 2) * \\ &\& (((Q_p(2:nx-1)) * ABS((Q_p(2:nx-1)))))) / \\ &\& (((A_p(1:nx-2) + A_p(2:nx-1)) / 2) ** 2) * \\ &\& (((R_c(2:nx-1)) ** (4/3)))) \end{aligned}$$

**Area of flow**-----

$$A_c(2:nx-1) = A(2:nx-1) - (dt/dx) * (Q_p(2:nx-1) - Q_p(1:nx-2))$$

**Discharge**-----

$$\begin{aligned} \text{parone}(2:nx-1) &= ((Q_p(2:nx-1) ** 2) / A_p(2:nx-1)) - \\ &\& ((Q_p(1:nx-2) ** 2) / A_p(1:nx-2)) \\ \text{partwo}(2:nx-1) &= g * ((0.5 * (A_p(2:nx-1) * A_p(2:nx-1)) / B(2:nx-1)) - \\ &\& (0.5 * (A_p(1:nx-2) * A_p(1:nx-2)) / B(1:nx-2))) \\ Q_c(2:nx-1) &= Q(2:nx-1) - (dt/dx) * (\text{parone}(2:nx-1) + \text{partwo}(2:nx-1)) + \\ &\& (g * dt * (A_p(2:nx-1) * \\ &\& (S_{0c}(2:nx-1) - S_{fc}(2:nx-1)))) \end{aligned}$$

**Height of the water**-----

$$H_c(2:nx-1) = A_c(2:nx-1)/B(2:nx-1)$$

**Final value (average of predictor and corrector steps)**-----

$$A(2:nx-1) = 0.5 * (A_p(2:nx-1) + A_c(2:nx-1))$$

$$Q(2:nx-1) = 0.5 * (Q_p(2:nx-1) + Q_c(2:nx-1))$$

$$H(2:nx-1) = A(2:nx-1)/B(2:nx-1)$$

**Courant number of Hydraulic part**-----

$$WAVAC(1:nx) = (g * (A(1:nx)/B(1:nx))) ** 0.5$$

$$V(1:nx) = Q(1:nx) / A(1:nx)$$

$$CFL(1:nx) = (dt/dx) * (ABS(V(1:nx)) + WAVAC(1:nx))$$

### Erosion part-----

$$V(1:nx) = Q(1:nx) / A(1:nx)$$

$$FR(K-1:o+1) = V(K-1:o+1) / (SQRT(g * H(K-1:o+1)))$$

$$SHLD(1:nx) = SHLDZR * \cos(SAEII) * (1 - (\tan(SAEII) / \tan(BETA)))$$

### Sediment transport equation formula-----

$$CR(i) = V(i) / (SQRT(H(i) *$$

$$\& g * ((Z(i-1) - Z(i+1)) / (2 * dx))))$$

$$STRS(i) = (H(i) * ((Z(i-1) - Z(i+1)) /$$

$$\& (2 * dx))) / ((RUR-1) * Dave)$$

$$PHII(i) = 4 * (((Dnine/Dten) ** 0.2) *$$

$$\& (((((Z(i-1) - Z(i+1)) / (2 * dx))) ** 0.6) * CR(i) *$$

$$\& (STRS(i) ** 0.5) * (STRS(i) - SHLD(i))))$$

$$QS(i) = B(i) * PHII(i) * (SQRT(g * (RUR-1) * (Dave ** 3)))$$

$$ALFA(i) = (((QS(i)) * (1 / (H(i) * (1 - (FR(i) ** 2)))) * (dt/dx)) ** 2)$$

### Sediment continuity equation-----

$$Zc(i) = ((1 - ALFA(i)) * Z(i) + ALFA(i) * (Z(i+1) + Z(i-1))) * (0.5))$$

$$Z(i) = Zc(i) - (dt / (2 * (1 - PRT) * dx)) * ((QS(i-1)) - (QS(i+1)))$$

### Save final result in main matrix-----

$$H(1:nx) = H(1:nx) + Z(1:nx)$$

$$h\_array(1:nx, it+1) = H(1:nx)$$

$$V\_array(1:nx, it+1) = Q(1:nx)$$

$$Z\_array(1:nx, it+1) = Z(1:nx)$$

$$H(1:nx) = H(1:nx) - Z(1:nx)$$

End do

### End of loop-----

Return

End

## 8.4 Appendix-D

In this part 14 embankment dams are numerically failed and modelled with TELEMAC-2D and SISYPHE software. These dam failures are modelled based on the following assumptions:

- All the dams are failed by overtopping flow with initial breach in the middle of the crest.
- All the dams have non-cohesive soil with same grain size ( $d_{50}=4.75$  mm) and same numerical configuration.
- All the dams have rectangular reservoir shapes.

In the following details of these numerical modelling are presented in more detail.

**Table 8-1.** List of embankment dam failure

No.	Height (m)	Volume (m <sup>3</sup> )	width of dam (m)	Up and downstream slopes (%)	cohesion	Mean diameter (m)
1	50	2000000	36	1V:1.7H	0.0	4.75
2	80	2000000	250	1V:1.7H	0.0	4.75
3	50	12000000	250	1V:1.7H	0.0	4.75
4	80	40000000	250	1V:1.7H	0.0	4.75
5	50	2000000	500	1V:1.7H	0.0	4.75
6	80	12000000	500	1V:1.7H	0.0	4.75
7	50	40000000	500	1V:1.7H	0.0	4.75
8	80	2000000	36	1V:1.7H	0.0	4.75
9	50	2000000	250	1V:1.7H	0.0	4.75
10	80	12000000	250	1V:1.7H	0.0	4.75
11	50	40000000	250	1V:1.7H	0.0	4.75
12	80	2000000	500	1V:1.7H	0.0	4.75
13	50	12000000	500	1V:1.7H	0.0	4.75
14	80	40000000	500	1V:1.7H	0.0	4.75

**Outflow hydrograph of embankment dam failure (chapter 5):**

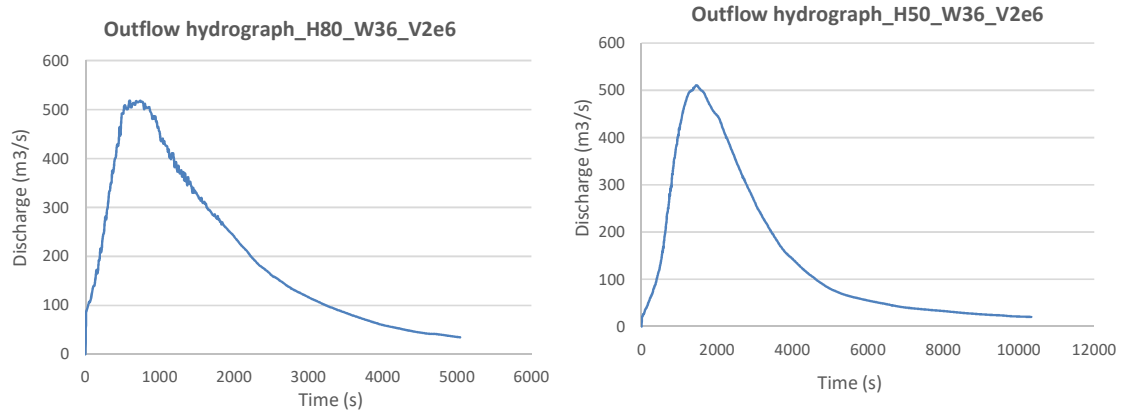


**Figure 8-3.** Outflow hydro graph for dam number 1 and 2

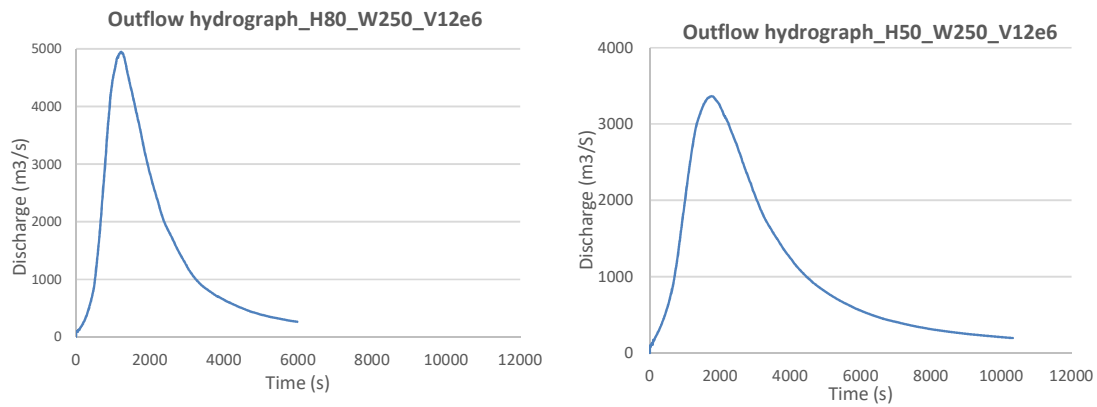


**Figure 8-4.** Outflow hydro graph for dam number 3 and 4

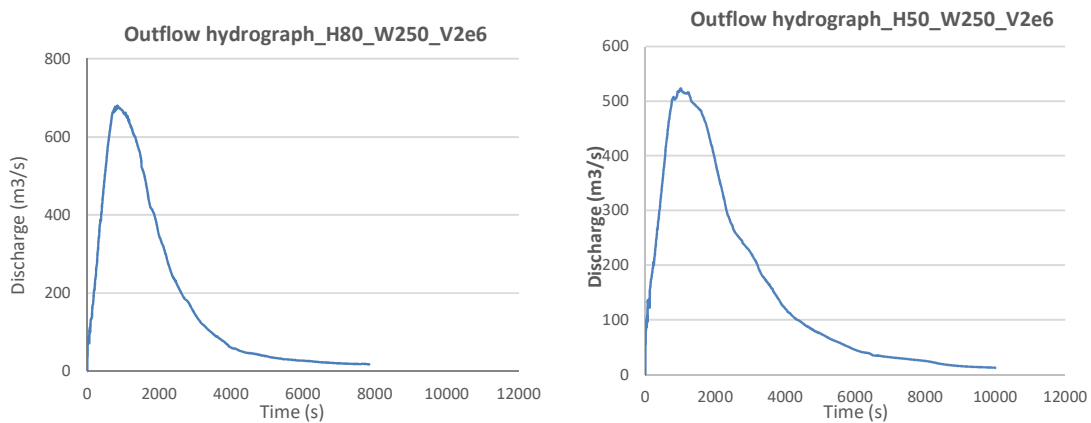


**Figure 8-5.** Outflow hydro graph for dam number 5 and 6

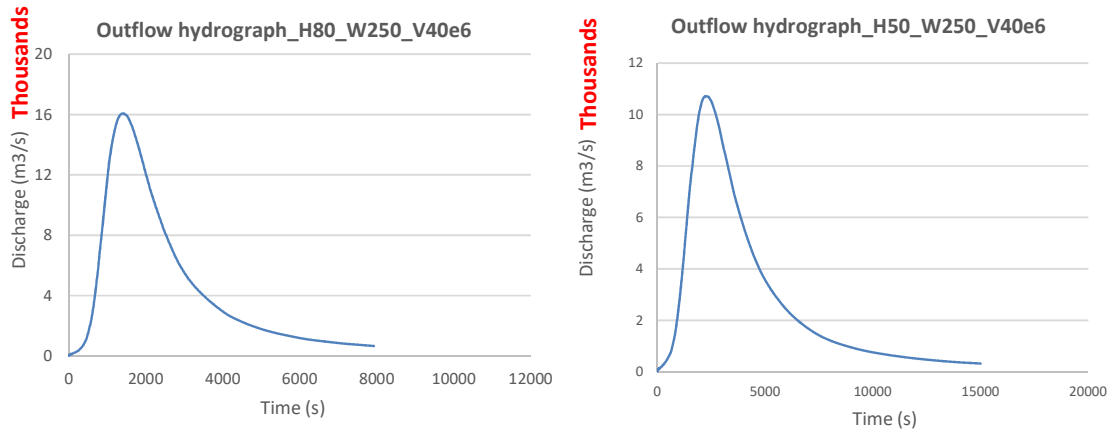


**Figure 8-6.** Outflow hydro graph for dam number 7 and 8

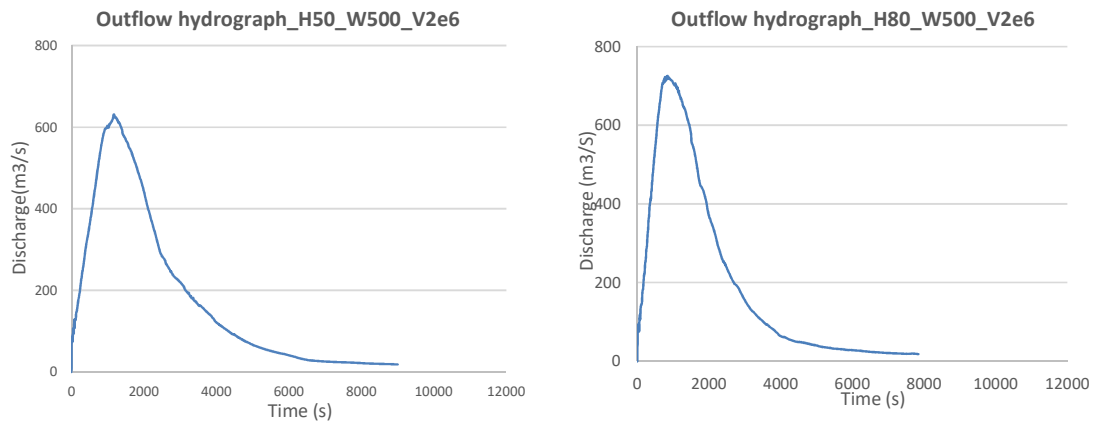


**Figure 8-7.** Outflow hydro graph for dam number 9 and 10

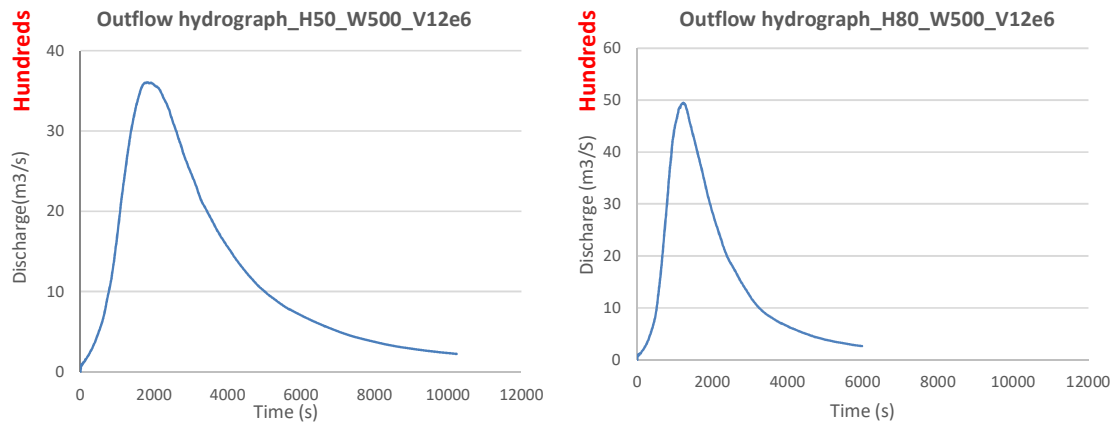


**Figure 8-8.** Outflow hydro graph for dam number 11 and 12

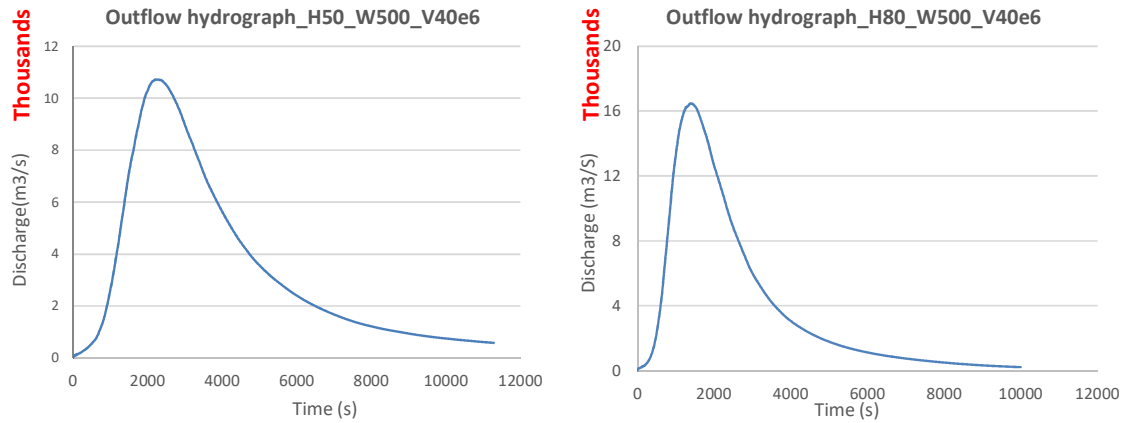


**Figure 8-9.** Outflow hydro graph for dam number 13 and 14

## 8.5 Appendix-E

### List of the peak outflow discharge curve in downstream of dams (chapter 5)

In this part 42 channels are numerically modelled with TELEMAC-2D software. These channels are modelled based on the following assumptions:

- All the channels have rectangular shape with 1% slope.
- All the channels have 20 km length with 10, 20 and 30 Strickler Roughness coefficients.
- All the channels are divided into 20 sections and a cross-section discharge is calculated for each of them

Results of these numerical modelling are presented in two parts:

- Peak outflow discharge curve (Appendix E).
- Flood wave Arrival time (Appendix F).

In the following details of peak outflow discharge curves are presented.

**Table 8-2.** List of the peak outflow discharge curve

No.	Channel length (km)	Channel width	Hydrograph No.	Manning number	Slope of the channel
1	20	36	1	10	1%
2	20	36	1	20	1%
3	20	36	1	30	1%
4	20	36	2	10	1%
5	20	36	2	20	1%
6	20	36	2	30	1%
7	20	250	7	10	1%
8	20	250	7	20	1%
9	20	250	7	30	1%
10	20	250	8	10	1%
11	20	250	8	20	1%
12	20	250	8	30	1%
13	20	250	3	10	1%
14	20	250	3	20	1%
15	20	250	3	30	1%
16	20	250	4	10	1%
17	20	250	4	20	1%
18	20	250	4	30	1%
19	20	250	5	10	1%
20	20	250	5	20	1%
21	20	250	5	30	1%
22	20	250	6	10	1%
23	20	250	6	20	1%
24	20	250	6	30	1%
25	20	500	13	10	1%
26	20	500	13	20	1%
27	20	500	13	30	1%
28	20	500	14	10	1%
29	20	500	14	20	1%
30	20	500	14	30	1%
31	20	500	11	10	1%
32	20	500	11	20	1%
33	20	500	11	30	1%
34	20	500	12	10	1%
35	20	500	12	20	1%
36	20	500	12	30	1%
37	20	500	9	10	1%
38	20	500	9	20	1%
39	20	500	9	30	1%
40	20	500	10	10	1%
41	20	500	10	20	1%
42	20	500	10	30	1%

**Peak outflow discharge curve in downstream of dams (chapter 5):**

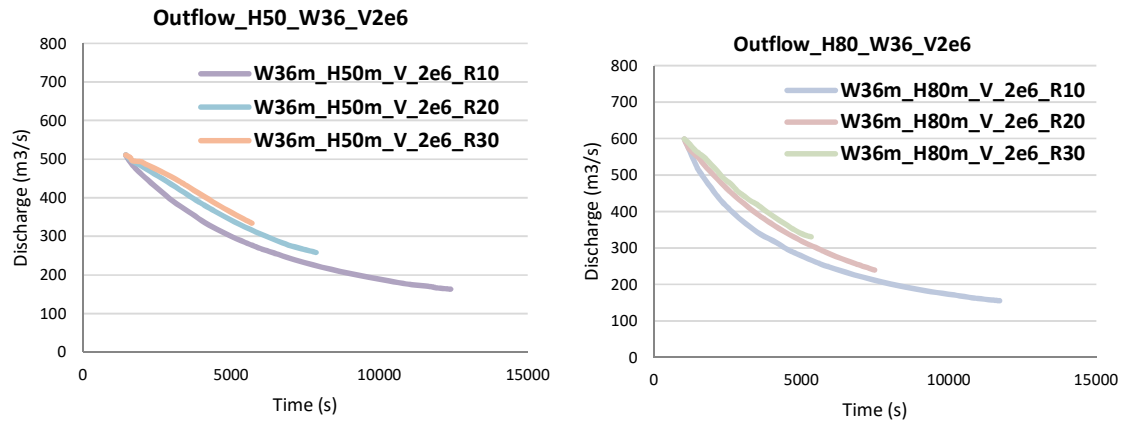


**Figure 8-10.** Peak outflow discharge curve for test number 1 and 6

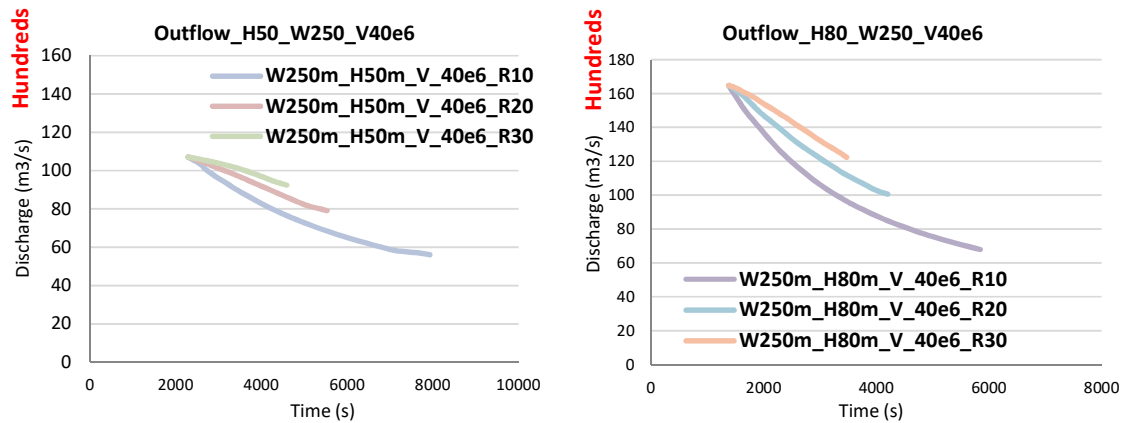


**Figure 8-11.** Peak outflow discharge curve for test number 7 and 12

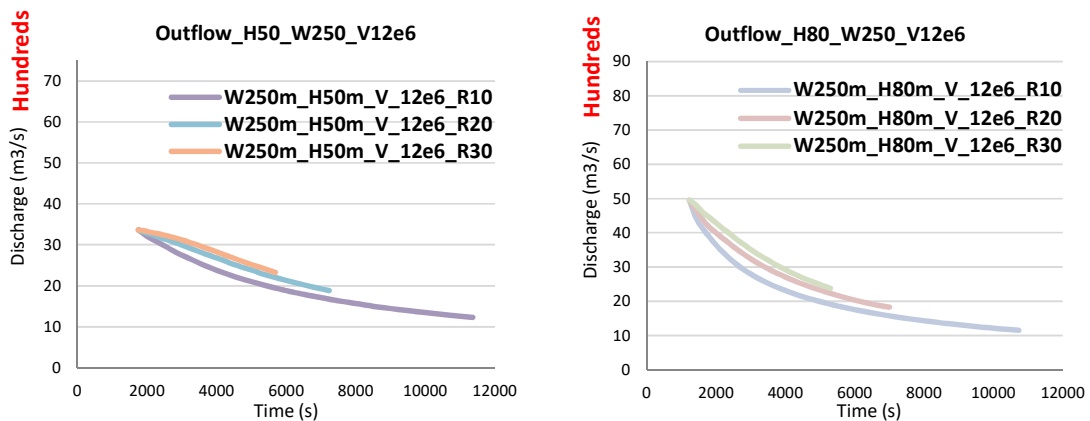


**Figure 8-12.** Peak outflow discharge curve for test number 13 and 18

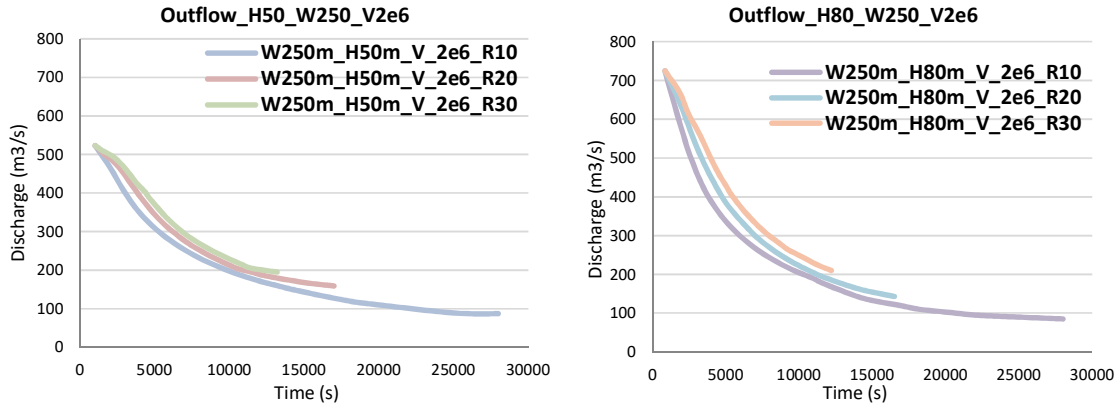


Figure 8-13. Peak outflow discharge curve for test number 19 and 24

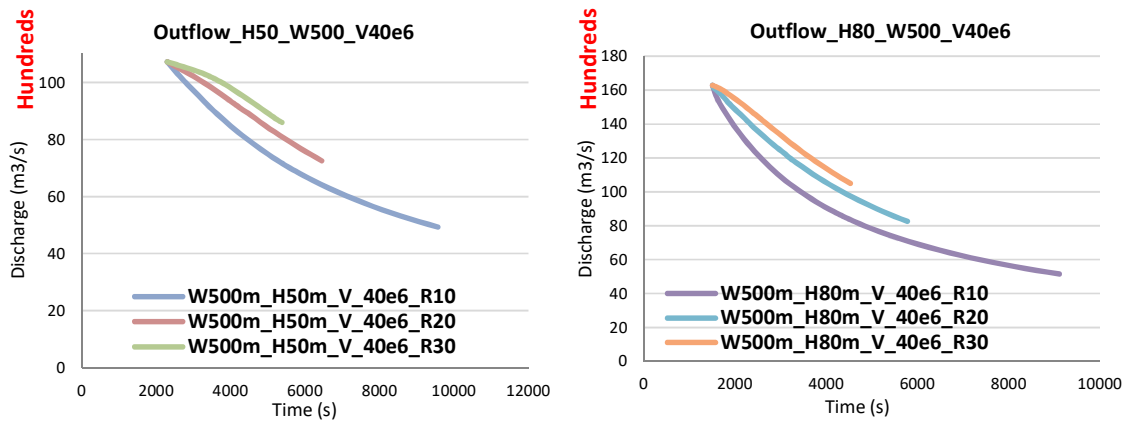


Figure 8-14. Peak outflow discharge curve for test number 25 and 30

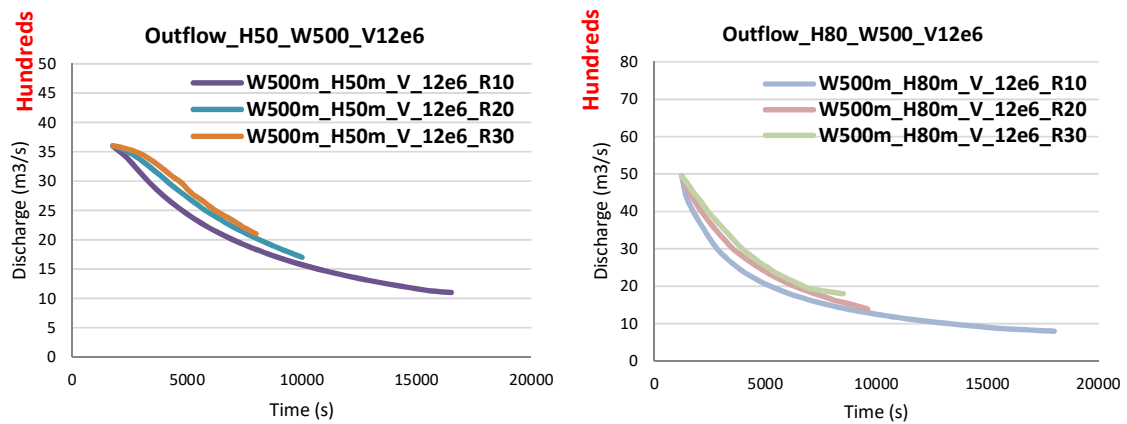
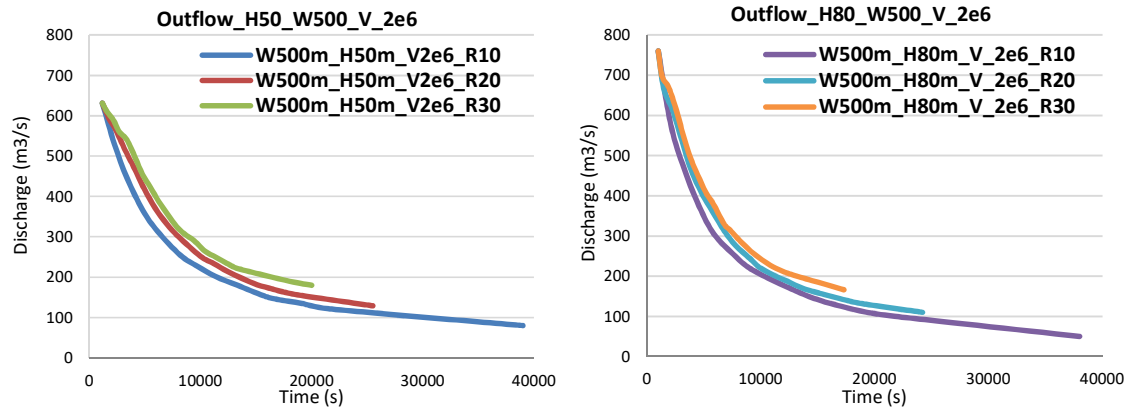


Figure 8-15. Peak outflow discharge curve for test number 31 and 36



**Figure 8-16.** Peak outflow discharge curve for test number 37 and 42

## Influence of different slopes on the peak outflow discharge curve

In this part 15 channels are numerically modelled with TELEMAC-2D software. These channels are modelled based on the following assumptions:

- All the channels have rectangular shape with 1%, 5% and 10% slope
- All the channels have 20 km length with 10, 20, 30 and 40 Strickler Roughness coefficients.
- All the channels are divided into 20 sections and a cross-section discharge is calculated for each of them

In the following details of this investigation are presented.

**Table 8-3.** List of the peak outflow discharge curve

Test No.	Height of the dam (m)	Width of the channel (m)	Reservoir volume (m <sup>3</sup> )	Slope	manning
40	50	500	12.0E+6	1%	10-20-30-40
			12.0E+6	5%	10
			12.0E+6	10%	10
34	50	500	2.0E+6	1%	10-20-30-40
			2.0E+6	5%	10
			2.0E+6	10%	10
16	50	250	12.0E+6	1%	10-20-30-40
			12.0E+6	5%	10
			12.0E+6	10%	10
22	50	250	2.0E+6	1%	10-20-30-40
			2.0E+6	5%	10
			2.0E+6	10%	10
4	50	36	2.0E+6	1%	10-20-30-40
			2.0E+6	5%	10
			2.0E+6	10%	10

**Compare influence of different slopes on the peak outflow discharge curve**

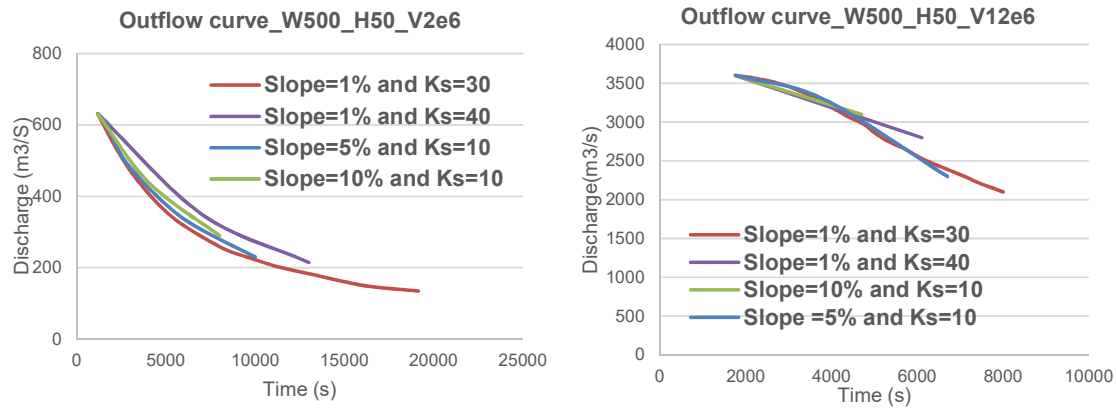


**Figure 8-17.** Peak outflow discharge curve for test number 34 and 40

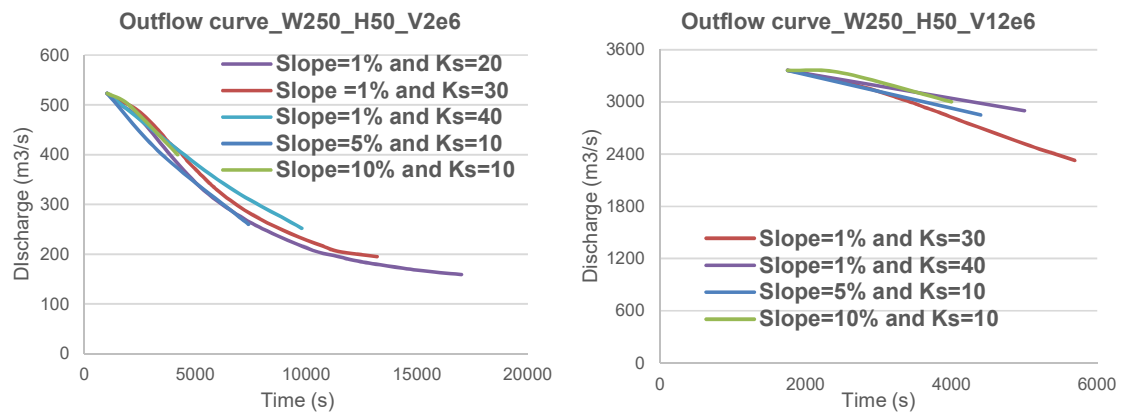


**Figure 8-18.** Peak outflow discharge curve for test number 22 and 16

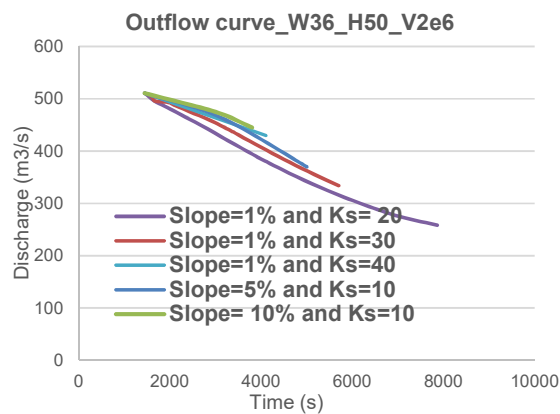


**Figure 8-19.** Peak outflow discharge curve for test number 4

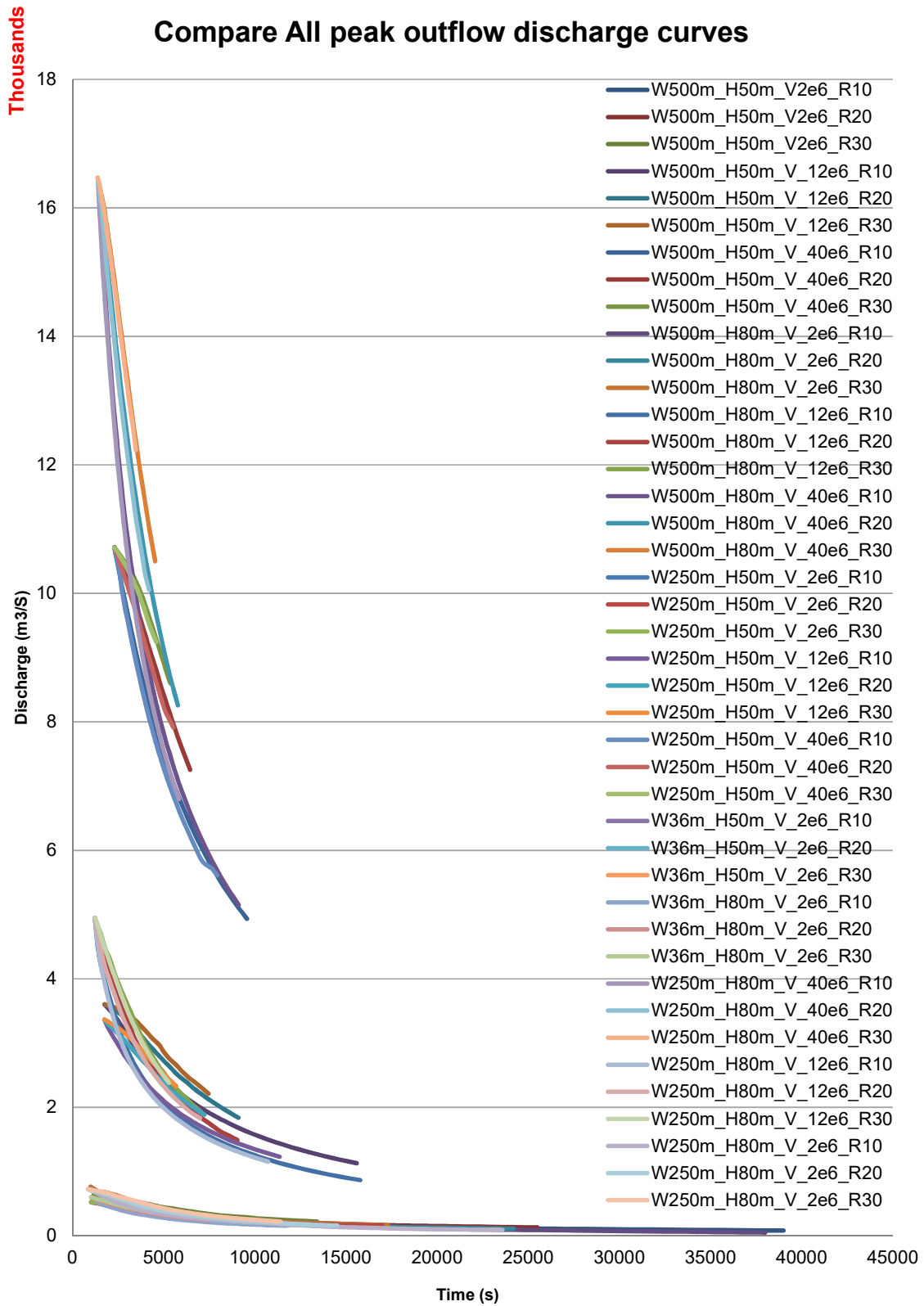


Figure 8-20. Compare all peak outflow discharge curve

## 8.6 Appendix-F

### List of the arrival time line in downstream of dams (chapter 5):

In this part 42 channels are numerically modelled with TELEMAC-2D software. These channels are modelled based on the following assumptions:

- All the channels have rectangular shape with 1% slope.
- All the channels have 20 km length with 10, 20 and 30 Strickler Roughness coefficients.
- All the channels are divided into 20 sections and a cross-section discharge is calculated for each of them

In the following details of the flood wave Arrival time are presented.

**Table 8-4.** List of the arrival time line

No.	Channel length (km)	Channel width	Hydrograph No.	Manning number	Slope of the channel
1	20	36	1	10	1%
2	20	36	1	20	1%
3	20	36	1	30	1%
4	20	36	2	10	1%
5	20	36	2	20	1%
6	20	36	2	30	1%
7	20	250	7	10	1%
8	20	250	7	20	1%
9	20	250	7	30	1%
10	20	250	8	10	1%
11	20	250	8	20	1%
12	20	250	8	30	1%
13	20	250	5	10	1%
14	20	250	5	20	1%
15	20	250	5	30	1%
16	20	250	6	10	1%
17	20	250	6	20	1%
18	20	250	6	30	1%
19	20	250	3	10	1%
20	20	250	3	20	1%
21	20	250	3	30	1%
22	20	250	4	10	1%
23	20	250	4	20	1%
24	20	250	4	30	1%
25	20	500	13	10	1%
26	20	500	13	20	1%
27	20	500	13	30	1%
28	20	500	14	10	1%
29	20	500	14	20	1%
30	20	500	14	30	1%
31	20	500	11	10	1%
32	20	500	11	20	1%
33	20	500	11	30	1%
34	20	500	12	10	1%
35	20	500	12	20	1%
36	20	500	12	30	1%
37	20	500	9	10	1%
38	20	500	9	20	1%
39	20	500	9	30	1%
40	20	500	10	10	1%
41	20	500	10	20	1%
42	20	500	10	30	1%

Arrival time line in downstream of dams (chapter 5)

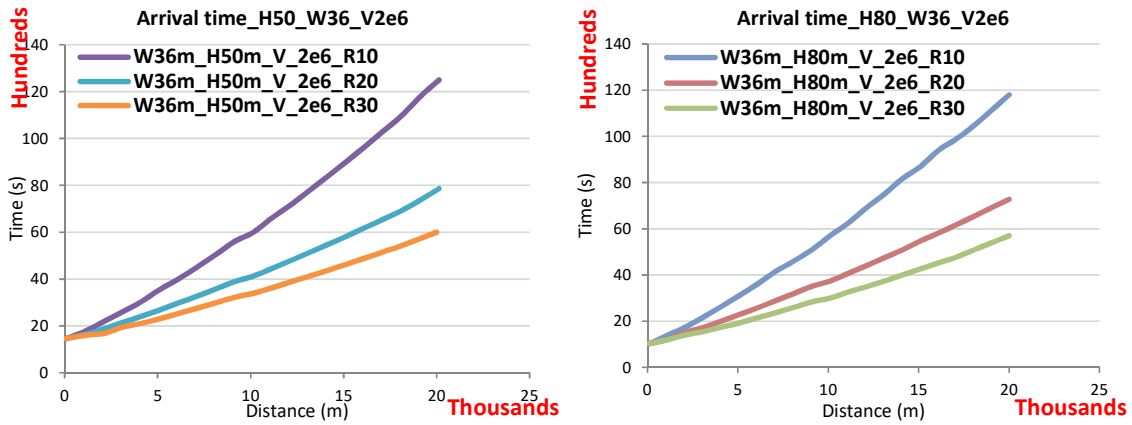


Figure 8-21. Arrival time for test number 1 and 6

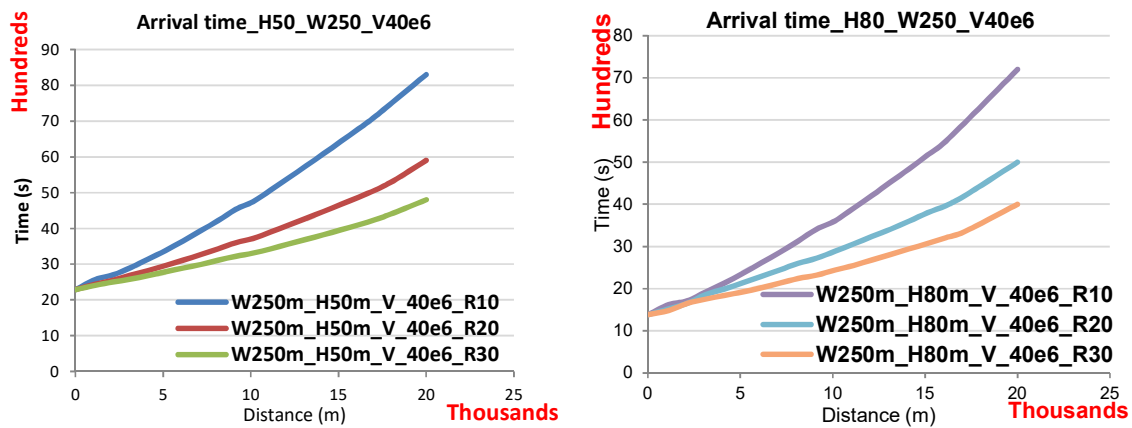


Figure 8-22. Arrival time for test number 7 and 12

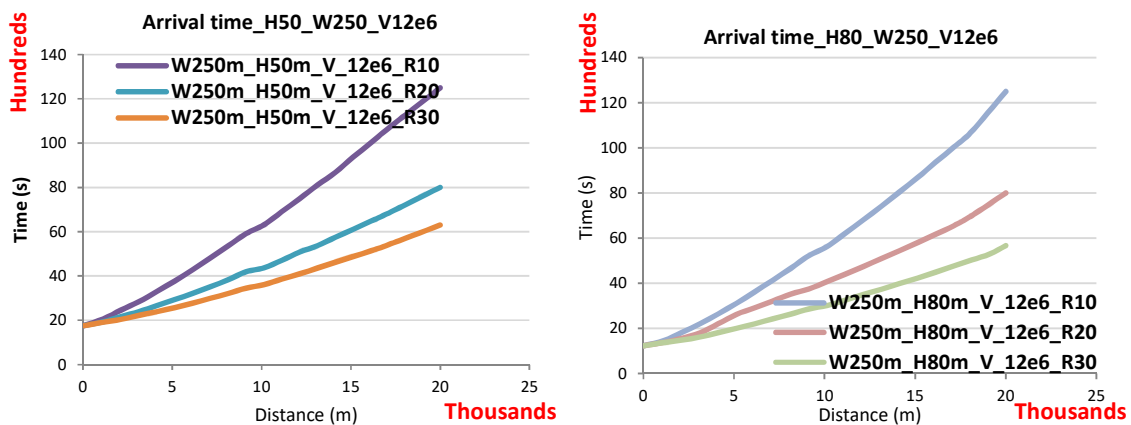


Figure 8-23. Arrival time for test number 13 and 18

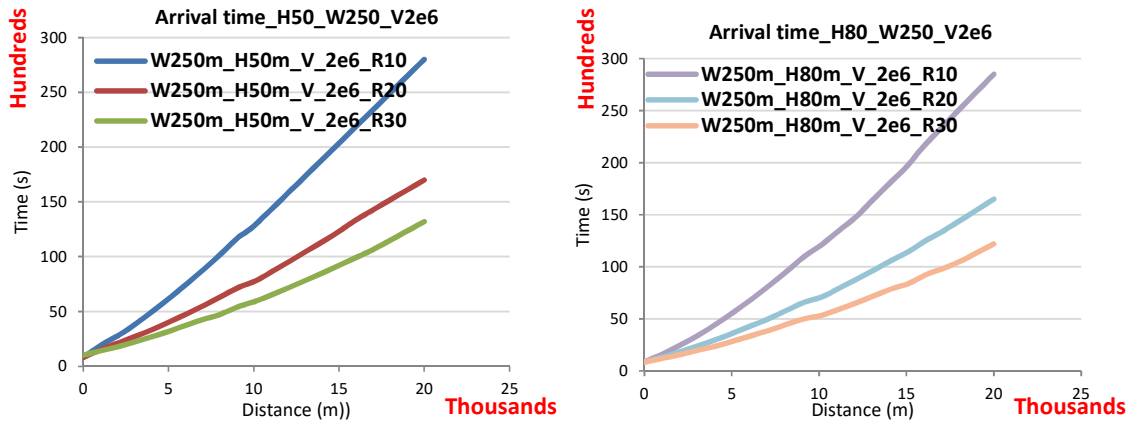


Figure 8-24. Arrival time for test number 19 and 24

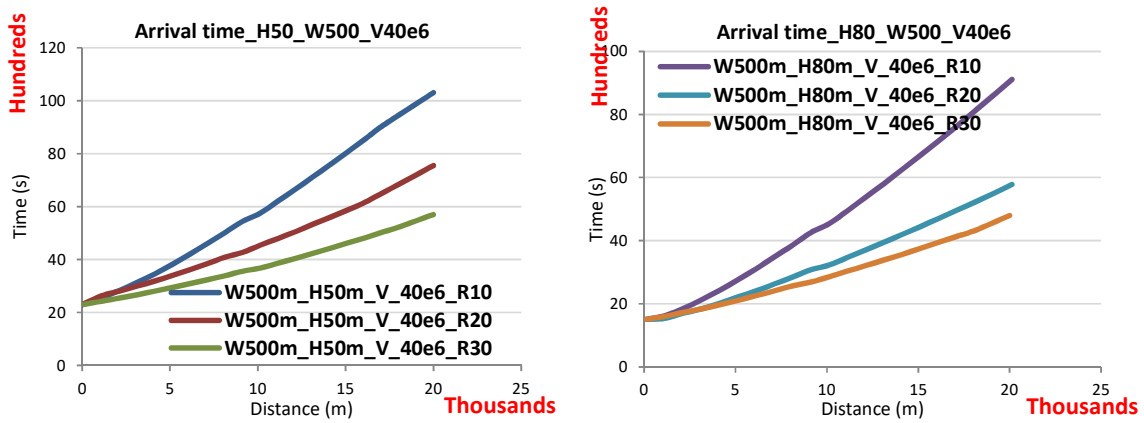


Figure 8-25. Arrival time for test number 25 and 30

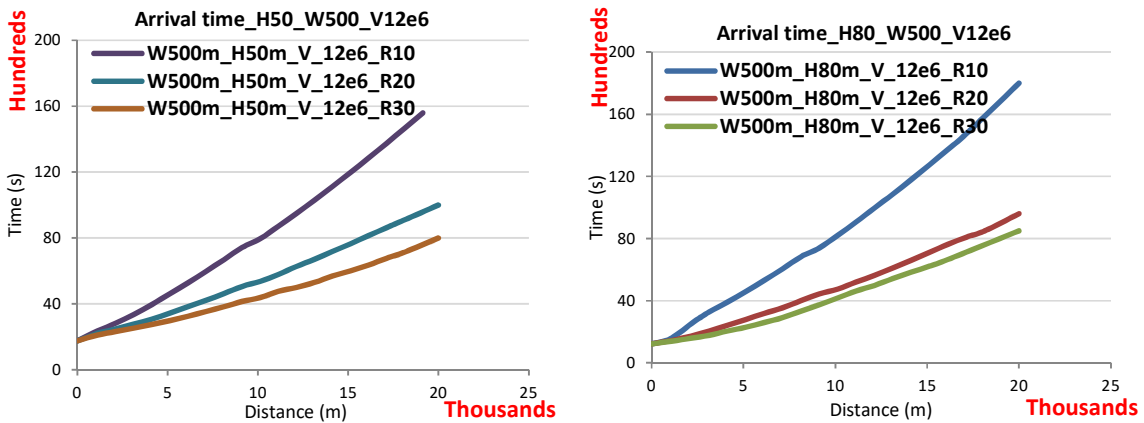


Figure 8-26. Arrival time for test number 31 and 36

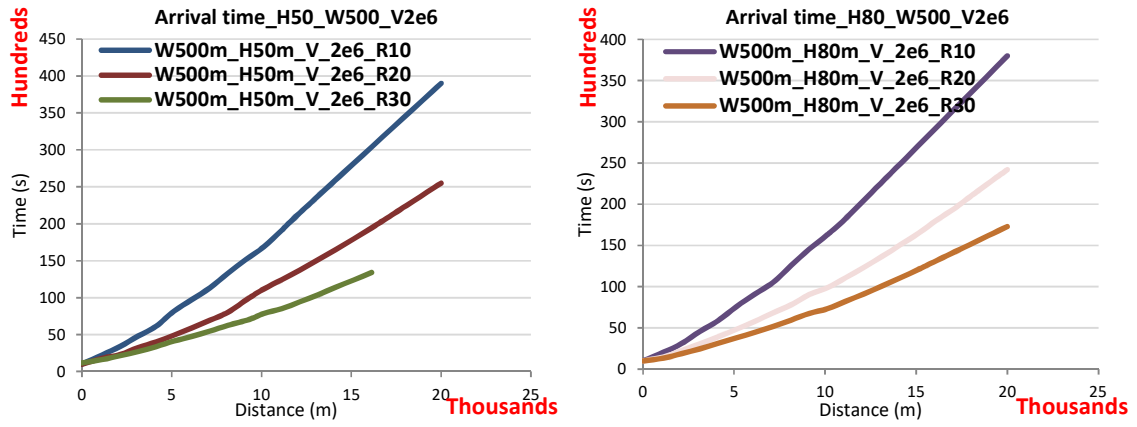


Figure 8-27. Arrival time for test number 37 and 42

### Influence of different slopes on the arrival time line

In this part 15 channels are numerically modelled with TELEMAC-2D software. These channels are modelled based on the following assumptions:

- All the channels have rectangular shape with 1% -5% and 10% slope.
- All the channels have 20 km length with 10-20- 30 and 40 Strickler Roughness coefficients.
- All the channels are divided into 20 sections and a cross-section discharge is calculated for each of them

In the following details of this investigation are presented.

**Table 8-5.** List of the arrival time line

Test No.	Height of the dam (m)	Width of the channel (m)	Reservoir volume (m <sup>3</sup> )	Slope	manning
40	50	500	12.0E+6	1%	10-20-30-40
			12.0E+6	5%	10
			12.0E+6	10%	10
34	50	500	2.0E+6	1%	10-20-30-40
			2.0E+6	5%	10
			2.0E+6	10%	10
16	50	250	12.0E+6	1%	10-20-30-40
			12.0E+6	5%	10
			12.0E+6	10%	10
22	50	250	2.0E+6	1%	10-20-30-40
			2.0E+6	5%	10
			2.0E+6	10%	10
4	50	36	2.0E+6	1%	10-20-30-40
			2.0E+6	5%	10
			2.0E+6	10%	10

Compare influence of different slopes on the arrival time line

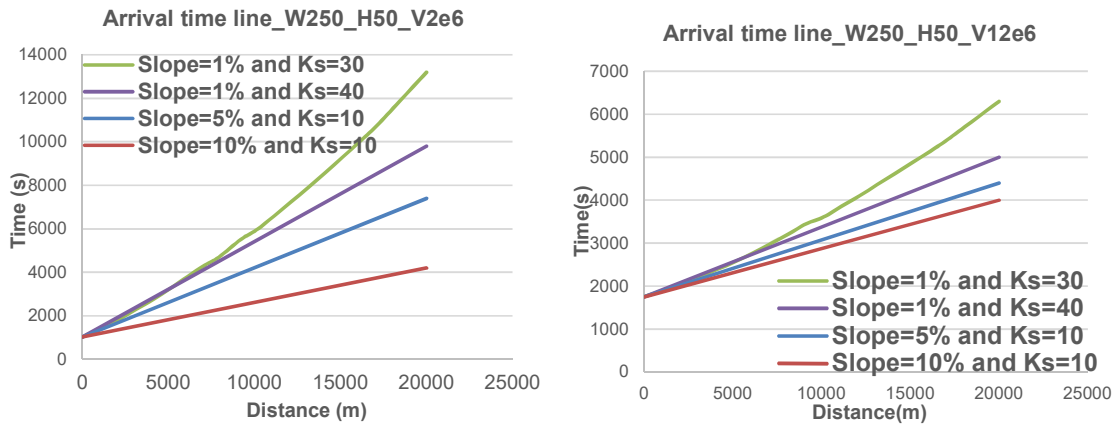


Figure 8-28. Arrival time for test number 22 and 16

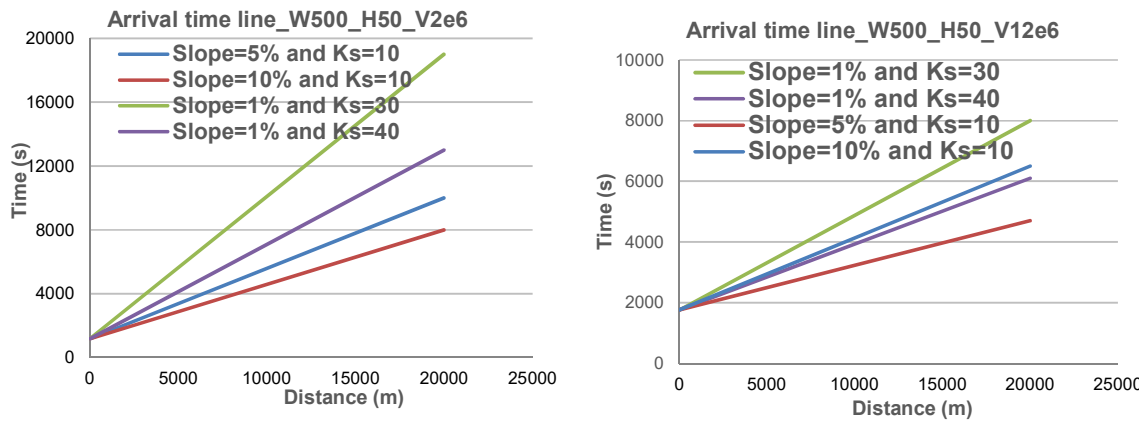


Figure 8-29. Arrival time for test number 34 and 40

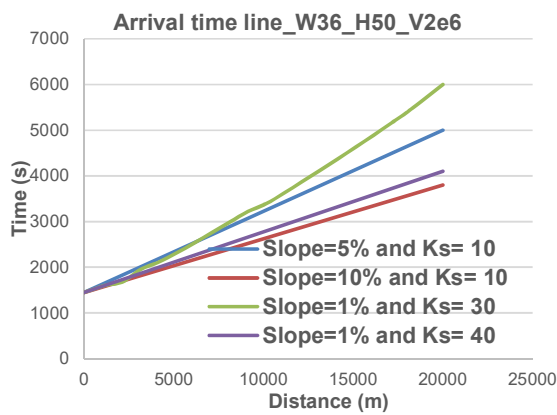


Figure 8-30. Arrival time for test number 4

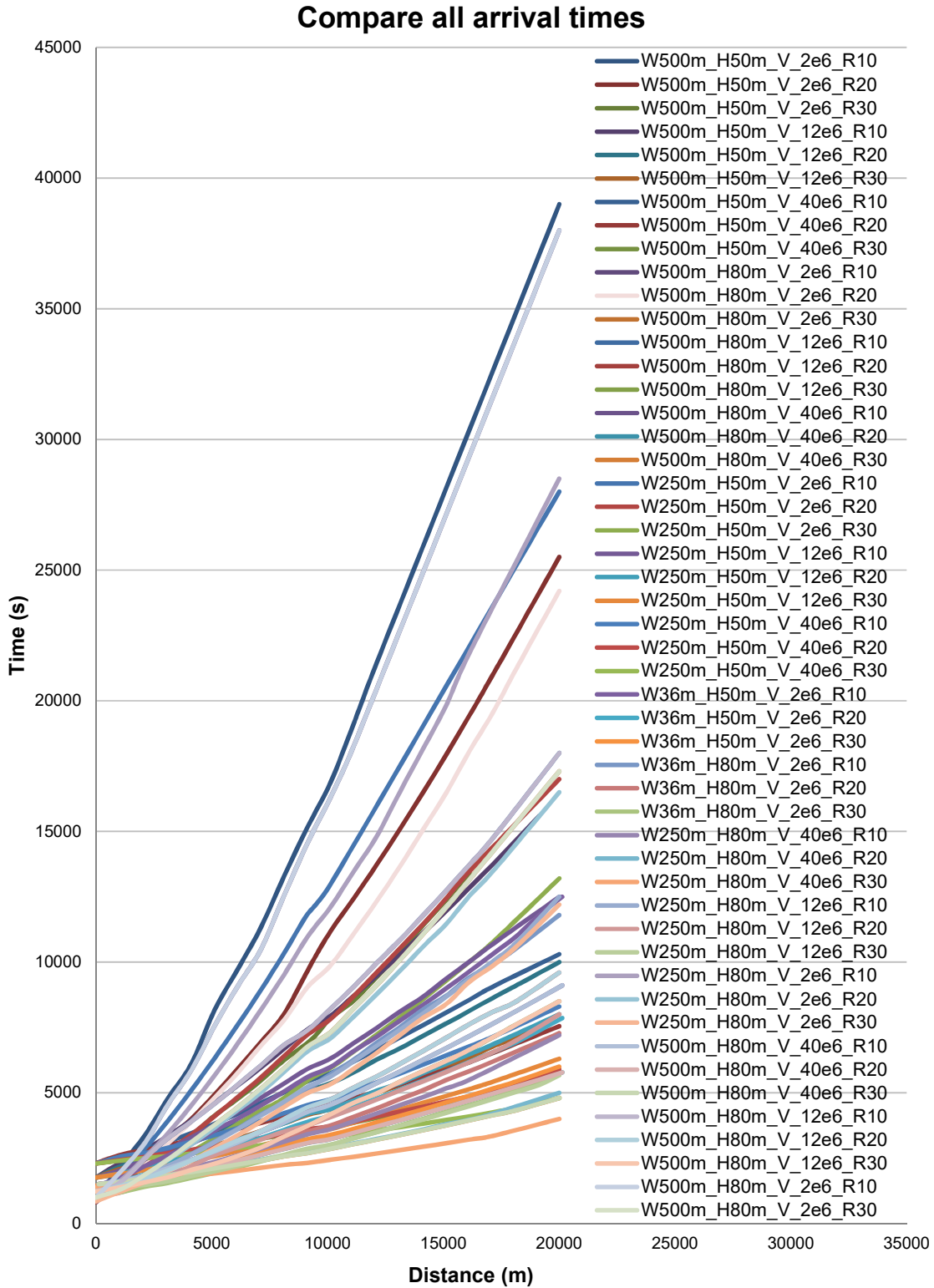
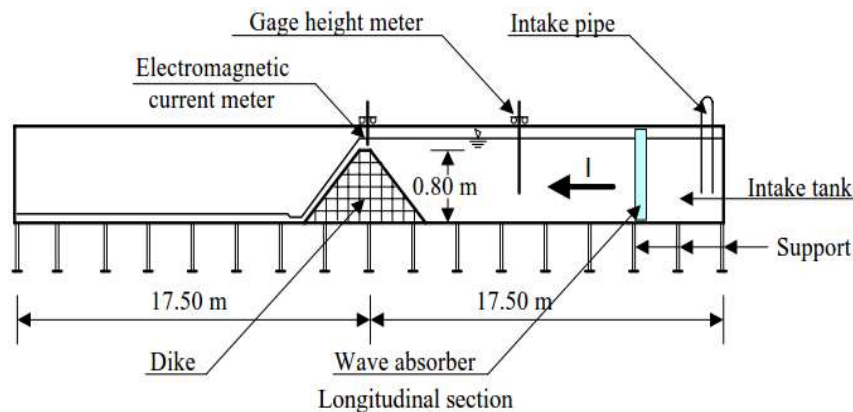


Figure 8-31. Compare all flood wave arrival time

## 8.7 Appendix-G

### Calibration the King Mongkut's University (small scale)

This test was performed in a flume with dimensions  $35\text{m} \times 1\text{m} \times 1\text{m}$ . A small scale dam is located in the middle of this flume with  $0.8\text{m}$  in height,  $0.3\text{m}$  width of the crest. The upstream slope of this dam is fixed at  $1\text{V}:3\text{H}$  and downstream of this dam varied from  $1\text{V}:2\text{H}$  to  $1\text{V}:5\text{H}$ . For all experimental tests, the initial water level in the reservoir is kept constant at  $0.83\text{m}$  and downstream water level is kept constant at  $0.03\text{m}$ . The soil porosity is  $0.35$  and soil density is  $2.65 \times 10^3 \text{ kg/m}^3$ .



**Figure 8-32.** King Mongkut's University dam failure tests

**Table 8-6:** Details of the King Mongkut's University dam failure tests

Flume	Height	Length	Width
Dimension(m)	1	35	1
Small scale dam	Height	Crest width	Crest Length
Dimension(m)	0.8	0.3	1

**Table 8-7.** Different slope in the King Mongkut's University dam failure tests

Run no.	Upstream slope	Downstream slope	Upstream inflow ( $\text{m}^3/\text{s}$ )	Initial upstream Level (m)	downstream Level (m)
1	$1\text{V}:3\text{H}$	$1\text{V}:2\text{H}$	$1.1 \times 10^{-3}$	0.83	0.03
2	$1\text{V}:3\text{H}$	$1\text{V}:3\text{H}$	$1.23 \times 10^{-3}$	0.83	0.03
3	$1\text{V}:3\text{H}$	$1\text{V}:4\text{H}$	$1.42 \times 10^{-3}$	0.83	0.03
4	$1\text{V}:3\text{H}$	$1\text{V}:5\text{H}$	$1.05 \times 10^{-3}$	0.83	0.03

### One-dimensional numerical modelling

In order to model the Chinnarasri et al. (2003) dam failure tests by using the 1-D program, a fixed spatial step  $\Delta x = 0.03$  m and a constant time step  $\Delta t = 0.01$  s are considered. The channel is assumed to be rectangular with a fixed width 1.0 m. Furthermore two boundaries are defined:

- Constant discharge at inflow
- Constant height of water at outflow

After running the numerical simulation, the measurement results are compared against the computational results as shown in the Figures 8-33 and 8-34.

Calibrated values for  $\omega$  parameter in the Smart equation are shown in the Table 8-8.

### TELEMAC-2D numerical modelling

Two similar dams with a mean grain size of 0.31mm and 2.0 mm are modelled by using TELEMAC-2D software. The experimental setup configuration for this software is represented by 22000 cells, which spatial step varies from 0.1 m for the reservoir and downstream, to 0.05 m for the dam. Furthermore, constant time step 0.05s is considered throughout the calculation. After running the numerical simulation, the computational results are compared with measurement results as shown in the Figures 8-33 and 8-34.

Calibrated values for  $\beta_{tel}$  parameter in the the Koch and Flokstra equation are shown in the Table 8-9.

**Table 8-8.** Calibrated  $\omega$  value

Slope (%)	$\omega$
Between 1V:5H and 1V:4H (20%-25%)	0.6-0.9
Between 1V:4H and 1V:3H (25%-33%)	0.9-1.1
More than 1V:2H (33%)	1.1-2.8

**Table 8-9.** Calibrated  $\beta_{tel}$  parameter

Slope (%)	$\beta_{tel}$
Less than 1V:4H (25%)	1.3
Between 1V:4H and 1V:3H (25%-33%)	2.0-3.5
More than 1V:2H (33%)	4.5-6.0

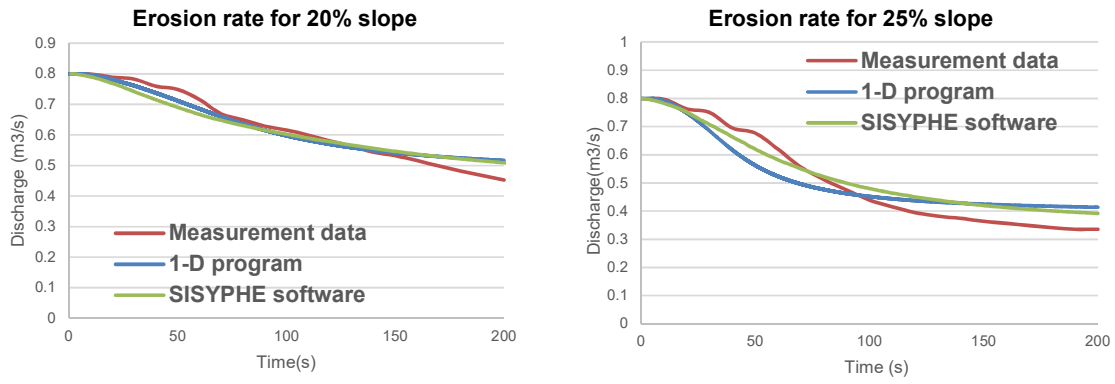


Figure 8-33. Erosion rate for 20% and 25% slope

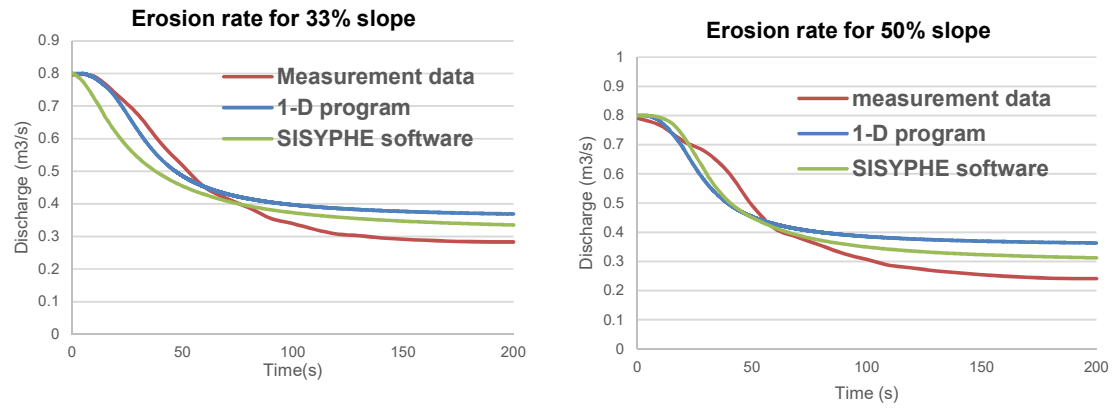


Figure 8-34. Erosion rate for 33% and 50% slope